5-2015

ADSORPTION OF DYES ON ACTIVATED CARBON FROM AGRICULTURAL WASTES

Maliha Parvin

United Arab Emirates University

College of Science

Department of Chemistry

ADSORPTION OF DYES ON ACTIVATED CARBON FROM AGRICULTURAL WASTES

Maliha Parvin

This thesis is submitted in partial fulfilment of the requirements for the degree of Master of Science in Chemistry

Under the Supervision of Professor Thies Thiemann

May 2015

Declaration of Original Work

I, Maliha Parvin, the undersigned, a graduate student at the United Arab Emirates University (UAEU), and the author of this thesis entitled "*Adsorption of Dyes on Activated Carbon from Agricultural Wastes",* hereby, solemnly declare that this thesis is an original research work that has been done and prepared by me under the supervision of Professor Thies Thiemann and Dr. Ahmed Soliman , in the College of Science at UAEU. This work has not been previously formed as the basis for the award of any academic degree, diploma or a similar title at this or any other university. The materials borrowed from other sources and included in my thesis have been properly cited and acknowledged.

Student's Signature_____ Date _____

Approval of the Master Thesis

This Master Thesis is approved by the following Examining Committee Members:

1) Advisor (Committee Chair): Thies Thiemann
   Title: Professor
   Department of Chemistry
   College of Science

   Signature _____ Date _____

2) Member: Ahmed A. Soliman
   Title: Instructor
   Department of Chemistry
   College of Science

   Signature _____ Date _____

3) Member: Ahmed Murad
   Title: Associate Professor, Vice-Dean COS
   Department of Geology
   College of Science

   Signature _____ Date _____

4) Member (External Examiner): Nathir al Rawashdeh
   Title: Professor
   Department of Applied Chemical Sciences
   Institution: Jordan University of Science and Technology

   Signature _____ Date _____

This Master Thesis is accepted by:

Dean of the College of Science: Professor Frederick Leung

Signature _____ Date _____

Dean of the College of the Graduate Studies: Professor Nagi T. Wakim

Signature _____ Date _____

Copy ____ of ____

Abstract

Adsorption of dyes as a remediation technique for dye-loaded wastewater remains an area of interest. On the one hand, adsorption using bio-derived, renewable sorbent materials can be seen as environmentally friendly, on the other hand adsorption can provide us with a trouble-free, commercially cheap operation. The main objective of this thesis is adsorption of the dyes Crystal Violet (CV) and Nile Blue (NB) on activated carbon derived from date palm leaf wastes. For this purpose, activated carbon was prepared via chemical treatment of palm leaf wastes with sulfuric acid (H_2SO_4), phosphoric acid (H_3PO_4), and nitric acid (HNO_3), respectively, with subsequent carbonization through thermal treatment. Dye adsorption studies with this activated carbon were carried out under different conditions, and the influence of different parameters such as temperature, time, pH, dye concentration, dose and particle size of activated carbon (AC) was investigated in batch experiments. Furthermore, dynamic sorption experiments were performed successively. The present study found AC from date palm leaves to be a promising low cost adsorbent to remove CV and NB from aqueous solutions.

Keywords: Activated carbon, dye adsorption, crystal violet dye, Nile blue dye, date palm leaf.

Title and Abstract (in Arabic)

امتصاص الأصباغ باستخدام الكربون النشط المشتق من المخلفات الزراعية

الملخص

امتصاص الأصباغ يلقى اهتمام كبيرا كطريقة لمعالجة مياه الصرف الصحي الملوثة بالأصباغ. و من ناحية, الامتصاص باستخدام المشتقات الحيوية، والمواد المتجددة و التي لها القدرة على الامتصاص يمكن أن ينظر له كطريقة صديقة للبيئة، و من جهة أخرى هذا الامتصاص يمكن أن يوفر لنا عملية اقتصادية رخيصة غير مكلفة و خالية من المتاعب. الهدف الرئيسي في هذه الدراسة هو امتصاص صبغات الكريستال البنفسجي والنيل الأزرق باستخدام الكربون النشط المشتق من نفايات أوراق النخيل. ولتحقيق هذا الهدف تم تحضير الكربون النشط باستخدام المعالجة الكيميائية لنفايات أوراق النخيل باستخدام أحماض مختلفة وتتضمن حمض الكبريتيك, و حمض الفوسفوريك , و حمض النيتريك, على التوالي , مع الكربنة اللاحقة باستخدام المعالجة الحرارية. ولقد أجريت دراسات عدة لامتصاص الأصباغ باستخدام الكربون النشط في ظل ظروف مختلفة. ولقد تم دراسة العوامل المختلفة التي تؤثر على عملية الامتصاص مثل درجة الحرارة, والوقت, ودرجة الحموضة, وتركيز الصبغة, وجرعة وحجم جزيئات الكربون النشطة في عدة تجارب مخبرية. وعلاوة على ذلك لقد أجريت بنجاح تجارب الامتصاص الديناميكية. كما اتضح في هذه الدراسة أن الكربون النشط المشتق من نفايات أوراق النخيل يعد واعدا كمادة منخفضة التكاليف لها القدرة على امتصاص وإزالة الملوثات العضوية كصبغات الكريستال البنفسجي والنيل الأزرق من المحاليل المائية .

الكلمات الرئيسية: الكربون النشط، امتصاص الصبغة، صبغة الكريستال البنفسجي ,صبغة النيل الأزرق، أورق النخيل.

Acknowledgements

Firstly, my ever big thank goes to almighty Allah (SWT) for giving me the ability to complete my postgraduate study with health and peace. Then, my thanks go to my principal supervisor Professor Thies Thiemann whose enthusiasm about and introduction to adsorption of dyes on activated carbon from agricultural wastes got me started. I am especially grateful and thankful to Dr Ahmed Soliman for introducing me to the exciting field of literary theory, along with his endless ideas and encouragement led to this and most other studies in which I have been involved.

I would like to thank my examining committee for their guidance, support, and assistance throughout my preparation of this thesis. I would like to thank the chair and all members of the UAEU Department of Chemistry for assisting me all over my studies and research. My special thanks are extended to Ahmed Taha of the Library Research Desk for providing me with the relevant reference material.

Special thanks are due to my parents, father-in-law, mother-in-law, husband, son, brothers, and sisters who helped me along the way. I am sure they suspected it was endless. In addition, special thanks are extended to Fatima Hassan Ali Alawalhi and Najla for their cordial friendship.

Dedication

To Professor Thies Thiemann and Professor Abbas Khaleel

Table of Contents

List of Tables

List of Figures

List of Abbreviations

AC	Activated Carbon
CV	Crystal Violet
NB	Nile Blue
UV	Ultra-violet Visible
IR	Infrared
FR	Flow Rate
COD	Chemical Oxygen Demand
NF	Nanofiltration
RO	Reverse Osmosis
UF	Ultrafiltration

Chapter 1: Introduction

1.1 Industrial Organic Dye-Stuff

In former times, dyes were gained mostly from mineral (inorganic) sources with the exception of some very expensive organic dyes from natural sources, such as of purpur from the mollusk Murex spp., scarlet from the Kermes insect and carmine from the Cochineal insect. In 1856, W. H. Perkin perfected the synthesis of the first organic dye “mauve”. In 1878, A. von Bayer synthesized indigo for the first time. In the early 1860s, H. Caro started working for BASF and developed a synthesis for alizarin. BASF also obtained a patent to manufacture methylene blue, and by 1901, 80% of the revenues of BASF (a company that nowadays employs 113000 people) came from dyestuff. Today, organic dyes are integrally associated with the textile industry.

The world-use of reactive dyes alone increased from 60.000 tons in 1988 to 178.000 tons in 2004 (182.000 tons in 2011). The world production of indigo dyes lies at 80.000 tons per year (in 2010), while 112.000 tons of naphthol dyes were produced annually by 2013 and Ghaly Furthermore, today, more than 10,000 different dyes are produced annually for different applications, 30% of which are used in excess of 1,000 tonnes per year. However, 90% of the textile products are used at the level of 100 tonnes per annum or less, making for the large variety of dyes used in the textile industry (Ghaly, Ananthashanker, Alhattab, & Ramakrishnan, 2014; Philips, 1996; UNSD, 2013; Soetaert, & Vandamme, 2010).

1.2 Classification System of Dyes

Dyes can be classified according to their chemical structure and their application. In term of chemical structure, dyes can be inorganic or organic compounds. Again, both groups can be subdivided into natural and synthetic compounds. According to the dyeing method, dyes can be divided into anionic, direct or disperse dyes, here based on their application (Hunger, 2007; Christie, 2014).

1.2.1 Dye Classification Based on the Chemical Structure of the Dye

1.2.1.1 Azo Chromophore

Azo compounds have the azo linker (two nitrogen atoms double bonded to each other: N=N) (Fig 1). Each nitrogen atom is bound to another group, which most often is an aryl group. There are dyes with one, two, three and even four azo groups in the molecule. The aromatic rings usually have chloro, hydroxyl, sulphate or nitro groups attached, either to increase the solubility of the dye in water or to enhance its interactions with the substrate. Today, azo dyes are widely used because of their good performance and cost effectiveness.

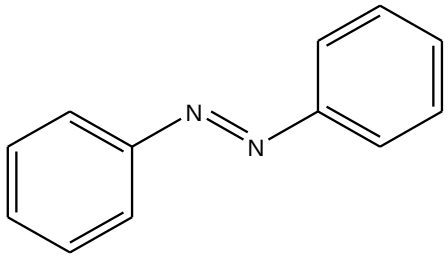

Figure 1: Azo group

1.2.1.2 Anthraquinone Chromophore

Anthraquinone (Fig 2) based compounds are considered to constitute the second most important class of textile dyes after azo dyes. Nevertheless, they do not show the large variety of colours that azo dyes do. In addition, it must be noted that anthraquinone dyes are expensive.

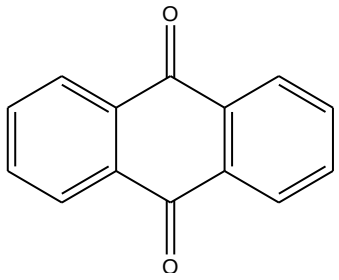

Figure 2: Anthraquinone group

1.2.1.3 Indigoid Chromophore

In 1878, Adolf von Bayer managed to synthesize indigo from phenylacetic acid. Indigo is extensively used to colour denim, popular mostly due to its characteristic of producing gradually fading blue shades (Fig 3).

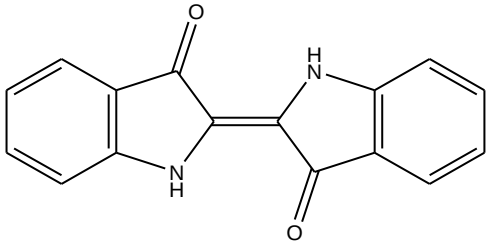

Figure 3: Indigo

1.2.1.4 Polymethine and Related Chromophores

This group of dyes includes aliphatic molecules with conjugated systems (Fig 4), the most well-known representative of which is the β-Carotene, which has a straight conjugated system. However, there are also dyes with aromatic structures in this class. These are used for colouring acrylic fibres and paper. Within this class of dyes, a number of arylcarbenium dyes are used in the basic process (cationic), and there are neutral and anionic dyes.

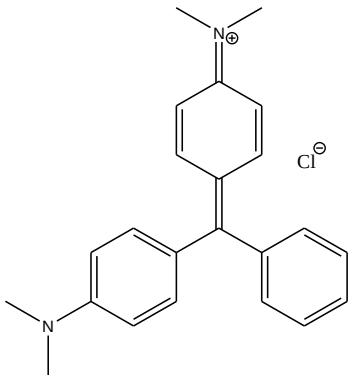

Figure 4: Malachite green, a triaryl carbenium dye

1.2.1.5 Phthalocyanine Chromophore

This group of dyes is formed by molecules exhibiting a macrocycle of benzopyrrole (indole) rings, usually with a metal ion in the centre (Fig 5). Copper phthalocyanine is widely used in plastics, paints and inks, as well as in the textile industry for dyeing and printing. The colours are extremely stable and strong, making them cost effective.

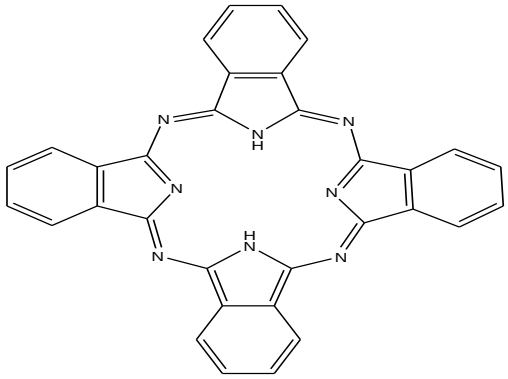

Figure 5: Phthalocyanine

1.2.1.6 Sulphur Compounds and Sulphur Containing Chromophores

Sulphur compounds and sulphur containing chromophores are prepared when sulphur is heated together with aromatic compounds, where sulphur dyes are polymers with heterocyclic rings and thiophenolic sulphur (Fig 6). Sulphur black is used in the textile industry with the highest tonnage of all sulphur containing dyes.

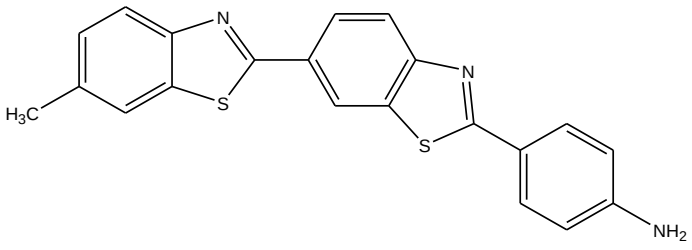

Figure 6: The presumed form of Sulphur dye

1.2.1.7 Metal Complexes and Chromophores

The most used commonly used metals in metal complex dyes are chromium, copper, iron, cobalt and nickel. The most important groups involved in complex formation with the metal ion are the hydroxyl (-OH), carboxy (-CO_2) and amino groups (-NH-).

1.2.2 Classification of Dyes According to Their Usage

According to the application method, dyes can be classified into acidic, basic, direct, mordant, vat, reactive, and disperse dyes (Table 1).

Class	Principal substrate	Application method	Chemical types
Acid	nylon, wool, silk, paper,inks, and leather	usually from neutral to acidic dyebaths	Azo (including premetallized), anthraquinone, triphenylmethane, azine, xanthene, nitro and nitroso
Azoic components and compositions	cotton, rayon, cellulose acetate and polyester	fiber impregnated with coupling component and treated with a solution of stabilized diazonium salt	Azo
Basic	Paper, polyacrylonitrile, modified nylon, polyester and inks	applied from acidic dyebaths	Cyanine, hemicyanine, diazahemi-cyanine, diphenylmethane, triaryl-methane, azo, azine, xanthene, acridine, oxazine, and anthraquinone

Direct	cotton, rayon, paper, leather and nylon	applied from neutral or slightly alkaline baths containing additional electrolyte	Azo, phthalocyanine, stilbene, and oxazine
Disperse	polyester, polyamide, acetate, acrylic and plastics	fine aqueous dispersions often applied by high temperature/ pressure or lower temperature carrier methods; dye may be padded on cloth and baked on/or thermofixed	Azo, anthraquinone, styryl, nitro, and benzodifuranone
Fluorescent brighteners	soaps and detergents, all fibres, oils, paints, and plastics	from solution, dispersion or suspension in mass	Stilbene, pyrazoles, coumarin, and naphthalimides
Food, drugs, and cosmetic dyes	foods, drugs, cosmetics		Azo, anthraquinone, carotenoid and triarylmethane
Mordant	wool, leather, and anodized aluminium	applied in conjunction with Cr salts	Azo and anthraquinone
Oxidation bases	hair, fur, and cotton	aromatic amines and phenols oxidized on the substrate	Aniline black and indeterminate structures
Reactive	cotton, wool, silk, and nylon	reactive site on dye reacts with functional group on fibre to bind dye covalently under influence of heat and pH (alkaline)	Azo, anthraquinone, phthalocyanine, formazan, oxazine, and basic
Solvent	plastics, gasoline, varnishes, lacquers, stains, inks, fats, oils, and waxes	dissolution in the substrate	Azo, triphenylmethane, anthraquinone, and phthalocyanine

Sulphur	cotton and rayon	aromatic substrate vetted with sodium sulphide and re-oxidized to insoluble sulphur-containing products on fibre	indeterminate structures
Vat	cotton, rayon, and wool	water-insoluble dyes solubilized by reducing with sodium hydrogensulfite, then exhausted on fiber and reoxidized	anthraquinone (including polycyclic quinones) and indigoids

Table 1: Summary of the classes of dyes according to their application (Hunger, 2007).

1.3 Adverse Effects of Dye-Loaded Wastewater

Emissions of organic pollutants from industrial activities are a major cause of degradation of water quality. Within this context, the developing countries contribute the largest amount of textile wastewater (World Bank, 2012). Waste water generated in major cities of India is estimated 38,354 million litres per day (MLD), but the sewage treatment capacity is only of 11786 MLD (Kaur, Wani, Sing, & Lal, 2012). Wastewater generation from this sector has been estimated as 55 $x10^6$ m^3 per day, of which 68.5$x10^3$ m^3 are dumped directly into local rivers and streams without prior treatment (MOWR, 2000).

Moreover, about 10% of dyes used in the textile industry are lost during the dyeing process, and 2% are directly discharged as aqueous effluents into the environment. Without adequate treatment, these compounds retain their colour and structural integrity under exposure to sunlight, soil, bacteria and sweat, and exhibit a

high resistance to microbial degradation in wastewater treatment systems. They remain in the environment for longer periods, if discharged without adequate treatment (Soloman, Basha, Velan, Ramamurthi, Koteeswaran, & Balasubramanian, 2009; Baban, Yediler, & Ciliz, 2010; Robinson, McMullan, Marchant, & Nigam, 2001).

Thus, waste materials from textile industries are usually discharged as wastewaters, which are high in colour, have decreased biochemical oxygen demand (BOD), increased chemical oxygen demand (COD), a change in pH, in temperature, and in turbidity and have toxic chemical content (Verma, Dash, & Bhunia, 2012). Also, the release of wastewater from the textile industry to the environment causes aesthetic problems as with the altered color of the water in such water bodies as lakes and rivers local people are affected. Besides this, the accumulation of colour obstructs sunlight penetration, thus further perturbing the ecosystem of the water (Georgiou, Aivazidis, Hatiras, & Gimouhopoulos, 2003). Because of the penetration of the waste into the soil, ground water systems can also be affected by these pollutants (Namasivayam & Sumithra, 2005). Apart from this, several dyes and their metabolites have proved toxic to aquatic life (aquatic plants, microorganisms, fish and mammals (Üstün, Solmaz, & Birgül, 2007).

It is noteworthy that some dyes are mutagenic. Moreover, due to a decrease of light penetration into the water due to the dyes, the photosynthetic activity of the aquatic system is affected (Ogugbue, & Sawidis, 2011). Dye waste effluents from factories can be a direct health risk (WHO, 2000; WHO, 2002). Thus, both sporadic and excessive exposure to colour effluents can make humans more vulnerable to immune suppression, respiratory and circulatory diseases, disorders of central nervous system, including

neurobehavioral disorders. Also, a link of exposure to dye wastes and the occurrence of allergies, autoimmune diseases up to multiple myeloma, leukaemia, and lung oedema has been reported. Other effects can include vomiting, hyperventilation, insomnia, profuse diarrhoea, salivation, and eye or skin infections (Foo, & Hameed, 2010).

Especially high health risk upon exposure to azo dyes have been noted such as of the gastrointestinal tract, skin, and lungs. Hemoglobin adducts with azo dyes with concomitant disturbance of blood formation, caused by the adsorption of azo dyes and their breakdown products have been recorded. Several azo dyes have been noted to cause damage to DNA material that can lead to the genesis of malignant tumors. Electron-donating substituents in ortho and para position to the azo linker can increase the carcinogenic potential of the dye. Some of the commercially used azo dyes (e.g. Direct Black 38, azodisalicylate) and their breakdown products have been found to induce cancer in humans and animals (Carmen, & Daniela, 2012).

1.4 Procedures for the Separation and Elimination of Dyes from Water

The problematic discussed above necessitates that remnant dyes are separated from wastewater. Procedures for the separation and elimination of dyes from water have to satisfy: firstly, those organic dye-wastes are separated from water environment and secondly, that at least a partial or better yet a complete mineralization or decomposition of the organic dye wastes occurs. Separation processes can be based on fluid mechanics (sedimentation, centrifugation, filtration and flotation) or on synthetic membrane separation techniques (micro-, ultra- and nanofiltration, reverse osmosis). Additionally, physico-chemical processes (i.e., adsorption, chemical precipitation, coagulation-

flocculation, and ionic exchange processes) can be used to separate dissolved, emulsified and solid components from the water environment (Babu, Parande, Raghu, & Kumar, 2007; Naveed, Bhatti, & Ali, 2006; Carmen, & Daniela, 2012).

Partial and complete mineralization or decomposition of dyes as pollutants can be achieved by biological and chemical processes. Biological methods are used in connection with activated sludge processes and membrane bioreactors. Chemical processes include the advanced oxidation of dyes with ozone, H_2O_2 which can be run concomitantly under UV-irradiation (Lai, Chen, Chen, Wan, Wen, & Shu, 2014; Wiesmann, Choi, & Dombrowski, 2007). The biological and chemical processes can also be combined.

1.4.1 Physical Treatment Methods for Dye-loaded Wastewater

1.4.1.1 Adsorption

Adsorption techniques have gained favour recently due to their efficiency in the removal of pollutants. Thus, adsorption techniques have been found to be among the most effective and proven treatments of dye-loaded wastewater. It is a rapid process of separation of the adsorbate from the aqueous phase of the waste water, producing a high quality water. It is a process, which is economically feasible (Choy, McKay, & Porter, 1999). This process consists in the transfer of soluble dyes from wastewater to the surface of a solid, highly porous material (the adsorbent). Adsorbents can be of organic or inorganic nature. Inorganic adsorbents are china clay, bentonite clays, silica gel, metal oxides, zeolites and fly ash (Gupta, Sing, Tyagi, Prasad, & Sing, 1992; (Özcan, Erdem, & Özcan, 2004; Zaharia, & Suteu, 2013). Typical natural organic adsorbents

that have been used are peat (Poots, McKay, & Healy, 1976; Viraraghavan, & Mihial, 1995; Bousher, Shen, & Edyvean, 1997) and woodchips (Poots, McKay, & Healy, 1976; Nigam, Armour, Banat, Sing, & Marchant, 2000; Robinson, McMullan, Marchant, & Nigam, 2001)

One of the most used adsorbents is activated carbon. Thus, using activated carbon remains the most commonly used method of dye removal by adsorption (Nassar, & El-Geundi, 1991).

1.4.1.2 Ionic Exchange

Ion exchange process is very effective to remove various heavy metals from wastewater. Ion exchange resins can be easily recovered and reused by regeneration operations (Abo-Farha, Adel-Aal, Ashour, & Garamon, 2009). Ions in solution are transferred to a solid matrix in this process, which can release different types of, but similarly charged ions (Zewail, & Yousef, 2015). It is a physical separation process, where the ions exchanged are not chemically altered. The main advantages of ion exchange are recovery of metal value, selectivity, less sludge volume produced and the meeting of strict discharge specifications. Furthermore, the ion exchange resin can be categorized based on functional groups such as cationic exchange resins, anion exchange resins, and chelating exchange resin (Lee, Kuan, & Chern, 2007)**.**

1.4.1.3 Membrane Processes

Membrane filtration has the ability to work in combination with other effluent treatments. This method is not only restricted to organic contaminants and

microorganisms present in wastewater but to salts membrane filtration has been used for color removal, BOD reduction, salt reduction, polyvinyl acetate (PVA) recovery, and latex recovery, among others. The method is resistant to temperature. The membrane filtration can be detrimentally influenced by microbes. The remaining, concentrated residue after separation can pose removal problems. The technique suffers from high capital cost and has a risk of clogging. Frequent membrane replacement is one more disadvantage of this process. This method is suitable, if the effluent contains a low concentration of dyes. The common membrane filtration types are Micro-Filtration (MF), Ultra-Filtration (UF), Nano-Filtration (NF), and Reverse Osmosis (RO). The choice of the membrane process is influenced by the required quality of the final effluent (Anjaneyulu, Chary, & Raj, 2005; Robinson, McMullan, Marchant, & Nigam, 2001).

1.4.1.3.1 Micro-Filtration

This treatment is suitable for dye baths and rinsing baths, which contain pigment dyes (Babu, Parande, Raghu, & Kumar, 2007). Microfiltration can be used as a pretreatment for nano-filtration or reverse osmosis (Ghayeni, Beatson, Schneider, & Fane, 1998). It can separate suspended solids and colloids, using macromolecules with pores of 0.1 to 1 micron. MF performance leads typically to >90% reduction for turbidity. Usually, microfiltration membranes are made from specific polymers such as poly (ether sulfone), poly (vinylidienefluoride), poly (sulfone), poly (vinylidene difluoride), polycarbonate, polypropylene, polytetrafluoroethylene (PTFE), among others. Ceramic, glass, carbon, zirconia coated carbon; alumina and sintered metal

membranes are used where unusual chemical resistance or high temperature action is required (Naveed, Bhatti, & Ali, 2006).

1.4.1.3.2 Ultra-Filtration

This method can separate macromolecules and particles from water, but usually only 31-76% of dye-stuff in typically dye-containing waste water can be removed by this method. The treated wastewater is not allowed to be reused for sensitive processes, but 40% of such treated wastewater can be reused in the textile industry for rinsing, washing, etc., where salinity of the water is not a big deal. Usually, ultrafiltration is used as a pretreatment for reverse osmosis or in combination with a biological reactor or to remove metal hydroxides (reducing the heavy metal content to 1 ppm or less) (Mignani , Nosenzo, & Gualdi, 1999; Babu, Parande, Raghu, & Kumar, 2007).

1.4.1.3.3 Nano-Filtration

Nano-filtration (NF) is often used to separate effluents from a textile plant. The process has demonstrated its ability to decolorize solutions. NF techniques lead to a sharp reduction in chemical oxygen demand (COD) (up to 94% in a cross flow cell). However, NF modules are extremely sensitive to fouling by colloidal material, macromolecules and polymers. Therefore, extensive pretreatment is required. Almost all NF and RO membranes are thin film composite membranes (Naveed, Bhatti & Ali, 2006; Chakraborti, Purkait, DasGupta, & Basu, 2003).

1.4.1.3.4 Reverse Osmosis

Reverse osmosis (RO is used in reclamation of municipal wastewaters in treatment plants and is used to remove most types of ionic compounds, all mineral salts, hydrolyzed reactive dyes and chemical auxiliaries. Alike NF, RO is very sensitive to fouling and the influent stream must be carefully pretreated. The smaller the pore size of the RO, the higher the operating pressure, the capital investment and the operating costs (Kent, Farahbaksh, Mahendran, Jaklewicz, Liss & Zhou, 2011; Babu, Parande, Raghu, & Kumar, 2007; Naveed, Bhatti, & Ali, 2006).

1.4.1.4 Coagulation-Flocculation and Precipitation

Coagulation is one of the main technologies used in wastewater treatment. It is a complex phenomenon which involves several inter-related parameters. Therefore, it is very critical to state how well a coagulant will function. Basically, in this process small particles are converted into larger aggregates (flocs) and previously dissolved organic matter adsorbs onto the particulate aggregates. Hence, these impurities can be removed in consequent sedimentation/flotation and filtration steps. The coagulation method contains three consecutive steps: coagulant formation, colloid/particle destabilization and particle aggregation. After adding treatment chemicals, the coagulant formation and colloid/particle destabilization can be promoted in a fast-mixing stage. Afterwards, particle aggregation (floc formation) is promoted in a flocculation stage, where interparticle collisions create large floc particles amenable to separation from the treated water. In water and waste-water treatment practice, the terms ‘Coagulation’ is used to describe the initial process whereby the original colloid dispersion is destabilized ,

mostly by charge neutralization and the term ‘Flocculation’ describes the subsequent process whereby the destabilised colloids in the micron and sub-micron size range undergo aggregation and particle growth into millimeter-sized flocs. Since the coagulation stage, and the early phase of the flocculation, occur very rapidly, their distinction in a practical treatment sense has very slight meaning (Zouboulis, Moussas, & Vasilakou, 2008; Jiang & Graham, 1998; Verma, Dash, & Bhunia, 2012).

1.4.1.4.1 Electrocoagulation

Electrocoagulation (EC) is an electrochemical technique related to chemical coagulation. It involves the supply of coagulant ions (Al^{3+}, Fe^{3+}). Coagulant ions are produced by an electric current to a sacrificial anode which is placed into a process tank. The features of the particle aggregates (flocs) generated during the electrocoagulation process differ dramatically from those generated by chemical coagulation. Therefore, flocs generated in an electrocoagulation process has less bound water and more shear resistance and are more readily filterable. Additional advantages of electrocoagulation over chemical coagulation are: the amount of chemicals needed is lower, the salinity of the wastewater does not increase and the economic cost for the treatment is also lower. Furthermore, the gas bubbles generated at the cathode can contribute to the flotation of the flocs, which can be easily recovered. Finally, at the end of the process the generated sludge is separated by filtration (Chen, 2004; Mollah, Morkovsky, Gomes, Kesmez, Parga, & Cocke, 2004) EC has been applied to treat wastewaters containing food waste (Hanafi, Assobhei & Mountadar, 2010), dyes (Martínez-Huitle & Brillas, 2009), oil, suspended particles, etc. (Xu, & Zhu, 2004; Can, Kobya, Demirbas, & Bayramoglu,

2006; Canizares, Martínez, Rodrigo, Jiménez, Sáez, & Lobato, 2008; Canizares, Martínez, Rodrigo, Jiménez, Sáez, & Lobato, 2008)

1.4.2 Chemical treatment

1.4.2.1 Irradiation

The irradiation treatment is a promising technology to eliminate organic contaminants, and disinfect harmful microorganism using gamma rays or electron beams and electron beam accelerators are more suitable for versatility and lower costs.

A high quantity of dissolved oxygen is required for an organic dye to be effectively broken down by irradiation. The dissolved oxygen is consumed very rapidly and so a constant and adequate supply is required. Dissolved oxygen is required to break down the effluents by irradiation . So, a regular and sufficient supply of oxygen is necessary. This process is very important for sanitary engineering (Borrely, Cruz, Del Mastro, Sampa, & Somessari, 1998; Dascalu, Acosta-Ortiz, Ortiz-Morales, & Compean, 2000).

1.4.2.2 Oxidative processes

Chemical oxidation represents the transformation of pollutants by chemical oxidation agents. The modern textile dyes are resistant to mild oxidation conditions such as those existing in biological treatment systems. Therefore, efficient dye and colour removal must be accomplished by more powerful oxidising agents such as chlorines, ozone, Fenton reagents, UV/peroxide, UV/ozone, or other oxidising procedures or

combinations (Guomin, Guoping, Mei, & Yongjian, 2009; Kepa, Stanczyk-Mazanek, & Stepniak, 2008).

1.4.2.2.1 Oxidative Processes with Hydrogen Peroxide

Peroxidases treatment can decolorize of a wide spectrum aromatic dyes from polluted water. Advanced oxidation processes are involved in the preparation of hydroxyl radicals (Glaze, Kang, & Chapin, 1987). Peroxidases can catalyze degradation/transformation of aromatic dyes either by precipitation or by opening the aromatic ring structure. Also, peroxidases have been employed for the remediation of commercial dyes. Dyes were decolorized by the action of peroxidases in the presence of redox mediators (Husain, 2010). It was reported that the H_2O_2/O_3 was used to remove cyanide contamination from drinking water (.Herney-Ramírez, & Madeira, 2010)

1.4.2.2.2 Ozonation Process

Ozonation can cause significant resolubilization of precipitated dyes. Complete removal of dye precipitate should be accomplished prior to treatment of wastewater via ozonation. Nevertheless, the decolorization of seven common textile dyes by the ozonation process has been reported. Higher gas-phase ozone concentrations lead to higher decolorization rates due to more rapid ozone transfer. In general, a greater ozone utilization efficiency was achieved at lower pH levels. Where direct ozone reactions predominate (Adams, & Gorg, 2002). The main advantage of using ozone in water treatment is that ozone can be applied in its gaseous state and therefore does not increase the volume of the wastewater and sludge. A disadvantage of ozonation is its short half-

life, typically being 20 min, the destabilisation by the presence of salts, pH, and temperature, and the additional costs for the installation of ozonation plant (Venkatesh, Quaff, Pandey, & Venkatesh, 2014).

1.4.2.2.3 Oxidation Process with Sodium Hypochlorite

This treatment implies the attack at the amino group of the dye molecule by Cl^+, initiating and accelerating azo-bond cleavage. An increase of chlorine concentration favors the dye removal and decolorization process, as does the decrease of pH of the medium. Dyes containing amino or substituted amino groups on a naphthalene ring (i.e., dyes derived from aminonaphtol- and naphtylamino-sulphonic acids) are most susceptible to chlorine decolorization (Omura, 1994; Hamada, Nishizawa, Yoshida, & Mitsuishi, 1998). This treatment is unsuitable for dispersive dyes, and is becoming less frequently used due to the negative effects of releasing toxic aromatic amines into watercourses (Slokar, & Le Marechal, 1998).

1.4.2.2.4 Photochemical Oxidation Process

The combination of H_20_2/UV constitutes an attractive process for the oxidative degradation of organic pollutants dissolved in aqueous systems. The use of hydrogen peroxide as an oxidant has great advantages in contrast to other methods of chemical or photochemical water treatment. The oxidant is commercially availabile, thermally stable and has infinite solubility in water. Moreover, there are no mass transfer problems as seen with gases. Two hydroxyl radicals are formed for each molecule of H_20_2 photolyzed. However, there are also obstacles encountered with the H_2O_2/UV process.

The rate of chemical oxidation of the contaminant is limited by the rate of formation of hydroxyl radicals. As a result, the small absorption cross section of H_20_2 at λ = 254 nm is found to be a real disadvantage, especially, when the organic substrates will act as inner light filters. Reactive hydroxyl radicals are the main disadvantage of all oxidative degradation processes (Legrini, Oliveros, & Braun, 1993; Drogui, Elmaleh, Rumeau, Bernard, & Rambaud, 2001).

1.4.2.2.5 Electrochemical Oxidation Process

The electrochemical treatment of dye-containing effluents is a promising technique (Charoensri, Kobayashi, Kimura & Ishii, 2006). This technique offers an alternative solution to many environmental problems in the process industry, because electrons provide a versatile, efficient, cost-effective, easily automatable, safe and clean reagent (Contaminant, 2014; Saratale, Saratale, Parshetti, Chang, & Govindwar, 2009).

1.4.3 Biological Treatments

There are different biological treatments, performed under aerobic or anaerobic or combined anaerobic/aerobic conditions. The processing, quality, adaptability of microorganisms, and the reactor type are key parameters for removal efficiency (Reemtsma, & Jekel, 2006; Cardenas-Robles, Martinez, Rendon-Alcantar, Frontana, & Gonzalez-Gutierrez, 2013). Biological treatment systems can be used in combination with chemical processes.

1.5. Activated Carbon as Sorption Material in Adsorption Processes

Activated carbons are the most versatile and frequently used adsorbents, and activated carbons are widely used for purifying contaminated water. Their large internal surface area and pore volume, their ability to adsorb most dye pollutants and the low cost associated with them make activated carbons one of the most practical adsorbents Although carbon materials, especially carbon nanomaterials, can be synthesized by decomposition of alkanes and cycloalkanes (Ismadji, & Bhatia, 2001) or by using acetylene as the carbon source (Ramón, Gupta, Corbet, Ferrer, Movva, Carpenter, & Banerjee, 2011; Kasi, Kasi, Bokhari, & Afzulpurkar, 2013), the usual source of activated carbon are lignocellulose containing organisms (Nor, Lau, Lee, & Mohamed, 2013). Activated carbons derived from different plant sources have been used for the removal of dyes from wastewater. Some of these sources are agricultural wastes. A typical such source is bagasse, which is an agricultural/industrial by-product produced in large amounts by sugarcane mills. Bagasse is a cost-effective material and it has an inherent ability to adsorb waste chemicals such as dyes from aqueous systems (Singh & Tiwari, 2001).

Removal of dyestuff from aqueous solutions using bagasse was studied extensively (Duri, McKay, Geundi, & Wahab, 1990; Nassar, & El-Geundi, 1991; McKay, El-Geundi, & Nassar, 1997). Bagasse fly ash has also been used for the removal of colorants and dissolved organics from sugar mill effluent (Mall, Mishra, & Mishra, 1994; Kattri, & Singh, 1999). Applied bagasse as an adsorbent for the removal of malachite green from aqueous solutions. Monolayer adsorption of malachite green at

alkaline pH was observed as bagasse contains various oxides and hydroxylated species on the surface (Sing, & Tiwari, 2001). All these studies prove the utilization of a waste to treat another waste.

Other agricultural waste substrates for activated carbon that have been used are *neem* leaf powder, wheat straw, corn-cob, tree bark, rice husk, coconut shell powder, and ground sunflower seed shells. The activated carbons derived from the above have been used for the removal of dyes and organic colored matter from effluents (Bhattacharyya, & Sarma, 2003; Nigam, Armour, Banat, Singh, & Marchant, 2000; Anjaneyulu, & Hima Bindu, 2001b; Cazetta, Vargas, Nogami, Kunita, Guilherme, Martins, & Almeida, 2011).

Mixed adsorbent (oxygenated coconut shell activated carbon-fly ash-china clay) has been found to be very effective for the removal of basic dyes such as brilliant blue (BB 69) and brilliant red (BR 22) from industrial effluents (Anjaneyulu, & Hima Bindu, 2001b). Maximum removal of dye (98%) was achieved with mixed adsorbent (Nassar & El-Geundi, 1991; Raghavacharya, 1997; Anjaneyulu, Chary, & Raj, 2005). The removal of colour from combined pulp and paper mill effluent using bamboo dust carbon was found to be very effective at 99% at pH<7 and 3.1 g/l carbon dose with 2 h contact time (Bhattacharyya, & Sarma, 1997).

Zhang and Chuang (2001) reported that in their study that activated carbon removed colour effluents from a Kraft pulp mill at high pH. It was also observed that adsorption capacity of activated carbon is twice that of fly ash. It was suggested that powdered activated carbon could be used as an adsorbent for the pre-treatment for

subsequent biological processes, which resulted in an increased BOD_5/COD ratio besides removing color-causing organics (Ahn, Chang & Yoon, 1999). Adsorption on to activated carbon cloth (ACC) can be used as an alternative remediation water with residual color and low molecular weight dyes, which were found to be well adsorbed onto ACC (Pignon, Brasquet, & Le Cloirec, 2000; Babić, Milonjić, Polovina, & Kaludierović, 1999).

1.6 Purpose and Scope of This Work

In every country, the economy plays a vital role. So, if one would like to use adsorbents for effluent treatment, then one would need to find out low-cost adsorbents, where materials that would find little use otherwise would be best.

The Arabian Peninsula as an arid region has limited sources of thus far non-used agricultural wastes. One such non-used agricultural waste are date palm leaves. Date palms belong to the family *Palmae,* of genus *Phoenix,* species *dactylifera*. Mainly, they are grown in the Gulf States and on the Mediterranean coast. *Phoenix dactylifera* has been cultivated since prehistoric times in most of the Gulf, South-Asian and African countries. There are currently over 44 million date palms in the United Arab Emirates (UAE) that can be grouped into 199 different varieties, of which 8.5 million are in the Al Ain region. Together, they produce ~1 million tons of palm leaves annually, as agricultural waste. The common practice to get rid of these wastes is by burning, which causes a potential pollution impact on the environment. The date palm leaves (*Phoenix dactylifera*) as plant material possess cellulose (33.5%), hemicellulose (26%) and lignin (27%), as main components (Bendahou, Dufresne, Kaddami & Habibi, 2007). So, the

date palm leaflets can be used in the preparation of activated carbons for the removal of dyes.

While the United Arab Emirates does not have a very significant textile or leather industry, it is still of interest for the United Arab Emirates to develop the technology in this area and export this technique to other regions.

The aims of the work underlying this thesis are:

- To prepare activated carbons (using different activation methods) from date palm leaflets and utilize the carbons to adsorb dyes from aqueous solutions.
- To characterize the prepared activated carbon (AC) by available techniques (eg. by SEM, BET, FT-IR, TGA).
- To carry out sorption studies of different types of dyes on the prepared activated carbons

  i.) in batch experiments

  ii.) in dynamic experiments (continuous flow experiment)
- To model the sorption process
- To recycle the sorbent material and regenerate the spent adsorbent to be used in further cycles of adsorption.

Chapter 2: Methods

2.1 Preparation of Adsorbent

Naturally collected date palm leaflets from the United Arab Emirates University Campus at Maqam, Al Ain, Abu Dhabi, were cut into small pieces, and were washed 8-10 times with deionized water and air-dried for 24 h. The dried small pieces were soaked either in 25% (w/w) H_2SO_4, 5M HNO_3, 10M HNO_3, 15M HNO_3 or 5M H_3PO_4, 10M H_3PO_4 for 24 hours. The mixture was filtered using a porcelain Buchner funnel under vacuum. For carbonization, the impregnated leaves were washed with distilled water 8-10 times and were then kept in an oven (CARBOLITE) for 24 h at 250°C ± 1°C for the HNO_3 and H_3PO_4 impregnated leaves and for 5h, 10, 15, 20, 24 h at 250°C ± 1°C for the H_2SO_4 impregnated leaves.

The activated carbon was allowed to cool to room temperature and repeatedly washed with deionized water and 1% aq. $NaHCO_3$, respectively, until the pH of the supernatants remained constant at around pH 6.0 (pH-meter Orion 410 A+). Then, the obtained activated carbon was dried at 40 – 45 ^{o}C for 2 h to remove residual moisture, ground and sieved by standard steel meshes (Laboratory Test Sieves from Endecotts: apertures: 710 μm, 425 μm, 300 μm) to select particles between 300 μm and 425 μm in size.

The carbon was then stored in dry, clean and well closed polyethylene bottles for further use. Infrared spectra (Shimadzu IRPrestige 21 FT-IT spectrometer, measured as KBr pellets) were taken for the carbons activated at different temperatures. The weight-loss of the carbons was determined. The pH values of the activated carbon in deionized

water were measured. The surface area of the activated carbon was estimated from absorption isotherms.

2.2 Sorbates

Two dyes, namely Crystal Violet (CV) and Nile Blue (NB), were used in these studies as two single components (Fig. 7&8) respectively of CV and NB.

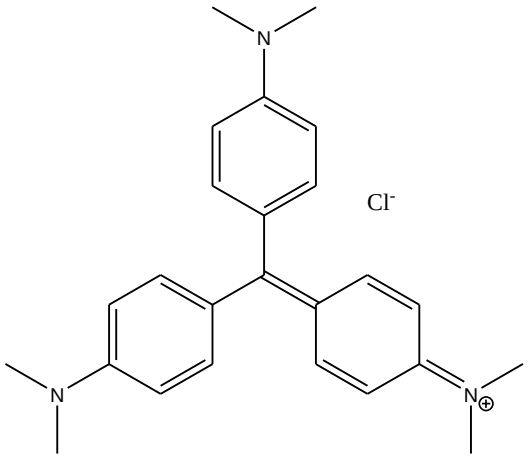

Figure 7: Chemical structure of Crystal Violet (CV)

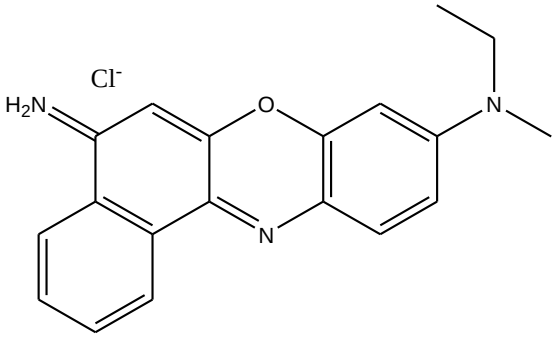

Figure 8: Chemical structure of NB

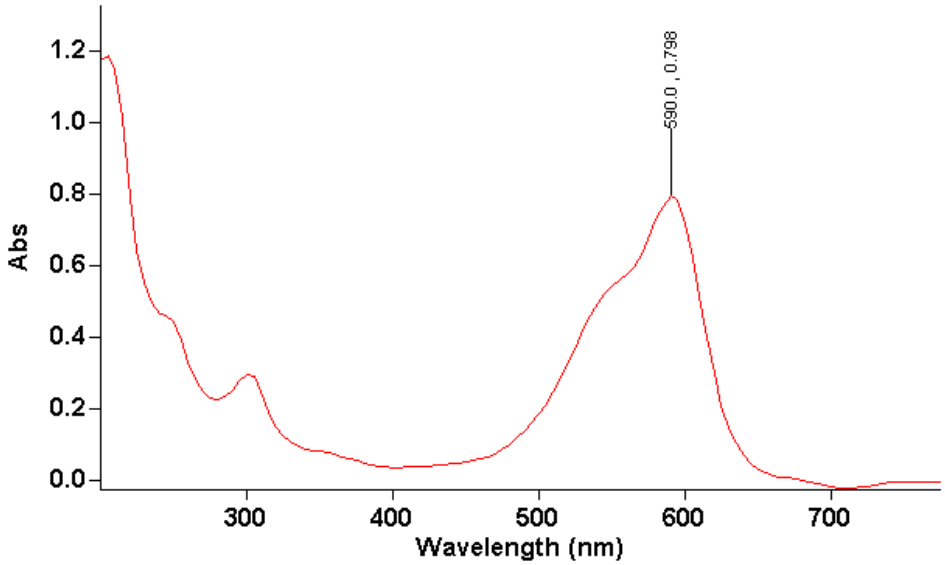

Figure 9: Absorbance of crystal violet (CV) at λ = 590nm (30 ppm CV), spectrum measured on a Cary 50 Conc. VARIAN UV-VIS spectrophotometer in water

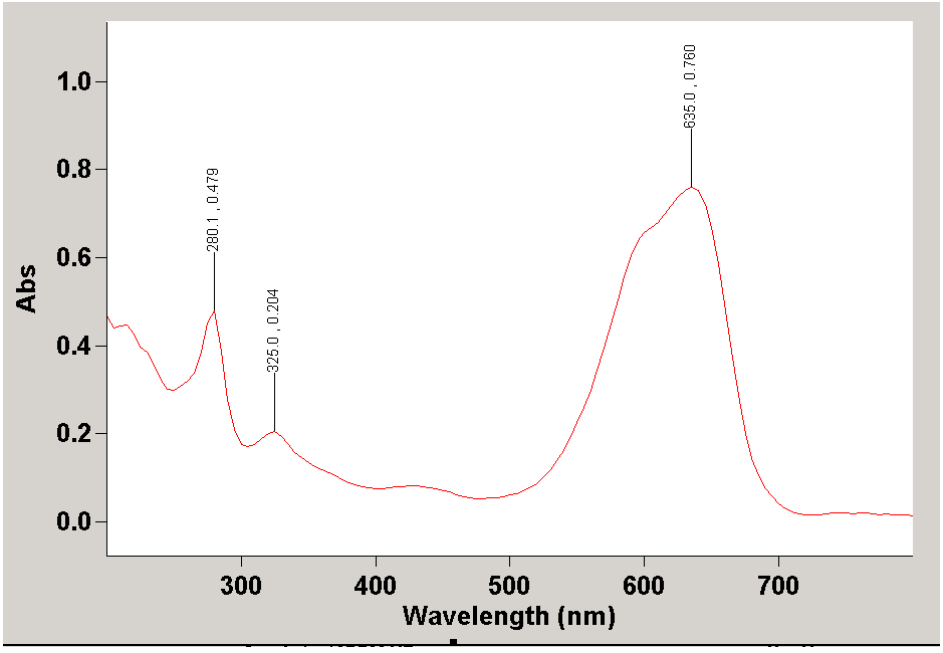

Figure 10: Absorbance of NB at λ = 635 nm (40 ppm NB), spectrum measured on a Cary 50 Conc. VARIAN UV-VIS spectrophotometer in water.

2.3 Preparation of the Dye Solution

A stock solution of dye (CV, NB, 1000 ppm) was prepared by dissolving 1 g of dye in distilled water and then making the volume up to 1000mL with water. It was stored in a volumetric flask for making other dilute solutions. Samples of different dye concentrations were prepared by dilution from the stock solution. Typically, solutions of 5 ppm, 10 ppm, 15 ppm, 20 ppm, 25 ppm, 30 ppm, 35 ppm, 40 ppm, 45 ppm, 50 ppm (for CV) and of 5 ppm, 10 ppm, 15 ppm, 20 ppm, 25 ppm, 30 ppm, 35 ppm, 40 ppm, 45 ppm, 50 ppm, 75 ppm and 100 ppm (for NB) were prepared. These solutions were used for constructing calibration curves and for kinetic and equilibrium studies.

2.4. Kinetic and Equilibrium Studies

2.4.1 Batch Experiments

The assessment of a solid-liquid adsorption system is usually based on two types of investigations: batch adsorption tests and dynamic continuous-flow adsorption studies.

Batch studies use the fact that the adsorption phenomenon at the solid/liquid interface leads to a change in the concentration of the adsorbate (ie., the dye to be studied) in the solution. Adsorption isotherms are constructed by measuring the concentration of adsorbate (dye) in the medium before and after adsorption, at a fixed temperature. For this, in general, adsorption data including equilibrium and kinetic studies are performed using standard procedures consisting of mixing a fixed volume of dye solution with a known amount of adsorbent (i.e. of activated carbon) under

controlled conditions of contact time, agitation rate, temperature and pH. At predetermined times, the residual concentration of the dye is determined by spectrophotometry using the maximum absorption wavelength of the dye. Dye concentrations in solution can be estimated quantitatively, generally according to Lambert-Beer law (which describes the linear relation between light absorbance and concentration of light-absorbing material: A = ε l c, where A = absorbance, c = concentration of the light absorbing material, and l = length of the pathway of light through the light absorbing material), using linear regression equations obtained by plotting a calibration curve for each dye over a range of concentrations. The adsorption capacity (adsorption uptake rate) is then calculated and is usually expressed in milligrams of dye adsorbed per gram of the adsorbent. For example, the amount of dye adsorbed at equilibrium, Q_e, is calculated from the mass balance equation given by Eq. 1

$$\mathbf{Qe} = \frac{\mathbf{V(C_0 - C_e)}}{\mathbf{m}} \qquad (1)$$

Where Co and Ce (in mg/L) are the initial and equilibrium dye concentrations, respectively. V (L) is the volume of dye solution and m is the mass of the dry adsorbent (in grams).

The equilibrium relationship between adsorbate in solution and adsorbed material is a fundamental characteristic of interest for the design of adsorption systems and can be described by adsorption isotherms, using different adsorption models available. The equilibrium adsorption isotherm gives an idea of the capacity of the adsorbent for the specific adsorbate under study. In the literature, batch methods are widely used to describe the adsorption capacity and the adsorption kinetics. These

processes are cheap and simple to construct and, consequently, often favoured in small- and medium-size process applications, using simple and readily available mixing tank equipment. Simplicity, well-established experimental methods, and easily interpretable results are some of the important reasons frequently evoked for the extensive usage of these methods. Another interesting advantage is the fact that, in batch systems, the parameters of the solution such as adsorbent concentration, pH, ionic strength, and temperature can be controlled and/or adjusted (Crini, & Badot, 2008).

In this thesis, adsorption equilibrium studies were performed by adding a fixed amount of activated carbon to a fixed volume of an aq. solution of CV and NB dye at different initial concentrations. The samples, contained in glass beakers, were agitated at different temperatures for a determined period in a shaker (LAB-LINE ORBIT ENVIRON-SHAKER). The adsorbent was then separated using a BECKMAN model TJ-6 centrifuge at 5000 rpm. The adsorbence of the supernatant dye was measured using a Cary 50 Conc. VARIAN spectrophotometer.

2.4.2 Dynamic Adsorption Studies

The performance of fixed-bed adsorption was complemented by dynamic studies. The efficiency of adsorbent materials for removing adsorbate from waste water of larger quantity can be studied with a dynamic adsorption system using a fixed-bed column loaded with adsorbent. From this study, we can determine the breakthrough and the running time of the column (before exhaustion) of the column. The breakthrough curves show the loading behavior of adsorbates to be removed, and is usually expressed in terms of adsorbed concentration (C_{ad}), inlet concentration (C_0), outlet concentration

(C_t) or normalized concentration of the adsorbate, defined as the ratio of outlet concentration to inlet concentration (C_t/C_0) as a function of time or volume of effluent for a given bed height.

The desired breakthrough concentration was determined as 10% of the inlet concentration, and the time required to reach the breakthrough point is defined as the breakthrough time. From the integration of the area under the breakthrough curve, using by eq. xx, we obtain the total capacity (q_{total}):

$$q_{total} = \frac{QA_c}{1000} = \frac{Q}{1000}\int_{t=0}^{t=t_{total}} C_{ad}\,dt \qquad (2)$$

Where Q is the volumetric flow rate (mL/min) and t_{total} is the total flow time (min) until breakthrough. The equilibrium bed capacity (q_{eq}) is derived as the total quantity adsorbed (q_{total}) per weight of adsorbent (W, in g):

$$q_{eq} = \frac{q_{total}}{W} \qquad (3)$$

In this thesis, the dynamic adsorption studies were conducted in a stainless steel adsorption column, with an inner diameter of 0.4 (cm) and 14 (cm) in height. At the bottom of the column, a stainless sieve was attached, followed by a layer of glass beads (0.5 g). Above the activated carbon was placed cotton and above that again glass beads (0.5 g) to weigh down the assemblage. The influent was pumped from the bottom through the column to avoid channelling due to gravity. The effluent was collected at regular time intervals and the concentration of dye in the effluent was measured by UV-

VIS spectrophotometry (Cary 50 Conc. VARIAN spectrophotometer). A peristaltic pump (MASTERFLEX C/L from Coll Parmer) was used with a flow rate of 0.88 ml/min. The flow rate was measured periodically to maintain the desired flow rate during the experiment. The experiments were performed at room temperature.

Chapter 3: Results and Discussion

3.1 Preparation of Activated Carbons from Date Palm Leaves

To prepare the activated carbon, the date palm leaves (dried, washed, dried and cut) were immersed in aq. mineral acids. After a given amount of time the aqueous solution was decanted and the remaining solid material was filtered off using a Buchner porcelain funnel or a kitchen mesh. The derived biomass was coarse enough to use these filters. Sintered glass filters tended to clog. In the case of impregnation with H_2SO_4 and HNO_3 of higher concentration (18 M H_2SO_4 and 15.6 M HNO_3) the treated leaves lost all consistency and could not be filtered off. The filtered, impregnated leaf mass was washed diligently with distilled water (8-10 times). Then, the leaves were transferred into a large glass beaker and heated in an oven at 250 ^oC.

To study the effect of heating time, the weight of activated carbon was recorded at different intervals at 250^0C for H_2SO_4 impregnation. The heating time was 5h, 10h, 15 h and 25 h, respectively. The percentage of weight loss increased with the increase of heating time. The result showed that the percentage of weight loss of AC increased with time, from 14 % after 5h to 67% after 25 h (Table 3, Fig 11). Interestingly, the weight loss significantly increases after 20h. This may be due to initial oxidation and functionalization of the carbon and subsequent rapid burn-off. Nevertheless, it must be noted that the adsorption capacity of the activated carbon heated at times less than 20h is less than the activated carbon heated for 25h, indicating that the burn-off might open pores on the carbon surface.

The same scenario was seen for carbons impregnated with HNO_3 acid of different molarity. Weight loss also increased with increasing molarity of the acid used for impregnation. The weight loss increased from 52% with 5M HNO_3 to 72% with 15.6M HNO_3 (Table 4, Fig 12).

Ash content determination of the leaves and the activated carbons was carried out be heating the samples for 24h. The ash content of the leaves was found to be 16.5w%. The ash content of AC-H_2SO_4 was found to be 25.2w%.

Activation method	Contact time (h)	Size of AC (μm)	Name of Activated Carbon	Temperature (^{0}C)
H_2SO_4	24	<300	AC-H_2SO_4	250
HNO_3		300	AC-HNO_3	
H_3PO_4		425	AC-H_3PO_4	
		710		

Table 2: List of activation methods used with the labelling of the activated carbons, subsequently used throughout the text

Time (h)	Weight loss of leaves (%)	Activation method
5	14.2	H_2SO_4
10	21.5	
15	24.8	
20	34.3	
25	67	

Table 3: Weight loss of activated carbon with different contact times

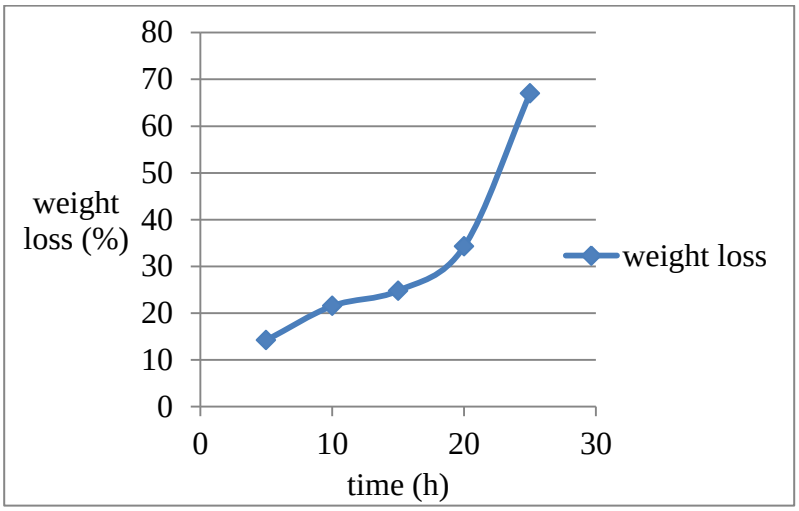

Figure 11: Weight loss of activated carbon versus activation time using 25w% H_2SO_4

Molarity (M)	weight loss (%)	Activation method	Activation time (h)
5	52	HNO_3	24
10	66		
15.6	71.9		

Table 4: Weight loss of AC treated with HNO_3 of different molarity (heated at 250 ^oC)

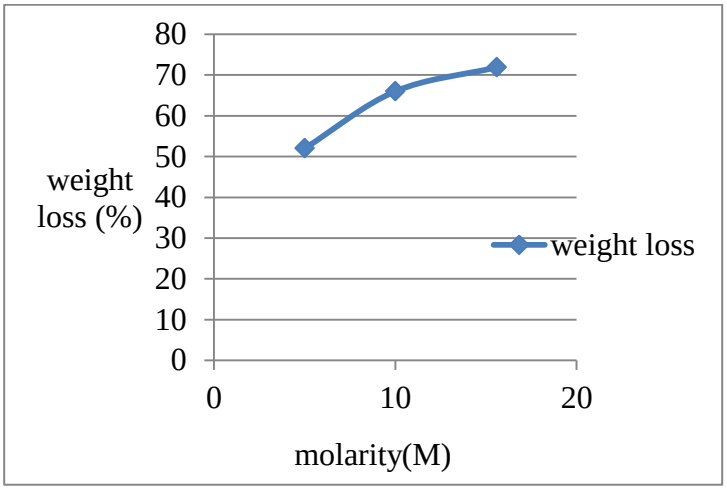

Figure 12: Weight loss of AC treated with HNO_3 of different molarity (heated at 250 ^oC)

molarity for different acid(M)	weight loss	Activation method
4.5	67	H_2SO_4
10	66	HNO_3
10	35	H_3PO_4

Table 5: Weight loss of AC treated with different types of acid

Time (h)	removal efficiency %
5	4.2
10	4.2
15	7.6
20	19.5
24	48

Table 6: Effect of heating time (250 ^{o}C, with carbon impregnated with 25w% H_2SO_4) on the adsorption capacity of the neutralized AC, measured as the removal efficiency (%) of crystal violet [CV] (25 ppm CV, 50 mg AC)

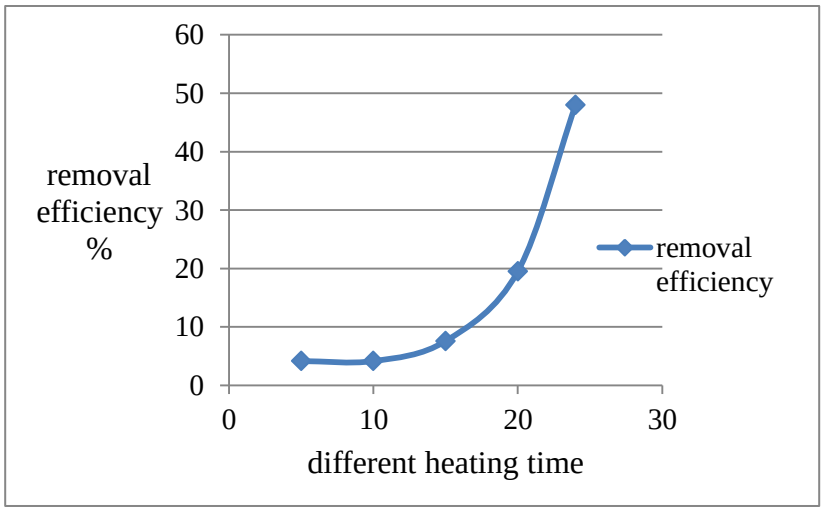

Figure 13: Effect of heating time (250 ^{o}C, with carbon impregnated with 25w% H_2SO_4) on the adsorption capacity of the neutralized AC, measured as the removal efficiency (%) of crystal violet [CV] (25 ppm CV, 50 mg CV, 50 mg AC).

To study the effect of heating time on the adsorption capacity of the AC, the equlibrium adsorption was recorded for different heating time's intervals. The percentage of removal efficiency is increased with the increase of heating time (Fig 13). The result showed that percentage of removal efficiency increases from 4.1% to 48% with increasing the heating time from 5 h to 25 h.

The activated carbons thus prepared were neutralized with sodium bicarbonate (2w% aq. $NaHCO_3$ for AC for 10M H_3PO_4, 15.6 M HNO_3 and 18M H_2SO_4 impregnated AC, 1w% aq. $NaHCO_3$ for 25w% H_2SO_4, 5M and 10 M HNO_3).

3.2 Characterization of AC

The differently activated carbons were submitted to IR spectroscopy (as KBr pellets). All carbon samples showed a strong absorption in the region of 1100 cm^{-1}. This absorption is very typical for activated carbons in general and has been ascribed to either a C-O stretching vibration or to a Si-O vibration, which may be due to inorganic silicates in the palm leaf (and therefor activated carbon) sample. In all cases, we have a broad O-H stretching vibration which may be partially attributed to moisture, but partially also to OH groups that may be found on the surface of the carbon. In Fig 15 and 16, but especially in Fig. 17 and 18, we find C-H stretching bands. Fig. 17 and 18 show small bands 600 – 800, which may be attributed to in-plane and out-of-plane aromatic deformation vibrations as well as CH bending modes.

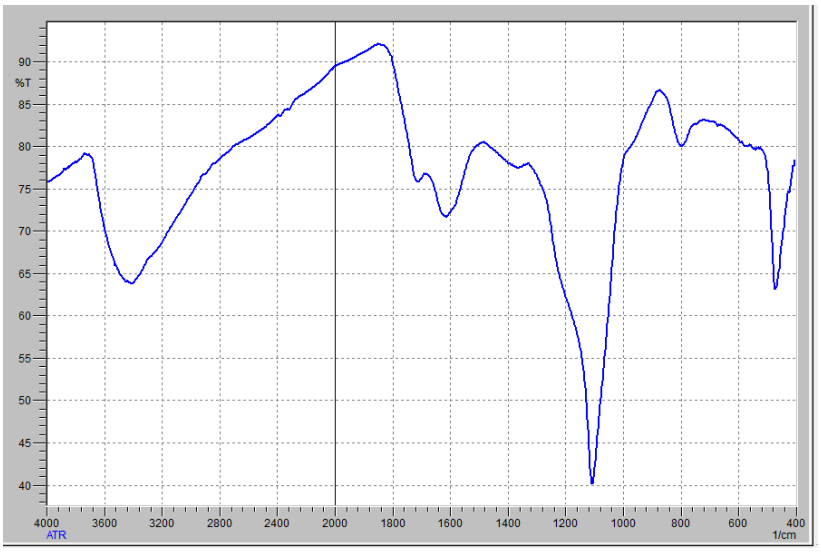

Figure 14: IR –spectrum of AC-H_2SO_4 (300 μm)

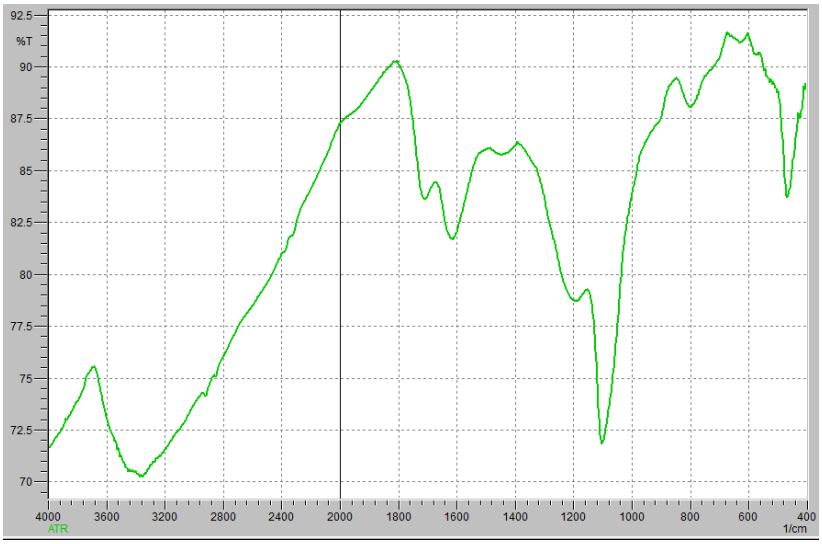

Figure 15: IR –spectrum of AC-H_3PO_4 (300 μm)

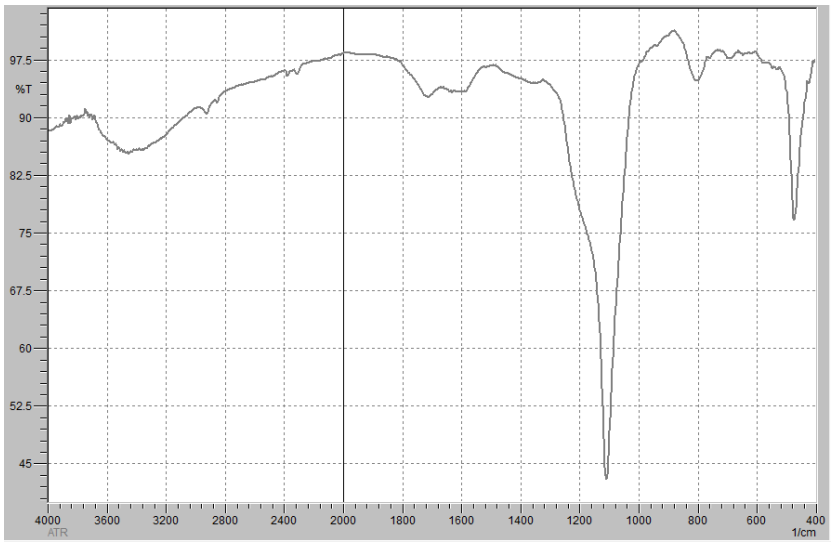

Figure 16: IR –spectrum of AC-HNO_3 (300 μm)

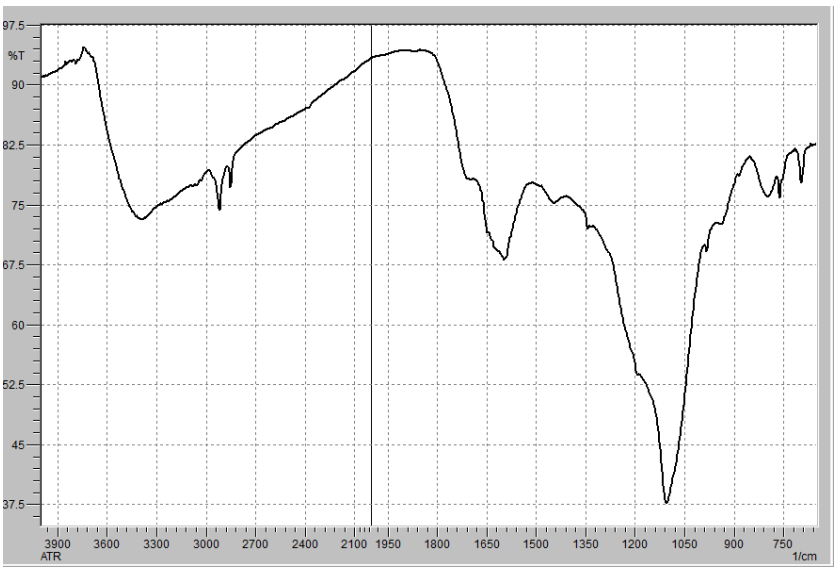

Figure 17: IR-spectrum of AC-H_3PO_4 (425 μm)

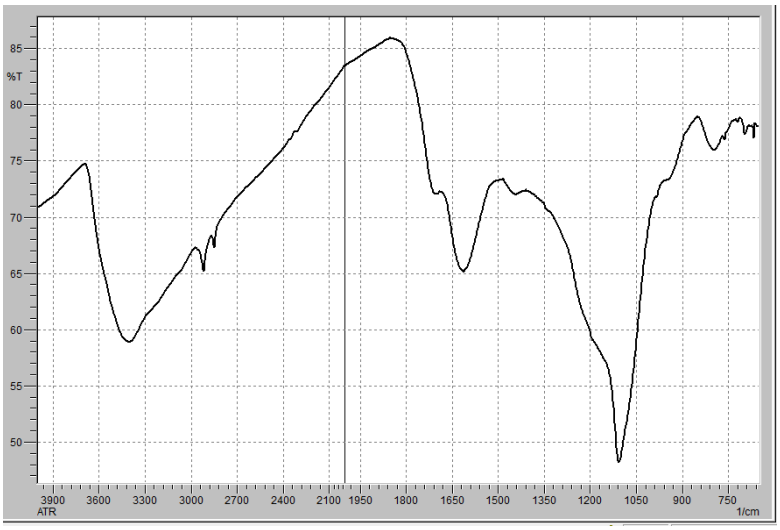

Figure 18: IR-spectrum of AC-H_3PO_4 (710 μm)

The surface area was determined for the activated carbon by Brunauer-Emmett-Teller analysis BET (QUANTA CHROME-NOVA 1000). The surface area (S_{BET}) of AC were found 20.5 m^2g^{-1}, 8.5 m^2g^{-1}, 53.84 m^2g^{-1} for AC-HNO_3, AC-H_2SO_4 and AC-H_3PO_4 (all 425 μm particle size), respectively. This study shows a higher surface area for phosphoric acid treatment of date palm leaflets.

3.3 Adsorption Studies

3.3.1 Introduction

For the adsorption studies, two dyes were chosen, namely crystal violet (CV) and Nile blue (NB). Crystal violet (CV) is also known as basic violet 3, gentian violet, and methyl violet 10B. Its IUPAC name is *N*-[4-[bis [4-dimethylamino)-phenyl]-methylene]-2, 5-cyclohexadien-1-ylidine]-*N*-methylmethanaminium chloride (of the molecular formula $C_{25}H_{30}N_3Cl$ and with the molecular weight 407.98). It belongs to the

class of triaryl methane dyes. The absorption maximum is at λ = 589 - 594 nm in aqueous solutions.

CV is used as a pH indicator (yellow [acidic] to violet with the transition at a pH 1.6). In the medical community, it is the active ingredient in Gram's stain, and is employed as a bacteriostatic agent. It prevents fungal growth in poultry feed (Al-Kadhemy & Abbas, 2013; Lin & Chen, 1995). Crystal violet dye is also widely used in animal and veterinary medicine as a biological stain (Saeed, Sharif & Iqbal, 2010).

CV is a typical cationic dye and belongs to the class of triaryl methane dyes, extensively applied for dyeing nylon, wool, silk, leather, and cotton in textile industries. It also finds applications in paints and printing inks (Ma, Song, Pan, Cheng, Xin, Wang, & Wang, 2012; Mittal, Mittal, Malviya, Kaur, & Gupta, 2010). Crystal Violet is harmful by inhalation, ingestion and skin contact, and has also been found to cause cancer and severe eye irritation to human beings. It is poorly degraded as recalcitrant molecule by microbial enzymes, and can persist in a variety of environments. Only a few reports noted degradation of Crystal Violet by microbial organisms. Crystal Violet (CV) was found to be adsorbed successfully from water by montmorillonite (MMT) and iron modified montmorillonite (MMT-Fe) has been used as a catalyst to degrade it in a Fenton-type process. Adsorption of Crystal Violet (CV) onto NaOH modified rice husk (Chakraborty, Chowdhury, & Saha, 2011). Activated carbons derived from male flowers of the coconut tree, palm kernel fibers (PKF), coniferous pine bark powder (CPBP), grapefruit peel (GFP), bottom ash (BA), powdered mycelial biomass of *Ceriporialacerata* P2, acid-activated sintering process red mud (ASRM), a power plant waste, and de-oiled soya (DOS) were used to remove crystal violet (Ahmad,2009;

Mittal, Mittal, Malviya, Kaur, & Gupta, 2010; Saeed, Sharif, & Iqbal, 2010; Senthilkumaar, Kalaamani, & Subburaam, 2006; El-Sayed, 2011; Lin, He, Han, Tian, & Hu, 2011; Zhang, Zhang, Guo, & Tian, 2014).

The molecular formula of Nile Blue (9-(diethylamino)benzo[a]phenoxazin-5-ylidene]azanium chloride) is $C_{20}H_{20}ClN_3O$, and its molar mass is 353.845 g/mol. Nile blue is a fluorescent dye. It is used as a stain in biology and histology. It has been used for fluorescence resonance energy transfer (FRET) studies (Maliwal, Kuśba, & Lakowicz, 1995; Lakowicz, Piszczek, & Kang, 2001). Also, this dye has been used to monitor events which depend on solvent polarity (Lee, Suh, & Li, 2003; Das, Jain, & Patel, 2004; Krihak, Murtagh, & Shahriari, 1997). Nile Blue tends to have a higher affinity for cancerous cells than healthy ones (Nikas, Foley, & Black, 2001) and it is a photosensitizer for oxygen (Lin, Shulok, Wong, Schanbacher, Cincotta, & Foley, 1991). These two properties together can be useful in photodynamic therapy. However, two properties of Nile Blue in aqueous media are limiting for many applications, specifically 1) low solubility and 2) low quantum yield. Nile blue changes its color (from blue to red) in the region of pH 10.1 – 11.1.

Adsorption of Nile blue from aqueous solutions using residue acid mixture obtained from dimethyl terephthalate distillation residue, natural clay, copolymers of acrylamide and mesaconic acid (CAME), sulfonated phenol-formaldehyde resin, activated sludge, acrylamide-maleic acid hydrogels have been studied (Güçlü, 2010; İyim, & Güçlü, 2009; Üzüm, & Karadağ, 2006; İyim, Acar, & Özgümüş, 2008; Mihara, Inoue, & Yokota, 2005; Saraydin, Karadağ, & Güven, 1996). Another derivatives of

Nile blue is Nile Blue sulphate. It was adsorbed on alumina from aqueous solution (Saleem, Afzal, Mahmood, & Hameed, 1994).

3.3.2 Adsorption studies – General Procedures

At the beginning, the adsorption of both dyes CV and NB were studied using all types of activated carbon produced above by adding a certain amount of AC to a solution of dye (50 mL) of different concentrations. The mixtures were shaken using a LAB-LINE ORBIT ENVIRON-SHAKER. Samples were taken at different intervals and the residual concentration of dye in the supernatant.

The following experiments were carried out with both dyes:

3.3.2.1 Determination of the effect of the dose of AC on the adsorption

3.3.2.2 Determination of the effect of the initial concentration of dye with a fixed dose of AC

3.3.2.3 Comparison experiments using differently activated carbons (ACs)

3.3.2.4 Comparison experiments using activated carbons of different mesh size

3.3.2.5 Determination of the effect of the pH of the solution on the adsorption of the dyes studied.

3.3.2.1 Determination of the Effect of the Dose of AC on the Adsorption (Dye Removal Efficiency)

Firstly, the effect of dosage of AC on the dye removal from the aqueous solutions was studied. The determination of AC dosage is important because it determines the efficiency of dye removal and may also be used to predict the cost of AC per unit of solution to be treated. As expected, the efficiency of dye removal increases

significantly as adsorbent dosage increases. The effect of dose of adsorbent on the percentage removal of CV and NB dye is shown in (Fig. 19). The graph indicates that already 0.1 g of AC leads to 100% for CV and 90% for NB. 0.2 g of AC leads to virtually quantitative removal of both CV and NB (1.25 mg [3.1 μmol] CV, 2.25 mg [6.35 μmol] NB). At this point the adsorption is 6.25 mg CV per g of AC and 11.2 mg NB per g of AC. It was also noted that the time required to reach equilibrium decreased at higher doses of adsorbent.

The percentage of dye removal was calculated using the following relationship:

$$\%Removal\ of\ dye = \frac{C_0 - C_e}{C_0} \times 100 \quad (4)$$

Where C_o and C_i are the initial and final (equilibrium) concentrations of the dye (mgL^{-1}), respectively.

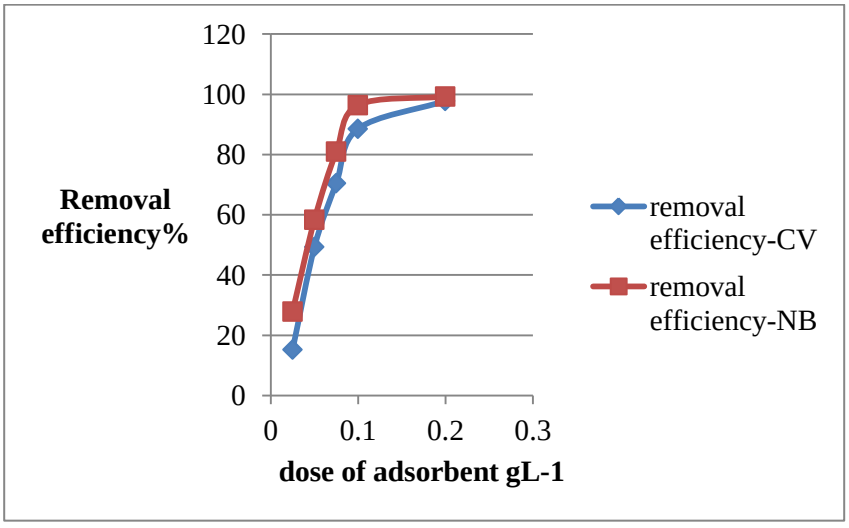

Figure 19: Effect of dose of adsorbent on the removal efficiency of dyes (CV 50 mL of 25 ppm solution, NB 50 mL of 45 ppm solution)

3.3.2.2 Determination of the Effect of the Initial Concentration of Dye with a Fixed Dose of AC

The effect of initial concentration of CV and NB dye on the removal by AC was studied as shown in (Fig 20). The percentage removal of the dye was found to decrease with the increase in initial dye concentration with a fixed AC dose. This indicates that there are lack of available active sites required for the high initial concentration of CV and NB. From the graph, we obtain that nitric acid activated AC (300 μm) is more efficient in CV removal than sulfuric acid activated AC (300 μm). Nile blue (NB) is more readily removed than crystal violet (CV) with sulfuric acid activated AC (300 μm). An initial calculation of the adsorption capacity of sulfuric acid activated AC (300 μm) for CV gives 45 mg CV/ g AC.

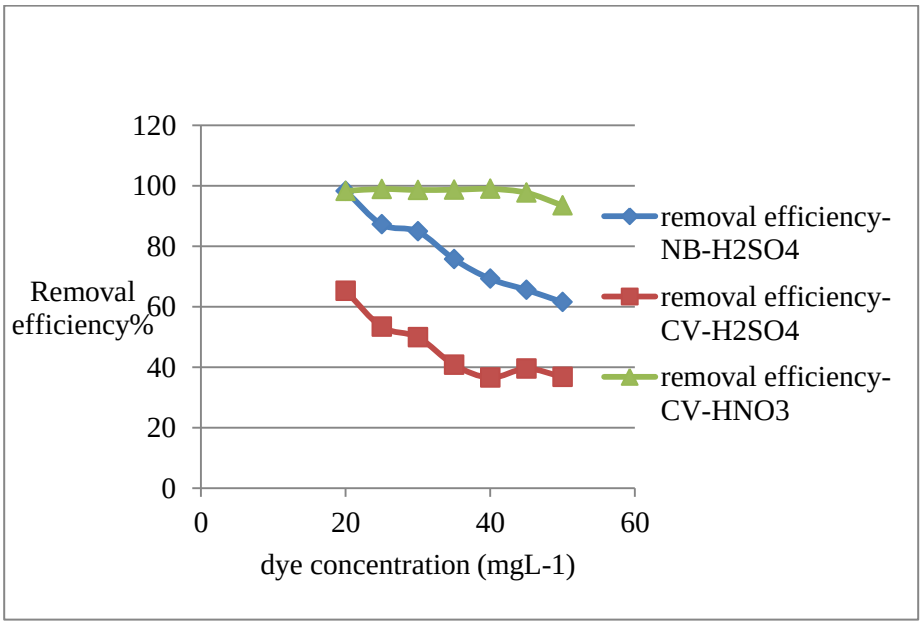

Figure 20: Effect of initial concentration of dye with 50 mg AC and 50 mL dye solution at pH 5.2 (CV) and at rt.

3.3.2.3 Comparison Experiments Using Differently Activated Carbons (ACs)

The effect of different activation methods of AC on the adsorption of CV and NB on AC was studied further as shown in (Fig. 21, 22). For this, 25 mL of aq. solutions of CV (25 ppm) and NB (40 ppm) were contacted with 0.05 g AC (300 μm). Again, the highest percentage removal of both dyes was found with AC produced by the HNO_3 (15.6 M HNO_3) activation method [vs. 25% H_2SO_4 and 10 M H_3PO_4 treatment]. The results show that the 95% of CV and 92% of NB dye could be removed by HNO_3 activated AC under these conditions. On the other hand, only 20% of CV and 33% NB dye was removed by H_3PO_4 activated AC. The removal efficiency for both dyes with H_2SO_4 activated AC lies in between HNO_3 and H_3PO_4 treated ACs. The sorption equilibrium is reached much more quickly with NB than with CV.

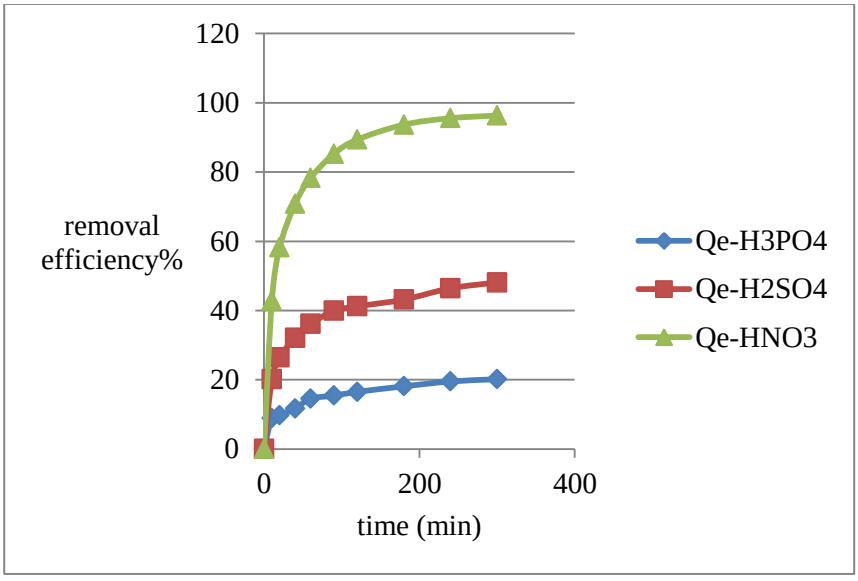

Figure 21: Effect of different AC activation methods on the removal efficiency of CV. c_0=25 ppm, 0.05 g AC= 300μm

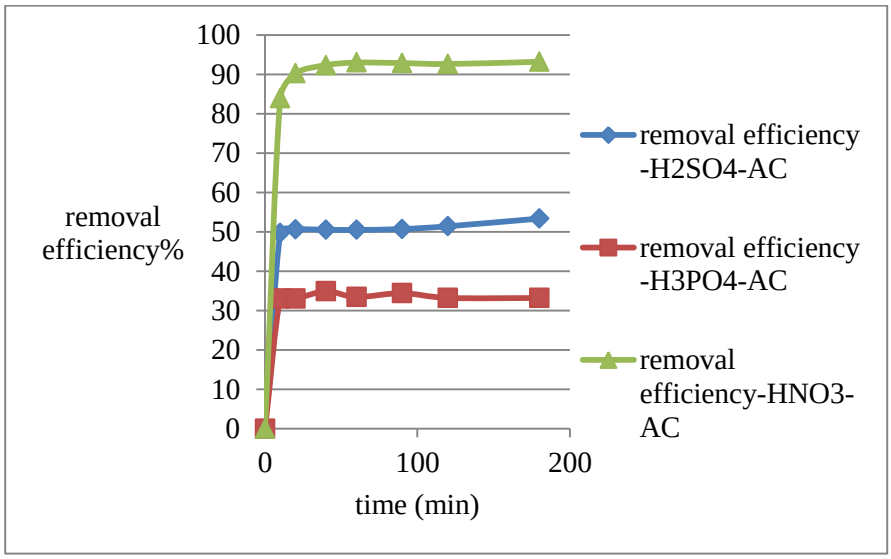

Figure 22: Effect of different AC activation methods on the removal efficiency of NB. c_0=40 ppm, 0.05 g AC= 300μm

3.3.2.4 Comparison Experiments Using Activated Carbons of Different Mesh Size

An investigation on the effect of mesh size (<300 μm, 300 μm, 425 μm and 710 μm) on the adsorption capacity of the AC was carried out at 24^{0}C, pH 5.23, 188 rpm shaking frequency, 0.05 g of AC and 50 mL of dye solution (25 ppm CV and 40 ppm NB).

Mesh size of an adsorbent plays a very important role in the adsorption capacity of the AC towards dyes. The relationship of adsorption capacity to mesh size depends on two criteria: (i) the chemical structure of the dye molecule (its ionic charge) and its chemistry and (ii) the intrinsic characteristic of the adsorbent (*ie.*, its crystallinity and porosity). Fig. 23 and Fig. 24 show the effect of mesh size of H_2SO_4 and HNO_3 activated ACs on the adsorption of CV, where Q_t is the time-dependent adsorption ([mg] of adsorbate / [g] adsorbent at time [t]). It can be noted that the AC of the smallest mesh

size shows the greatest adsorption. Small particle sized AC is expected to have the largest surface area for adsorption.

The increase in adsorption capacity with decreasing mesh size suggests that the dye preferentially adsorbs on the outer surface and does not fully penetrate the particle due to steric hindrance of the large dye molecules. Nevertheless, the equilibirium is reached more quickly with smaller size AC, so this may mean that some penetration occurs. From the effect of different activation methods, we know that HNO_3 treated AC gives the highest adsorption of CV. For this reason, the adsorption kinetics of CV on H_2SO_4-AC and HNO_3-AC were also studied with ACs of different sizes. From Figures 26 and 28, we can see that the data fits better pseudo 2^{nd} order kinetics overall and that the rate constant is increasing with decreasing particle size (Tables 7, 8). Nevertheless, it must be noted that at the initial stage of the adsorption, 1^{st} order kinetics may well operate.

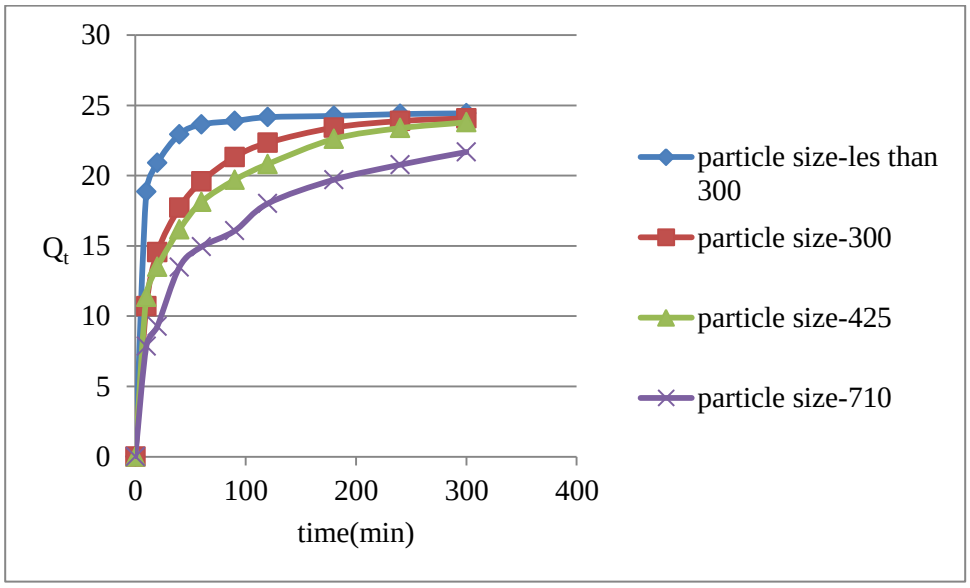

Figure 23: Effect of particle size on time-dependent adsorption (Q_t) of CV with <300, 300, 425, 710 μm AC-HNO_3

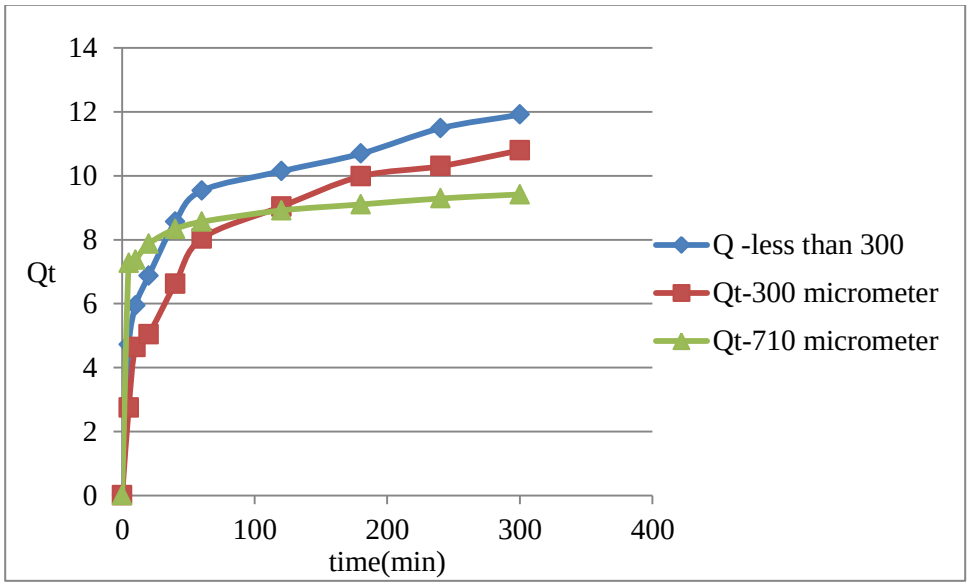

Figure 24: Effect of particle size on time-dependent adsorption Q_t of CV (25 ppm) with <300, 300, 425, 710 μm AC-H_2SO_4

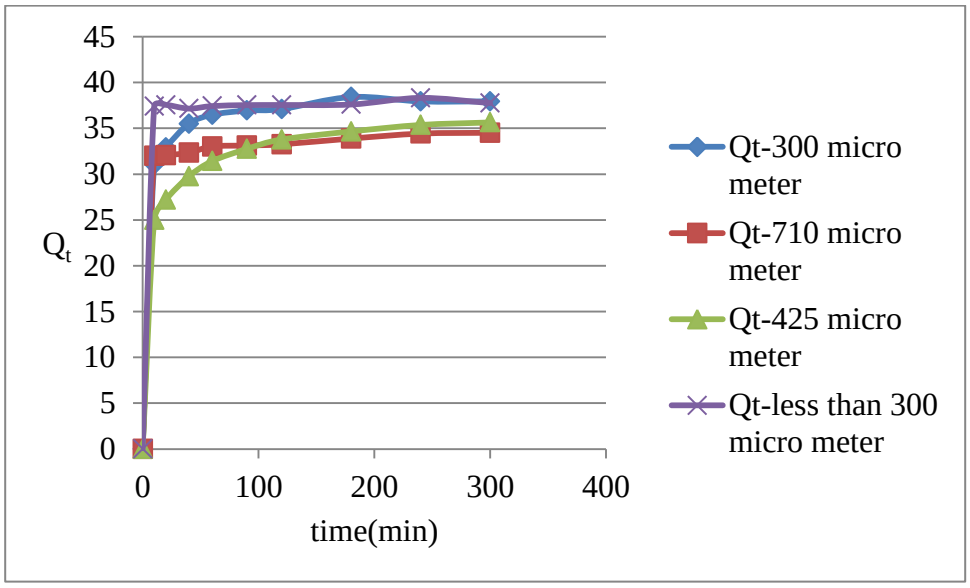

Figure 25: Effect of particle size on time-dependent adsorption Q_t of NB (40 ppm) with <300, 300, 425, 710 μm AC-HNO_3

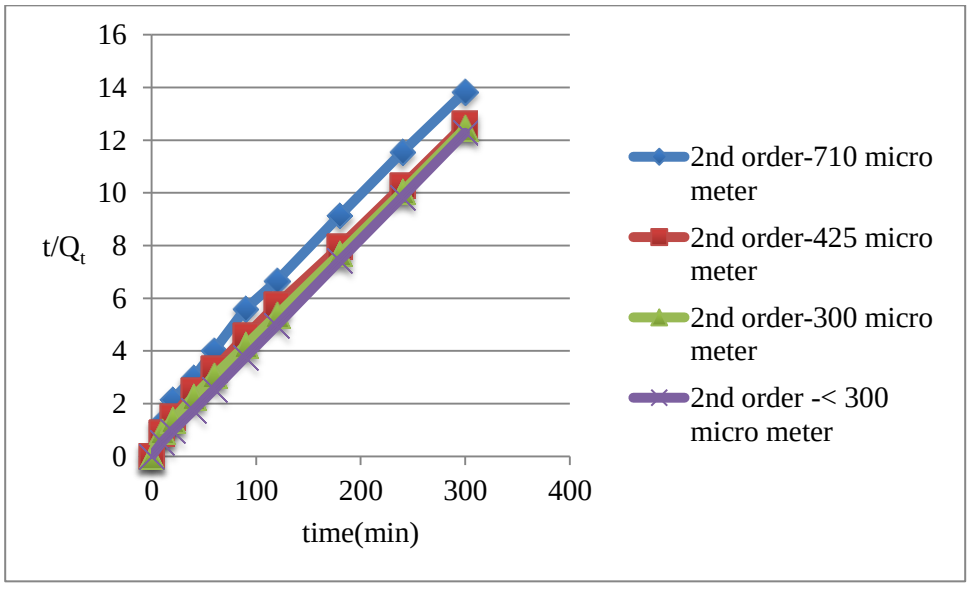

Figure 26: Adsorption follow 2nd order kinetics for 25 ppm CV on HNO_3-AC

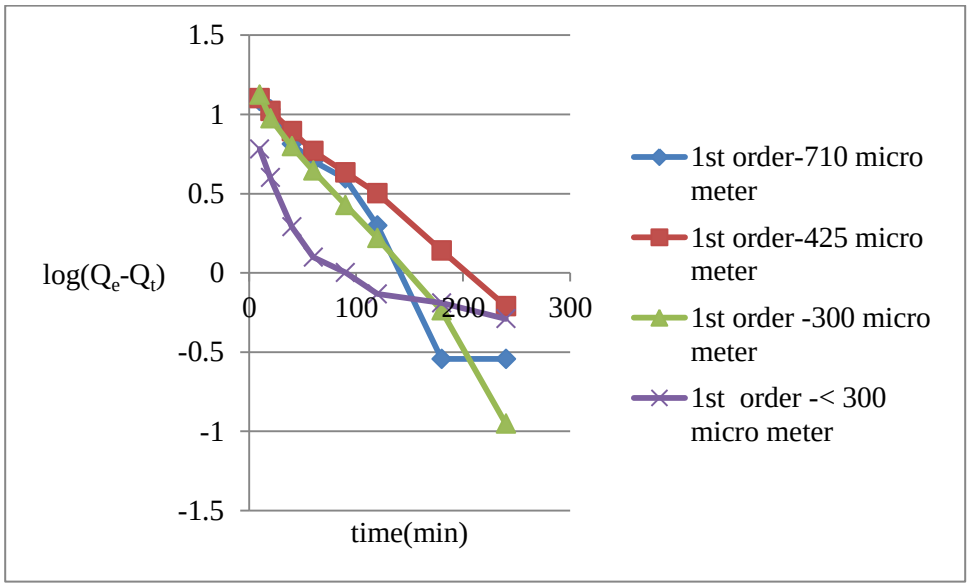

Figure 27: 1st order kinetics representation using adsorption data for 25 ppm CV on HNO_3-AC

Also, the adsorption of NB on HNO_3-Ac was studied (Fig 28) and was found to follow pseudo-2nd-order kinetics rather than 1st order kinetics (Fig 29), overall (Table 7). However, it cannot be excluded that initially the adsorption follows 1st order kinetics.

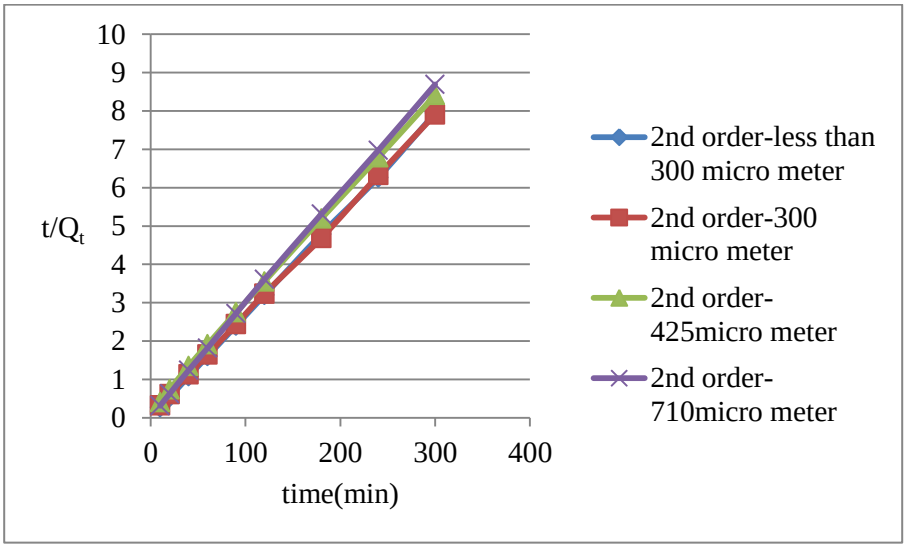

Figure 28: Adsorption follow 2nd order kinetics for 40ppm NB on HNO_3-AC

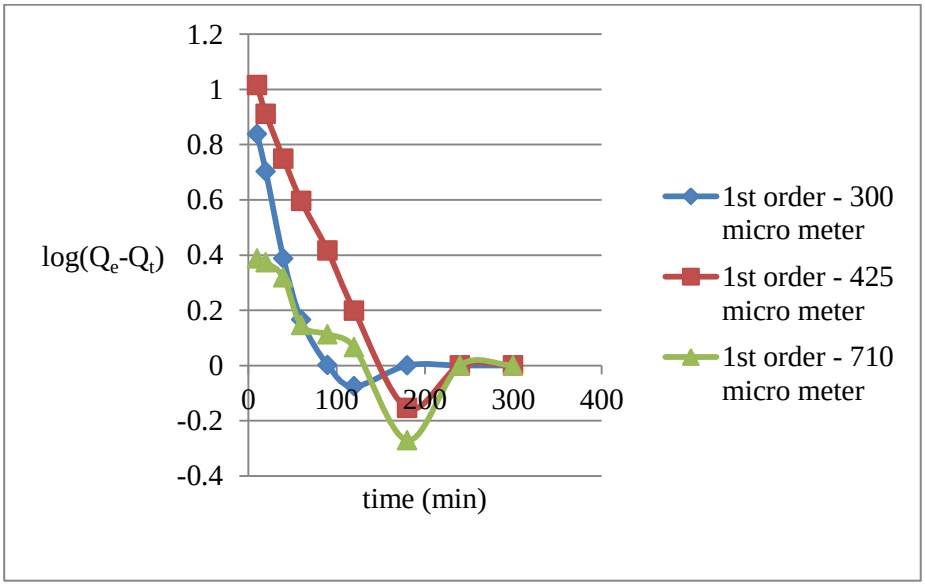

Figure 29: 1st order kinetics representation using adsorption data for 40ppm NB on HNO_3-AC

Size of AC	dye		Pseudo-first order			Pseudo-2nd order		
300µm	CV	Experimental adsorption capacity (q_e)	Rate constant (K_1)	Theoretical adsorption capacity (q_e)	R^2	Rate constant (k_2)	Theoreti-cal adsorpti-on capacity (q_e)	R^2
<300 µm		12.33	$8.52x10^{-3}$	5.5834	0.8272	$4.56X10^{-3}$	12.77	0.997
300 µm		12.03	$8.75x10^{-3}$	6.40	0.876	$3.7846x10^{-3}$	12.46	0.993
710 µm			$6.6787X10^{-3}$	1.59	0.466	0.0278	9.58	0.999

Table 7: Parameters for the adsorption of CV on H_2SO_4-AC of different mesh sizes

Size of AC	dye		Pseudo-first order			Pseudo-2nd order		
300μm	NB	Experimental adsorption capacity (q_e)	Rate constant (K_1)	Theoretical adsorption capacity (q_e)	R^2	Rate constant (k_2)	Theoretical adsorption capacity (q)	R^2
300 μm		37.94	$5.5272x10^{-3}$	3.199	0.5123	$8.47x10^{-3}$	38.46	0.9999
425 μm		35.36	$8.5211x10^{-3}$	7.268	0.7961	$3.39x10^{-3}$	36.49	0.9997
710 μm		34.42	$3.6848x10^{-3}$	2.0488	0.5746	0.01	34.72	0.9998

Table 8: Parameters for the adsorption of NB on HNO_3-AC of different mesh size

Size of AC	dye		Pseudo-first order			Pseudo-2nd order		
300μm	CV	Experimental adsorption capacity (q_e)	Rate constant (K_1)	Theoretical adsorption capacity (q_e)	R^2	Rate constant (k_2)	Theoretical adsorption capacity (q)	R^2
<300 μm		24.9	$7.8302x10^{-3}$	3.07	0.758	0.013	24.69	1
300 μm		24	0.013	9.57	0.7282	$2.47X10^{-3}$	25.35	0.9998
425 μm		24	0.01358	14.368	0.9946	$1.96x10^{-3}$	25.18	0.9983
710 μm		20	0.011	10.09	0.7379	$1.35x10^{-3}$	23.47	0.9961

Table 9: Parameters for the adsorption of CV on HNO_3-AC of different mesh size

3.3.2.5 Determination of the Effect of the pH of the Solution on the Adsorption of the Dyes Studied

The effect of the pH of the solution on the adsorption of the dye on the activated carbons prepared from date palm leaves was examined under the following conditions: at 25 °C, an initial concentration of 25 mg L^{-1} of CV, and 0.05 g of adsorbent. The pH of the solution was adjusted between pH 2 and pH 9 by adding either HNO_3 (6M) or NaOH (1 M) solution. The pH values of the solutions were measured using a pH-meter (Orion 9106 BNWP). Each solution was centrifuged at 300 rpm for 5 min before UV-VIS measurement. The residual concentration of the dye was determined as previously described, and the amount of adsorbed dye was calculated using Eq. 1 (p. xx). The experimental results showed no significant variation in the amount of solute adsorbed in the examined pH range (Fig. 30).

According to reported studies on the adsorption of dyes with different chemical structures, the effect of pH on the solute uptake by activated carbons can be highly, moderately or slightly significant. The adsorption can be affected by changes in pH of the solution because this parameter affects the degree of ionization of the dye and the surface properties of the sorbents.

For the dyes used in this work, the results related to the pH dependence are apparently surprising. However, a plausible explanation of this behaviour may be the presence of both negatively and positively charged functional groups in the dye molecules. Independent of the origin of this insignificant effect of the pH, this finding is

quite meaningful in the adsorption process application since it makes a pH adjustment of the effluent before treatment unnecessary.

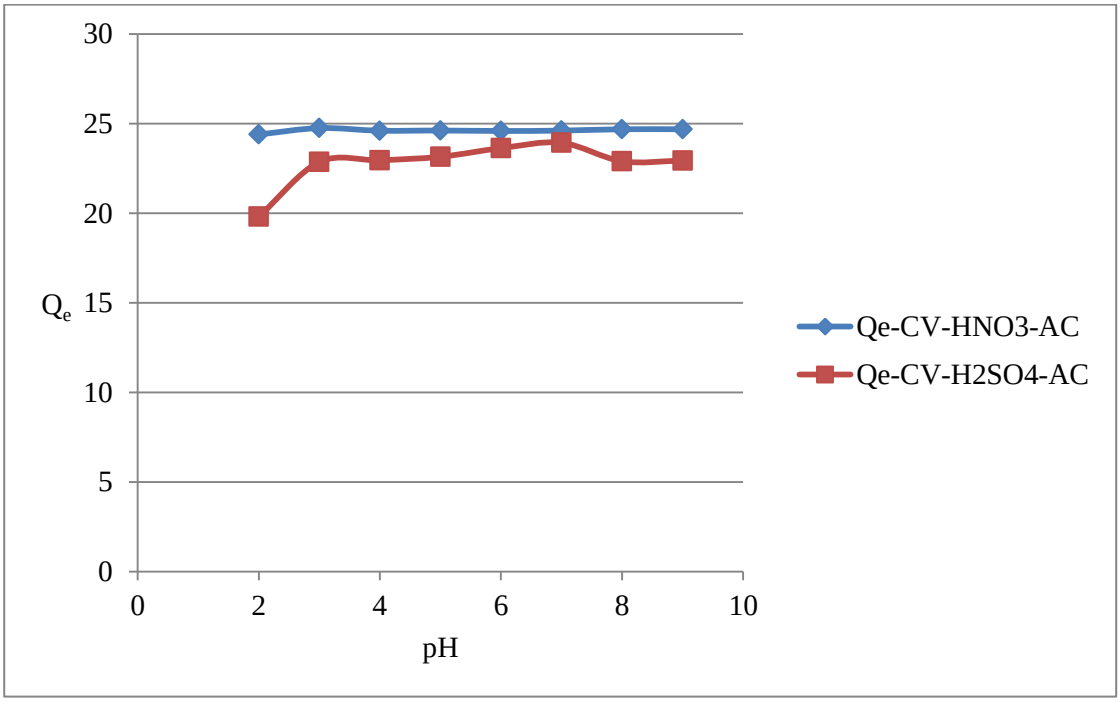

Figure 30: Effect of pH on CV

3.4.1 Equilibrium Studies

3.4.1.1 Langmuir Model

The Langmuir theory is based on the assumption of the adsorption leads to a mono-layer without interaction among the adsorbate molecules. The sorption takes place at specific sites within the adsorbent. Each site retains one molecule of the given compound. The adsorbent has a finite capacity for the adsorbate at equilibrium. A

saturation point is reached, where no further adsorption can occur. All sites are identical and energetically equivalent. The adsorbent is structurally homogeneous (Kundu, & Gupta, 2006; Cazetta, Vargas, Nogami, Kunita, Guilherme, Martins, & Almeida, 2011; Foo, & Hameed, 2010; Limousin, Gaudet, Charlet, Szenknect, Barthes, & Krimissa, 2007)

The following transformation is considered:

free site +solute =surface complex

The linear form of Langmuir isotherm is usually written as

$$\frac{C_e}{Q_e} = \frac{C_e}{Q_m} + \frac{1}{K_i} Q_m \quad (5)$$

The non-linear form of Langmuir isotherm is expressed as:

$$Q_e = \frac{Q_o b C_e}{1 + b C_e} \quad (6)$$

Where c_e is the liquid-phase equilibrium concentration (mg L^{-1}) of the adsorbate, Q_e is the amount of adsorbate adsorbed at equilibrium (mg g^{-1}) and Q_m is the theoretical maximum monolayer adsorbent capacity (mg g^{-1}). K_i is the Langmuire constant. Q_m and K_i are related to the adsorption efficiency and the energy of adsorption. They can be calculated from the linear plot of c_e/Q_e versus c_e (Soliman, El-Naas, & Chaalal, 2013).

3.4.1.2 Freundlich Model

Freundlich isotherm (1932) is the most basic known model for multilayer adsorption. It leads to an empirical equation which describes a heterogeneous system. This model is applied to adsorption on heterogeneous surfaces with an interaction between adsorbed molecules (Foo, & Hameed, 2010)

The Freundlich isotherm is expressed by the following empirical equation:

$$lnQ_e = lnK_F + \frac{1}{n}\ln C_e \quad (7)$$

This is the linear form of the Freundlich isotherm.

There exists also the non-linear form of the Freundlich isotherm, which can be expressed as

$$Q_e = K_F C_e^{\frac{1}{n}} \quad (8)$$

Where Q_e = solid phase equilibrium concentration (mg g^{-1}), c_e = liquid-phase equilibrium concentration (mg L^{-1}), and K_F = the Freundlich constant, with *n* giving an indication of the facility with which the adsorption process takes place. K_F (mg g^{-1}(L mg^{-1})$^{1/n}$) is the adsorption capacity of the adsorbent (i.e., the adsorption coefficient or distribution coefficient) and represents the quantity of dye adsorbed onto the activated adsorbant per unit of equilibrium concentration (Zhang, Zhang, Fernández, Menéndez, Niu, Peng, & Guo, 2010).

A value of 1/n close to 1 represents a linear relationship, while 1/n < 1 represents a non-linear relationship. The slope range of 1/n is a measure of the adsorption intensity or surface heterogeneity. The surface heterogeneity increases as 1/n approaches zero.

A value for 1/n below 1 indicates a Freundlich isotherm, while 1/n above one is indicative of cooperative adsorption (Fytianos, Voudrias, & Kokkalis, 2000). Higher values denote that the system approaches a rectangular isotherm (or irreversible isotherm), especially when the value of n > 10 (Table 10) (Kurniawan, Sutiono, Indraswati, & Ismadji, 2012). The K_F constant can be regarded as the maximum adsorption capacity of the adsorbent only with a very large value of *n*.

The linear plots of c_e/Q_e vs c_e (Fig 32) show that the adsorption of CV on AC-H_2SO_4 obeys the Langmuir isotherm model for CV. The experiments were also carried out with AC-HNO_3 (with CV) (Fig 34) and with AC-H_2SO_4 with Nile blue (NB) (Fig 37). The values of Q_m and K_i were determined for all adsorbents from the intercept and slopes of the linear plots of c_e/Q_e vs. c_e (Table. 11).

R^2 values are indicative of the actual deviation between the experimental points and the theoretically predicted data points and in our case (with R^2 greater than 0.94 for both AC-H_2SO_4 and AC-HNO_3, (Table 11) show a better correlation of the experimental data to the Langmuir model.

An important parameter is the Langmuir dimensionless constant separation factor or equilibrium parameter, R_L, which is defined by the following equation:

$$R_L = \frac{1}{1+bC_0} \quad (9)$$

Where c_o is the initial dye concentration in mgL^{-1}. The value of the separation factor R_L indicates the nature of the adsorption process given below (Tables 12).

In the present study, the values of R_L (Table 13) are observed to be in the range 0-1, indicating that the adsorption process is favorable for all types of prepared activated carbons. But for NB, R_L value almost zero which indicates that the adsorption process for NB by AC (H_2S0_4) is irreversible process.

The $_n$ values in the Freundlich equation were calculated as 3.35897, 6.10128 and 2.145 for the adsorption of CV on AC(H_2SO_4) , AC(HNO_3) and NB on AC (H_2SO_4), respectively. Since the values of *n* lie between 1 and 10, this indicates a favorable adsorption of AC (Table 11).

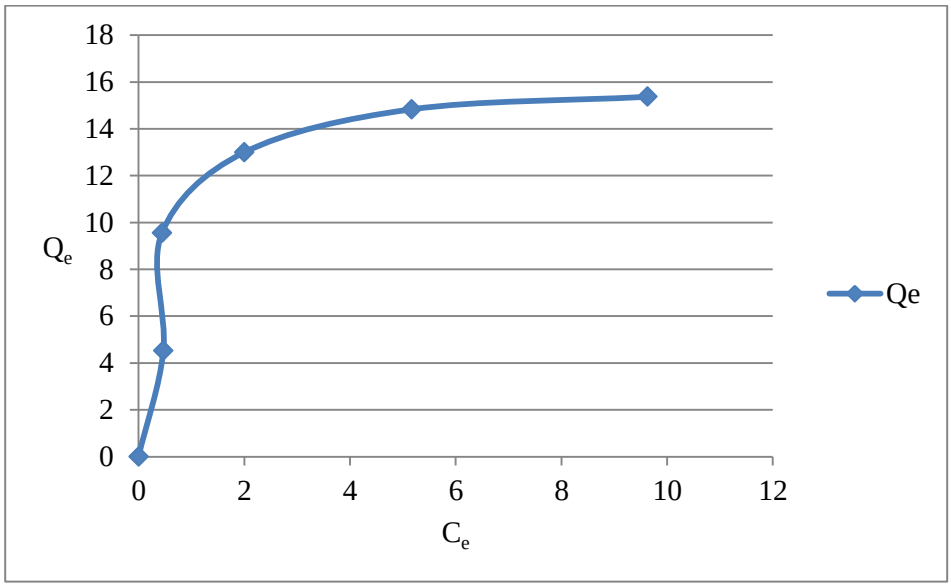

Figure 31: Q_e vs. c_e curve for CV with AC-H_2SO_4 (0.05 g, 300 μm, pH 5.2, measured at λ = 590 nm)

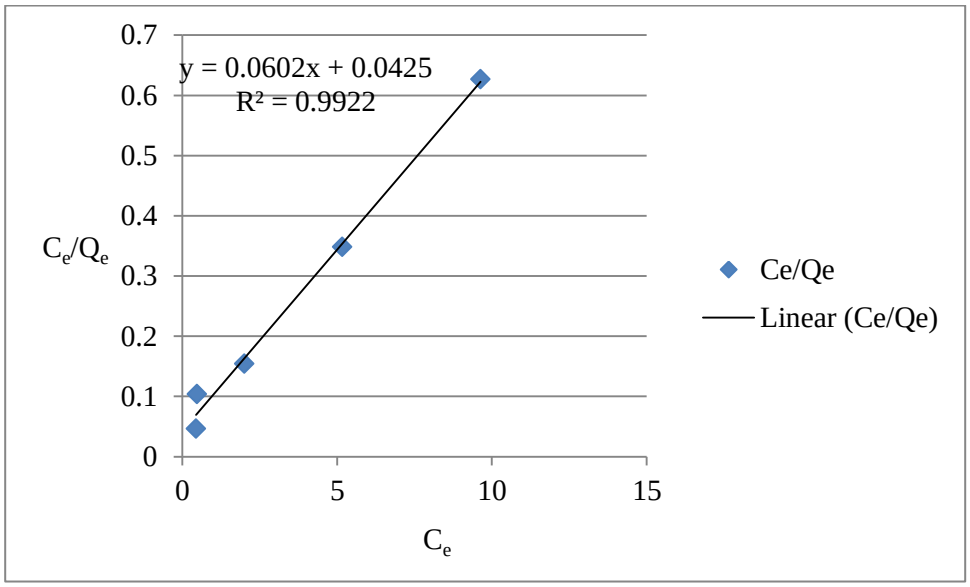

Figure 32: Langmuir isotherm for adsorption of CV on AC -H_2SO_4 (0.05 g, 300 μm, pH 5.2, λ = 590 nm)

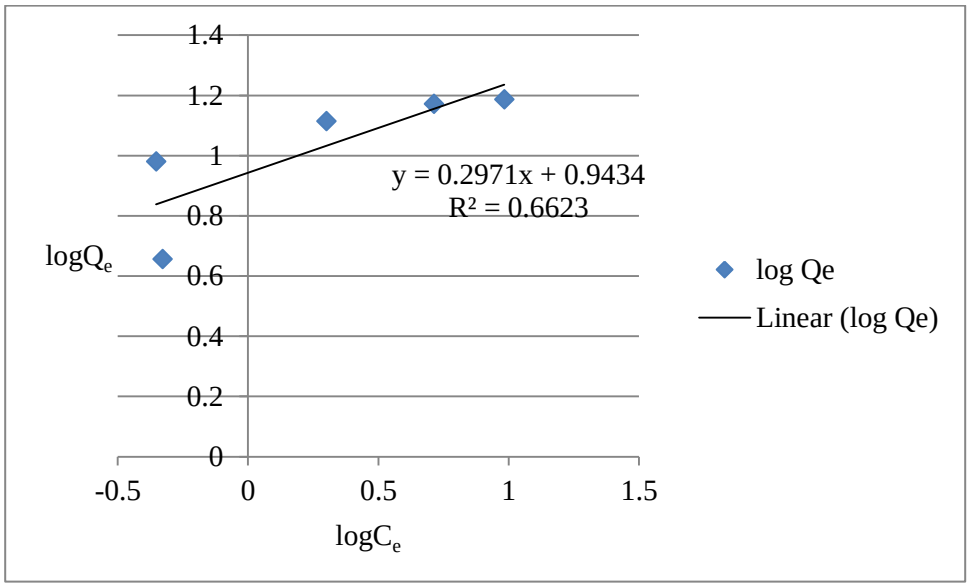

Figure 33: Depiction of the values with a Freundlich isotherm for the adsorption of CV on AC-H_2SO_4

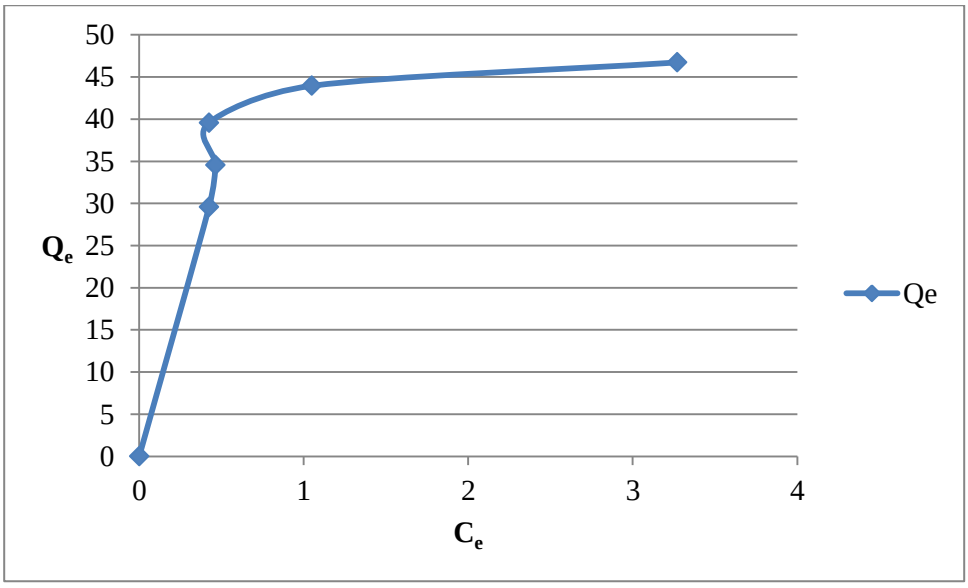

Figure 34: Q_e vs. c_e curve for CV on AC-HNO_3

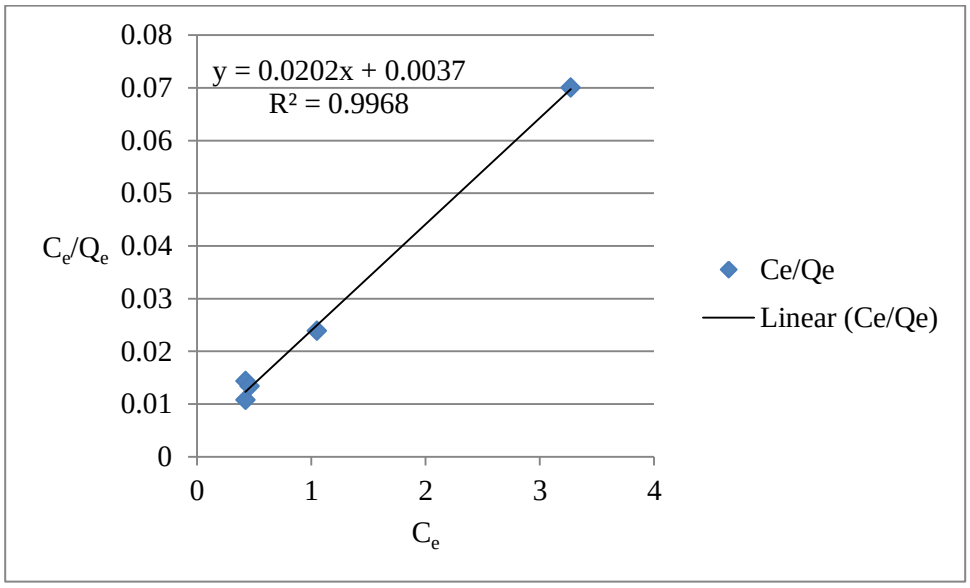

Figure 35: Langmuir isotherm for the adsorption of CV (25 ppm) on AC-HNO_3 (300 μm)

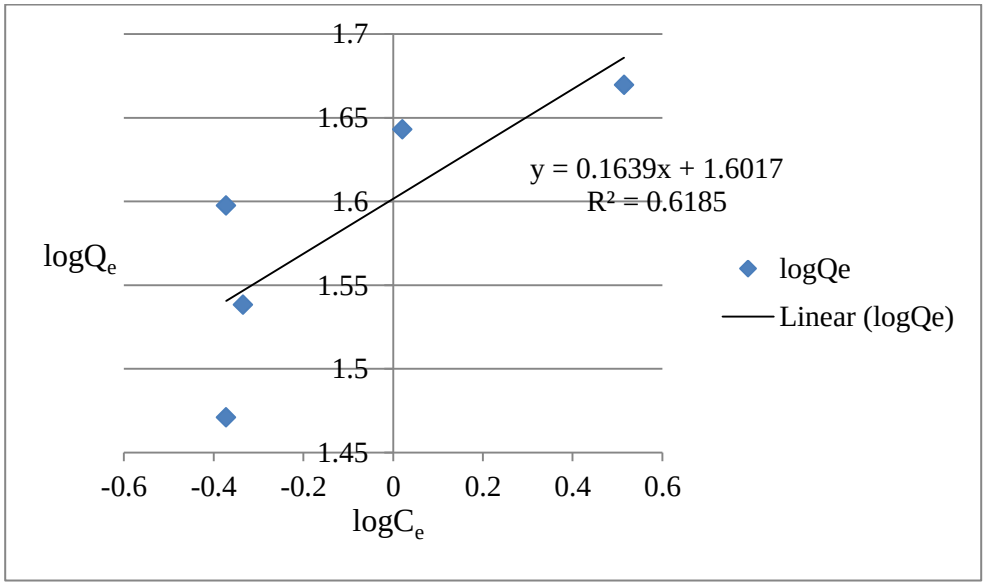

Figure 36: Depiction of the values as a Freundlich isotherm for the adsorption of CV (25 ppm) on AC-HNO_3 (300 μm)

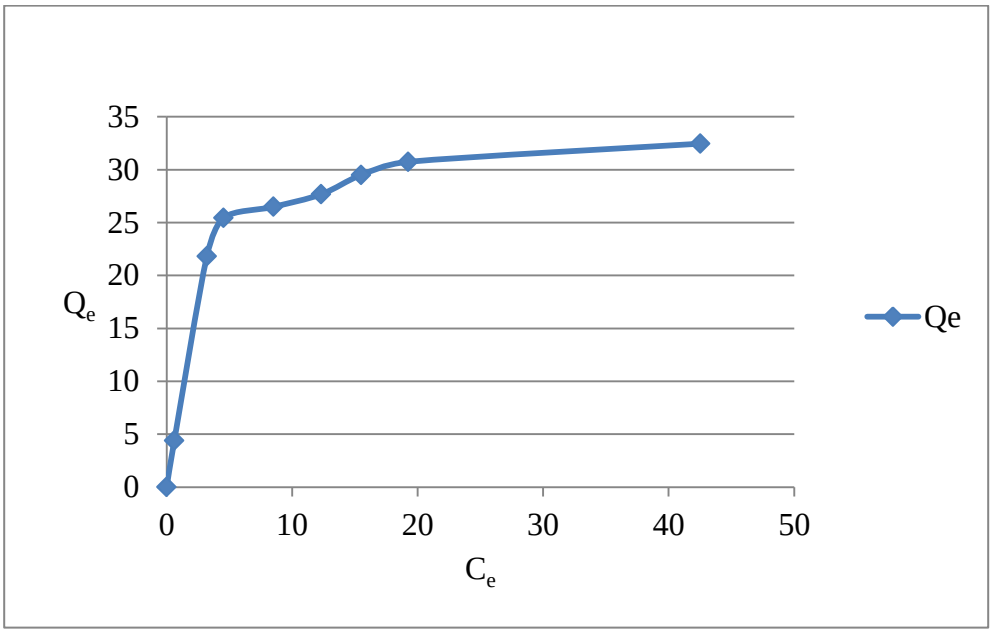

Figure 37: Q_e vs. c_e curve for the adsorption of NB on AC-H_2SO_4

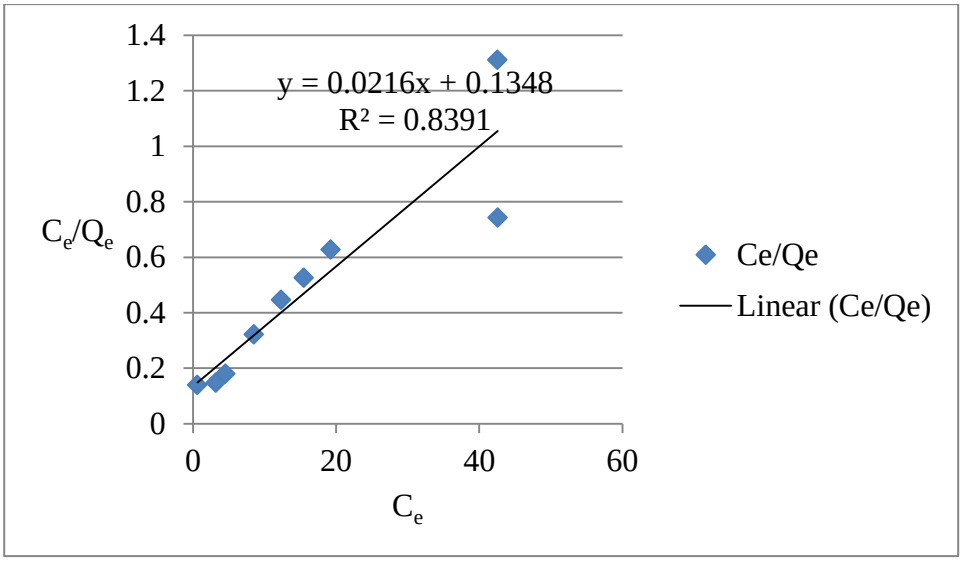

Figure 38: Langmuir isotherm for the adsorption of NB on AC-H_2SO_4

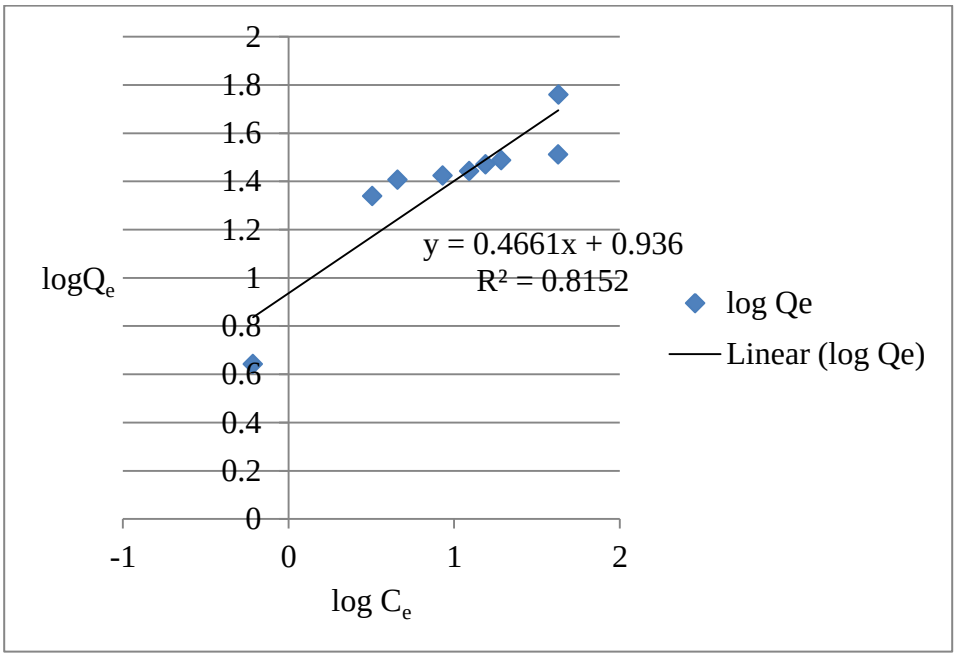

Figure 39: Depiction of the values for the adsorption of NB on AC-H_2SO_4 as a Freundlich isotherm

Slope of the Freundlich isotherm (1/n)	Nature of adsorption process of Freundlich model
1/n below 1	Normal Freundlich isotherm
1/n above 1	Co-operative adsorption
1/n close to zero	System is more heterogeneous (irreversible system)

Table 10: The nature of the adsorption process according to the value of 1/n

	Langmuir constant			Freundlich constants			
	Langmuir constant (Q_m)	Langmuir constant (K_L)	R^2	Freundlich constant ($K_{F)}$	1/n	n values of Freundlich	R^2
AC-H_2SO_4 for CV	16.66	1.42	0.992	8.77	0.2977	3.35897	0.6623
AC-HNO_3 for CV	49.50	5.459	0.997	39.967	0.1639	6.10128	0.6185
AC-H_2SO_4 for NB	46.296	343.44	0.839	8.629785	0.4661	2.145	0.8152

Table 11: Langmuir and Freundlich adsorption constants for CV adsorption on AC-H_2SO_4 and AC-HNO_3 and for NB on AC-H_2SO_4

R_L Value	Nature of adsorption process using the Langmuir model
R_L>1	unfavorable
R_L=1	linear
0<R_L<1	Favorable
R_L=0	Irreversible

Table 12: Meaning of the Langmuir dimensionless constant separation factor or equilibrium parameter (R_L) for the adsorption process

Dye concentration(CV)	Separation factor(Langmuir) - R_L (H_2SO_4) for CV	Separation factor(Langmuir) - R_L- (HNO_3) For CV	Separation factor(Langmuir) - R_L- (HNO_3) For NB
5	0.123		$5.82X10^{-4}$
10	0.0656		
15	0.0445		
20	0.0340		
25	0.0274		$1.16X10^{-4}$
30		$6.09X10^{-3}$	$9.7X10^{-5}$
35		$5.206X10^{-3}$	$8.3X10^{-5}$
40		$4.5587X10^{-3}$	$7.2X10^{-5}$
45		$4.05X10^{-3}$	$6.47X10^{-5}$
50		$3.65X10^{-3}$	$5.82X10^{-5}$
75			$3.8X10^{-5}$
100			$2.9X10^{-5}$

Table 13: Calculated values of the Langmuir dimensionless constant separation factor or equilibrium parameter (R_L) for the adsorption experiments of CV AC-H_2SO_4 and AC-HNO_3 and NB on AC-HNO_3 at different dye concentrations.

From Table. 13, it can be seen that the R_L values are in the range "$0<R_L<1$", so that the adsorptions can be seen as a favorable process. The R_L values for NB are close to 0.

As explained above, the adsorption of CV and NB on the tested activated carbons is well described by the Langmuir model, regardless of the experimental conditions (i.e. initial concentration, temperature or pH of solution). The Langmuir equation assumes a homogenous surface. An accurate fit means that the active sites are

homogeneously distributed over the surface for both adsorbents tested. The theory of Langmuir is actually based on the fixation of a monolayer of adsorbate molecules on the adsorbent's surface.

3.4.2 Kinetic Studies

3.4.2.1 Pseudo-first Order Model

The pseudo-first order model was first represented by Lagergren. This model is one of the most widely used models for describing the adsorption kinetics of a solute from aqueous solutions.

The pseudo-first order equation can be expressed as follows:

$$\frac{dQ_t}{dt} = k_1(Q_e - Q_t) \quad (10)$$

Where Q_t is the amount of dye adsorbed at time t (mg/g); Q_e is the amount of dye adsorbed at equilibrium and k_1 is a first order rate constant for the adsorption (L/min). After integration and applying boundary conditions t=0 to t= t and Q_t=0 to Q_t= Q_t, the integrated form of equation (1) becomes

$$\log(Q_e - Q_t) = \log(Q_e) - \frac{k_1}{2.303}t. \quad (11)$$

The equation is applicable to express experimental results. Mostly, it can differ from a first order equation in two ways:

1. The parameter k_1(*Qe*-*Qt*) does not represent the number of available sites.

2. The factor log (Q_e) is an adjustable factor and often it is found not equal to the intercept of a plot of log (Q_e- Q_t) against *t*, while in a true first order log (Q_e) should be equal to the intercept of a plot of log (Q_e- Q_t) against *t*.

To fit experimental data in equation (11), the equilibrium sorption capacity, q_e, must be known. In many cases q_e remains unknown as the chemisorption tends to become unmeasurably slow, and the amount sorbate is still significantly smaller than the actual equilibrium sorption capacity would give.

Normally in the literature, the pseudo-first order equation does not fit well for the whole range of contact time in the sorption process. It is usually applicable over the initial 20 to 30 minutes of the sorption procedure. Moreover, often one has to find some means of extrapolating the experimental data to $t = \infty$, or treat q_e as an adjustable parameter to be determined by trial and error. Therefore, it is essential to use experimental data and the trial and error approach to obtain the equilibrium sorption capacity, q_e, to analyze the pseudo-first order model kinetics (Ho, & McKay, 1998; Günay, Arslankaya, & Tosun, 2007).

3.4.2.2 Pseudo-second Order Model

The pseudo second-order equation is based on the sorption capacity of the solid phase. Contrary to other models (e.g., the 1st order kinetic model) it calculates the behavior over the whole range of adsorption. It considers a rate controlling step of the adsorption mechanism. The pseudo-second order chemisorption kinetic rate equation is expressed as:

$$\frac{dQ_t}{dt} = k(Q_e - Q_t)^2 \quad (12)$$

Where Q_e and Q_t are the sorption capacity at equilibrium and at time *t*, respectively (mg g^{-1}) and *k* is the rate constant of the pseudo-second order sorption process (g mg^{-1} min^{-1}). For the boundary conditions $t = 0$ to $t = t$ and $Q_t = 0$ to $Q_t = Q_t$, the integrated form of equation (12) becomes

$$\frac{1}{(Q_e - Q_t)} = \frac{1}{Q_e} + kt \quad (13)$$

Which is the integrated rate law for a pseudo-second order reaction. Equation (13) can be rearranged to obtain:

$$Q_t = \frac{t}{\frac{1}{kQ_e^2} + \frac{t}{Q_e}} \quad (14)$$

Which has a linear form:

$$\frac{t}{Q_t} = \frac{1}{kQ_e^2} + \frac{1}{Q_e}t \quad (15)$$

Where *h* can be regarded as the initial sorption rate as q_t/t *to* 0, hence

$$h = kQ_e^2 \quad (16)$$

Equation (15) can be written as:

$$\frac{t}{Q_t} = \frac{1}{h} + \frac{1}{Q_e}t \quad (17)$$

Equation (15) does not have the disadvantage of the problem with assigning an effective q_e.

If pseudo-second order kinetics are applicable, the plot of t/Q_t against *t* of equation (15) should give a linear relationship, from which Q_e and *k* can be determined from the slope and intercept of the plot and there is no need to know any parameter before (Ho, & McKay, 1998; Aksu, 2001).

The sorption capacity of active carbon derived from date palm leaves for CV and NB dyes were evaluated as a function of time and the results are shown below (for

CV: Fig 40,43 and 46; for NB: Fig 49). The sorption of the dyes on the ACs were treated with pseudo 2nd order and pseudo 1st order kinetics (for CV: Fig. 41, 44 and 47, Fig. 42,45 and 48, for NB: Fig. 50 and 51). In general, it was noted that the sorption increased with contact time. Equilibrium was established for CV on AC-H_2SO_4, HNO_3, H_3PO_4 after about 120 min and for NB equilibrium reached more quickly (after ca. 20 min.). Further increase in time resulted in no drastic removal of CV and NB dye from the aqueous solution. A maximum experimental sorption capacity of approximately 11, 24 , and 5, mg/g was observed for 25 ppm CV on AC-H_2SO_4, HNO_3 and H_3PO_4 (0.05 g), respectively. The maximum experimental adsorption capacity for NB was found to be 30 mg/g on AC-H_2SO_4. In the beginning, the rate of adsorption showed a rapid increase owing to the availability of a large number of exchanging sites and then gradually slowed, owing to saturation point achieved.

Correlation coefficients R^2 (Table 14) for pseudo 2nd order kinetics model are above 0.94 and suggest strongly that the sorption processes follow pseudo–second–order kinetics. Overall, sorption data of CV and NB dyes on date palm leaf derived ACs (for all activation methods tried) fit better the pseudo-second-order kinetics model for all concentrations than the pseudo-first-order kinetics model.

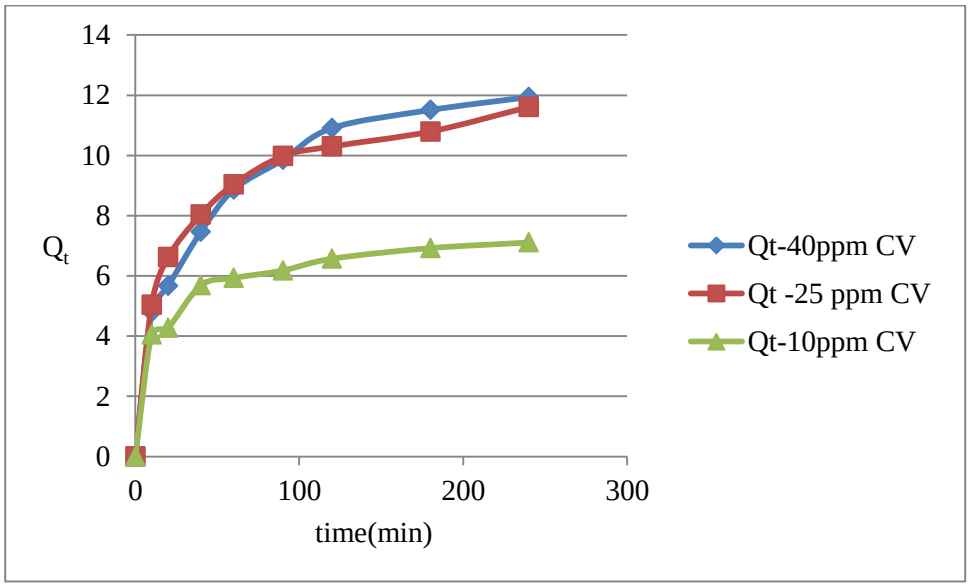

Figure 40: Adsorption of CV on AC-H_2SO_4 (0.05 g) vs. time for different conc. of CV

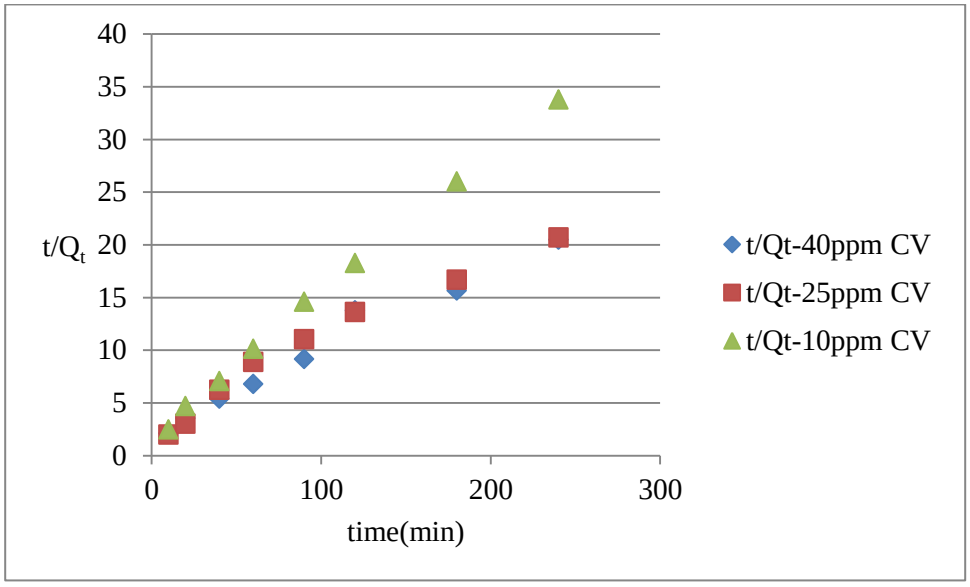

Figure 41: Presentation of the Adsorption of CV on AC-H_2SO_4 (0.05 g) as following pseudo-second order kinetics

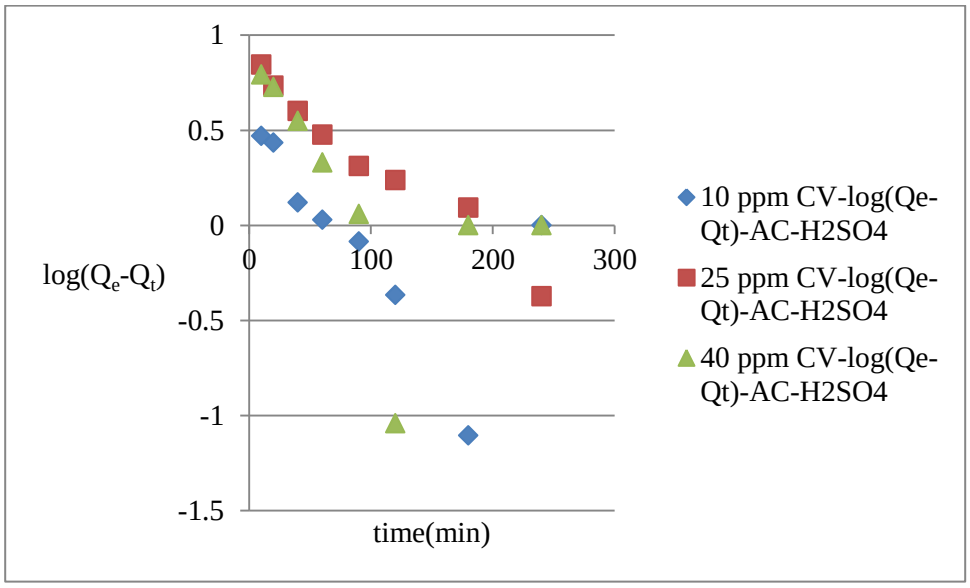

Figure 42: Presentation of the Adsorption of CV on AC-H_2SO_4 (0.05 g) as following first order kinetics

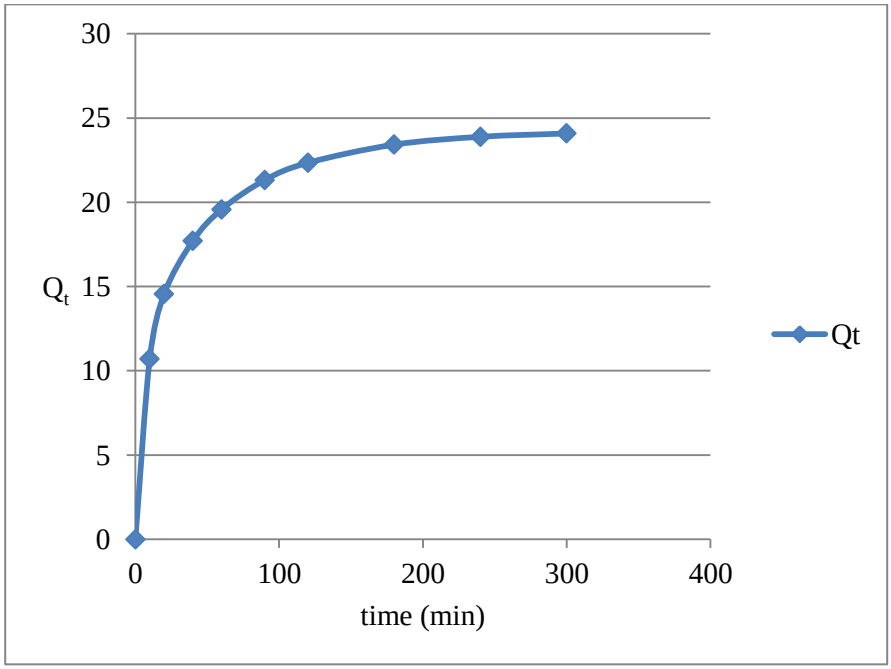

Figure 43: Adsorption of CV (25 ppm) vs. time on AC-HNO_3 (0.05 g)

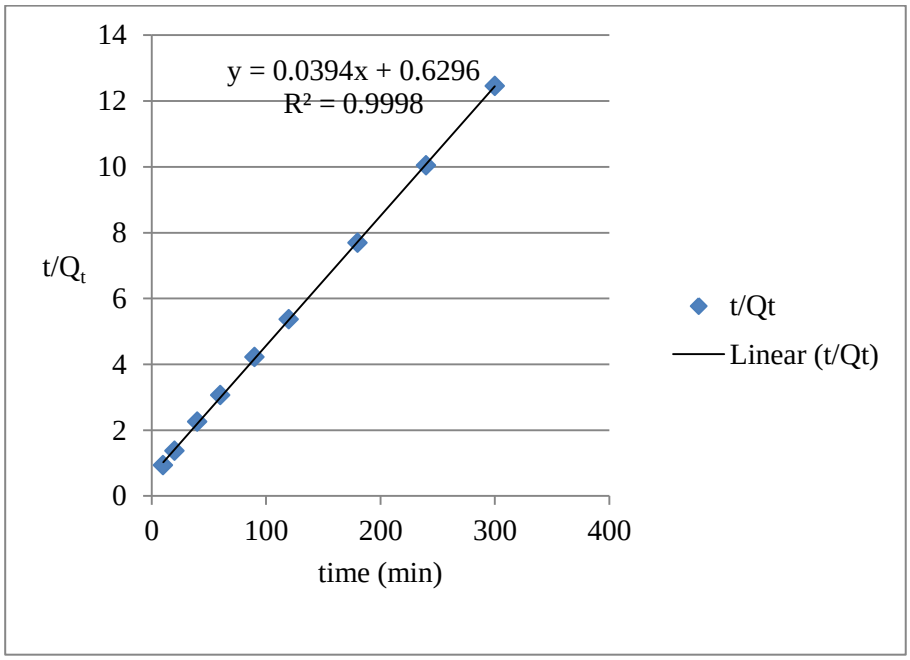

Figure 44: Presentation of the Adsorption of CV (25 ppm) on AC-HNO_3 (0.05 g) as following pseudo-second order kinetics

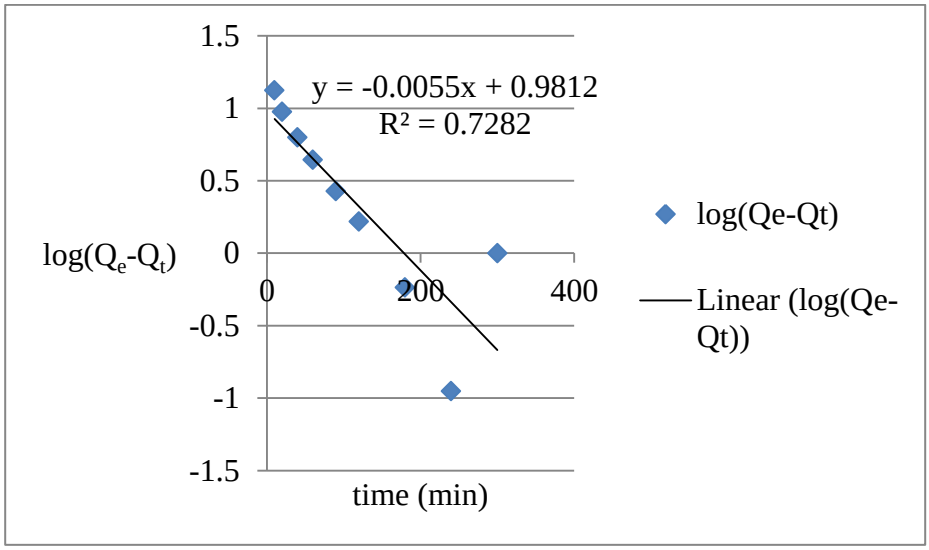

Figure 45: Presentation of the Adsorption of CV (25 ppm) on AC-HNO_3 (0.05 g) as following first order kinetics

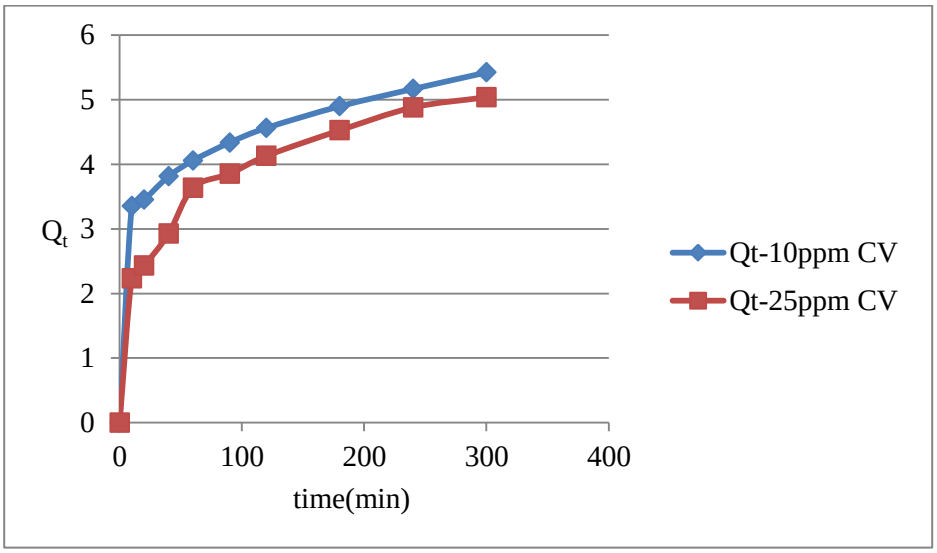

Figure 46: Adsorption of CV vs. time on AC-H_3PO_4 (0.05 g)

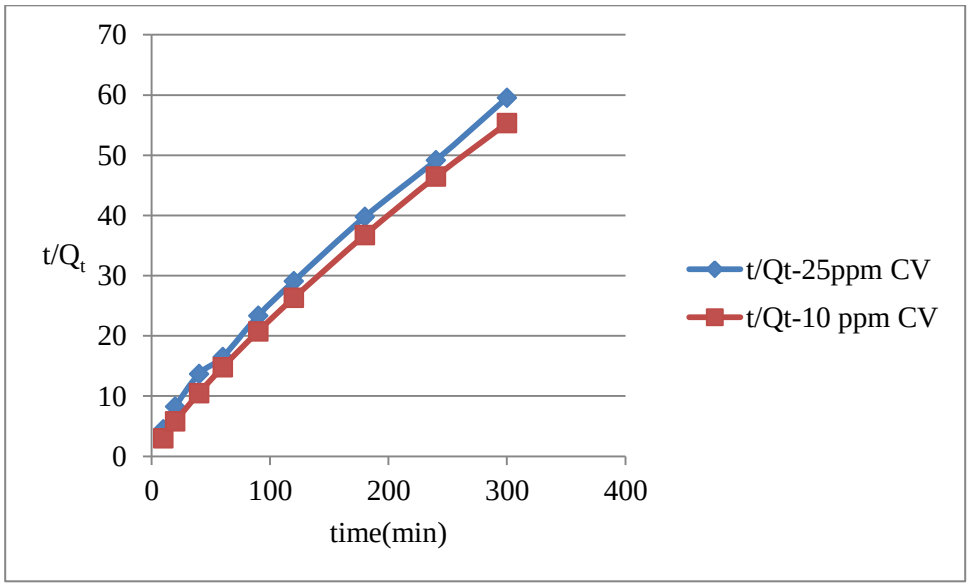

Figure 47: Presentation of the Adsorption of CV on AC-H_3PO_4 (0.05 g) as following pseudo-second order kinetics

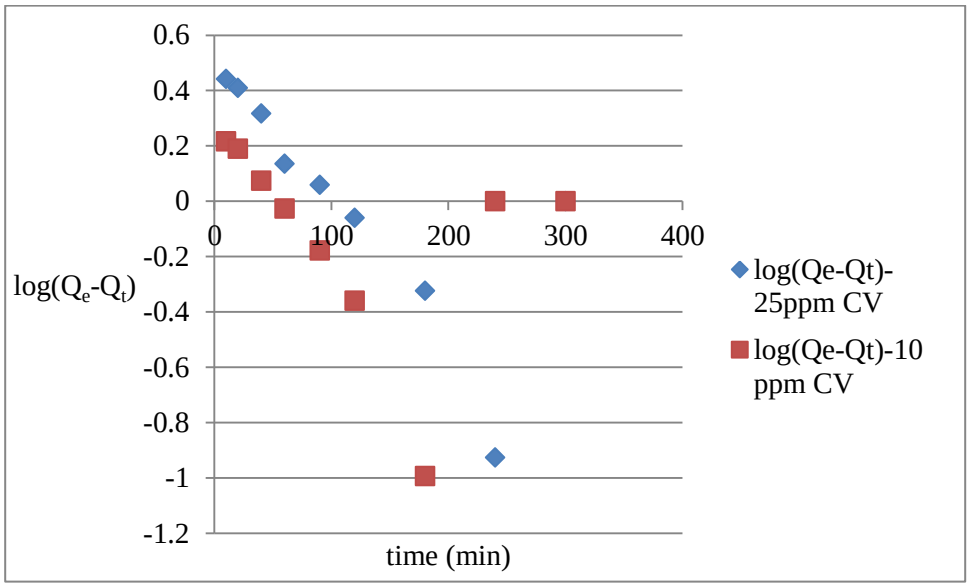

Figure 48: Presentation of the Adsorption of CV on AC-H_3PO_4 (0.05 g) as following first order kinetics

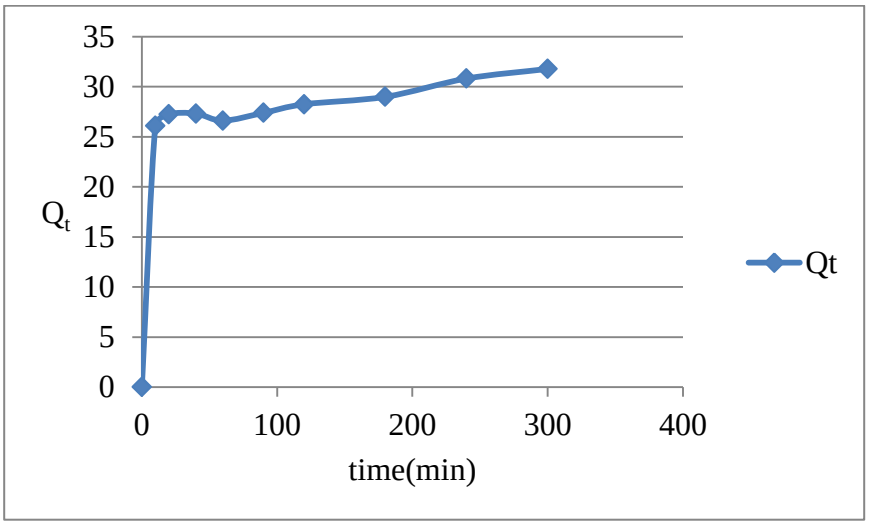

Figure 49: Adsorption of NB (40 ppm) vs. time on AC-H_2SO_4 (0.025 g)

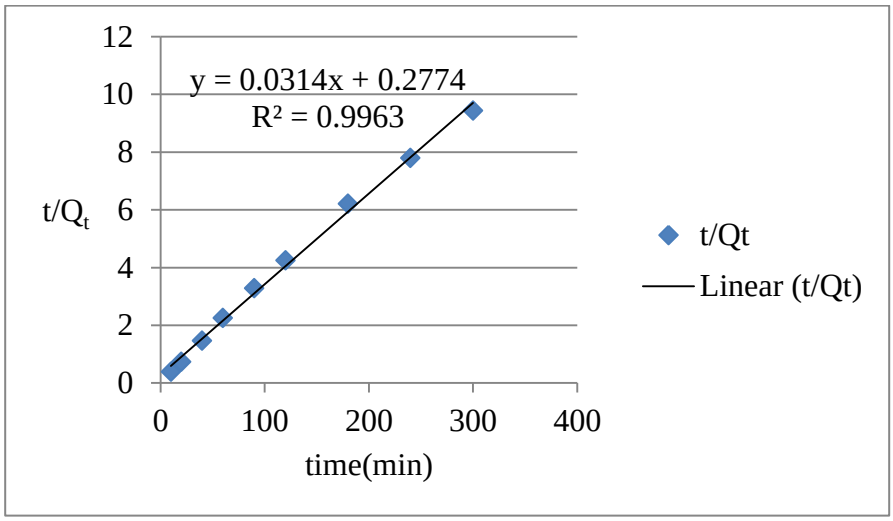

Figure 50: Presentation of the Adsorption of NB (40 ppm) on AC-H_2SO_4 (0.025 g) as following pseudo-second order kinetics

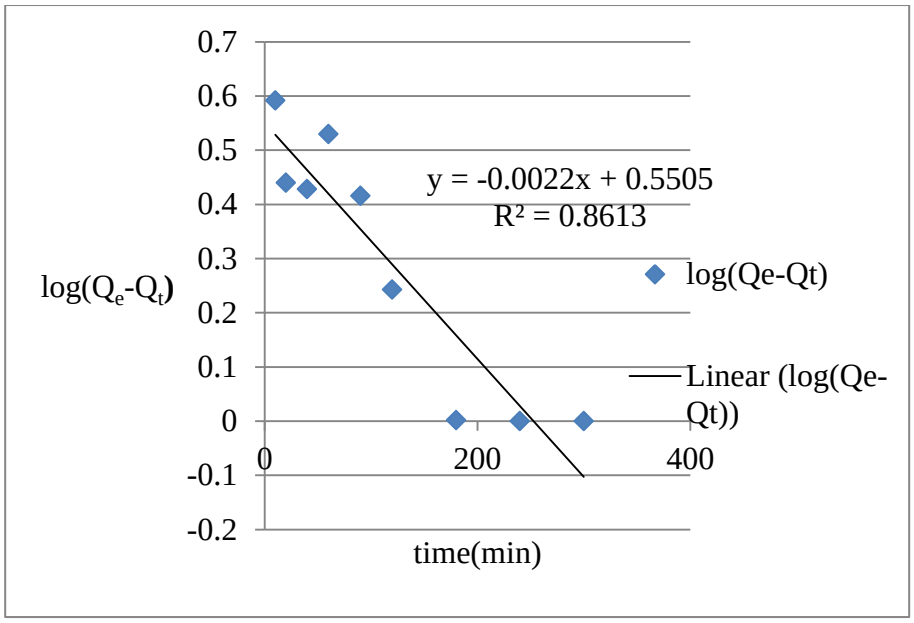

Figure 51: Presentation of the Adsorption of NB (40 ppm) on AC-H_2SO_4 (0.025 g) as following first order kinetics

			Pseudo-first order			Pseudo-2nd order		
Concentration of Dye	Dye Type	Experimental adsorption capacity(q_e)	Rate constant (K_1)	Theoretical adsorption capacity(q_e)	R^2	Rate constant(k_2)	Theoretical adsorption capacity(q)	R^2
10	CV-H_2SO_4 AC	7	0.0103	2.658	0.493	0.0099	7.434	0.998
25	CV-H_2SO_4 AC	11	0.0108	4.538	0.627	0.0038	12.224	0.992
40	CV-H_2SO_4-AC	11	0.0113	4.5519	0.461	0.0035	12.53	0.997
40	NB-H_2SO_4-AC	30	0.0051	3.55	0.861	0.0035	31.847	0.996
25	CV-HNO_3-AC	24	0.0126	9.5763	0.728	0.0025	25.38	0.999
10	CV-H_3PO_4-AC	5	0.0028	1.06	0.116	0.0099	12.56	0.995
25	CV-H_3PO_4-AC	5	0.0071	2.3254	0.539	0.0065	5.3966	0.994

Table 14: Comparison adsorption rate constants and calculated and experimental Q_e values when treating the adsorption processes with first and second order kinetics (for different concentrations of CV on AC-H_2SO_4,HNO_3,H_3PO_4 and NB on AC-H_2SO_4).

3.5 Thermodynamic Studies

3.5.1 Determination of ΔG, ΔH, and ΔS of the Adsorption of CV and NB on Palm leaflet Derived ACs

For the practical application for adsorption processes, it is important to understand the effect of temperature on the adsorption (for CV: Fig 53,59 ; for NB: Fig 56) The effect of temperature on the K_d values for CV and NB was studied at a constant dye concentration of 25 mg/l (25 ppm) and 40 ppm respectively , the results are shown in (for CV: Fig 62,64; For NB:63). The K_d values were calculated according to equation (18). The K_d value decreases with increasing reaction temperature (Table 15) from 30^0C to 43^0C ±1. The effect of temperature on sorption processes was analyzed by Van't Hoff plots, based on equation (19)

$$K_d = \frac{Q_e}{C_e} \quad (18)$$

$$lnK_d = \frac{\Delta S^0}{2.303R} - \frac{\Delta H^0}{2.303RT} \quad (19)$$

$$\Delta G^0 = \Delta H^0 - T\Delta S^0 \quad (20)$$

Where K_d is the distribution coefficient, T (K) is the absolute temperature, R is the gas constant (8.314 J/ (molK)), ΔS^o is the entropy change (J/mol) and ΔH^o is the enthalpy change (kJ/mol). Figure (62) shows a good linearity for the plot of ln K_d vs. T^-

[1]. The values of ΔH^o and ΔS^o were obtained from it. ΔG^o values were computed for each temperature by the Helmholtz relation (equation 20). In the case of the adsorption of CV on AC-H_2SO_4, the values of ΔH^o and ΔS^o were found to be -19.69 ($kJmol^{-1}\,k^{-1}$) and -.0617 ($kJmol^{-1}\,k^{-1}$), respectively. The values of of ΔH^o and ΔS^o associated with the adsorption of NB on AC-H_2SO_4 and CV on AC-H_2SO_4 and AC-HNO_3, along with the ΔG^o values, are shown in Table (16). The negative ΔH^o value indicates an exothermic process. The negative value of ΔS^o shows a decrease in the disorder and randomness at the solid-solution interface during the adsorption of the CV dye on the AC. The spontaneity of the sorption process is demonstrated by the negative value of ΔG^o. The absolute values of ΔG^o decrease with increasing temperature due to the negative value of ΔS^o. The thermodynamic data indicates that the sorption is governed mainly by a physisorption process. If the sorption process is solely physisorption, an increase in temperature will be lead to a decrease in sorption capacity.

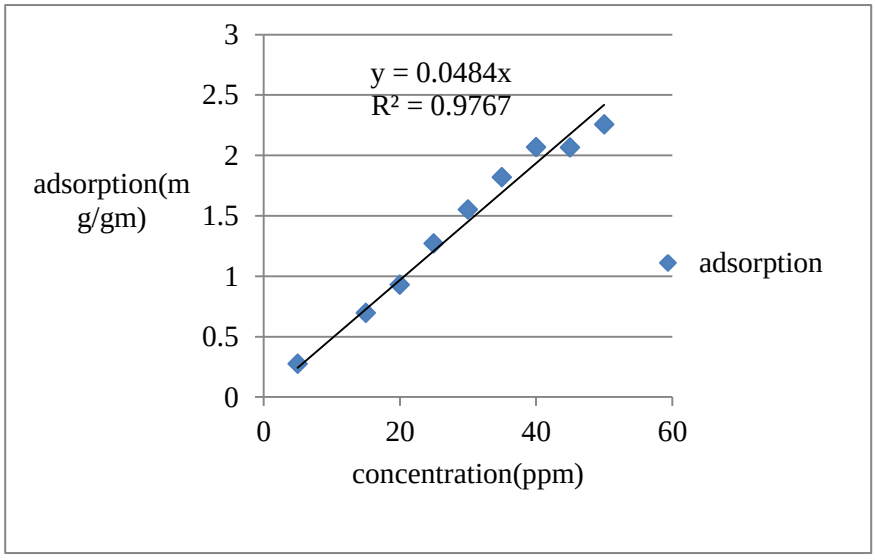

Figure 52: Typical calibration curve for CV (conc. vs. adsorption at λ = 305 nm)

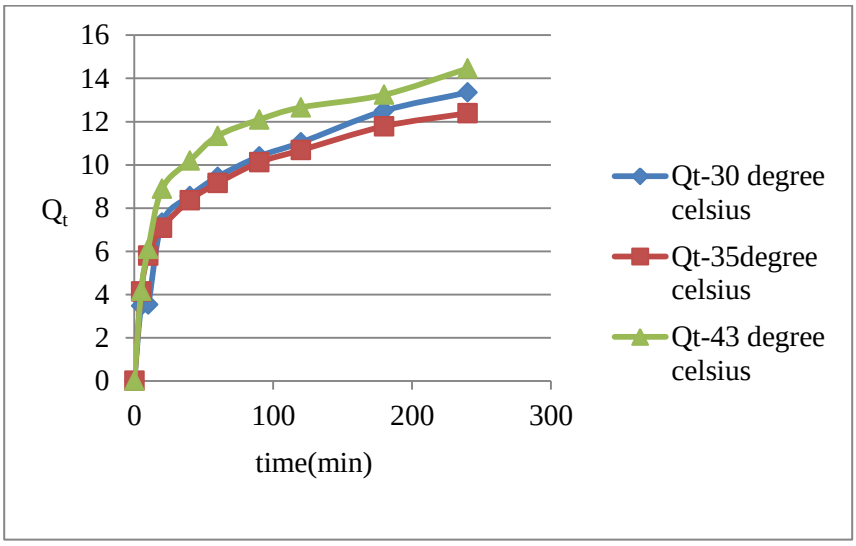

Figure 53: Effect of temperature on the adsorption of CV on AC-H_2SO_4 at 30^0, 35^0 and 43^0 C

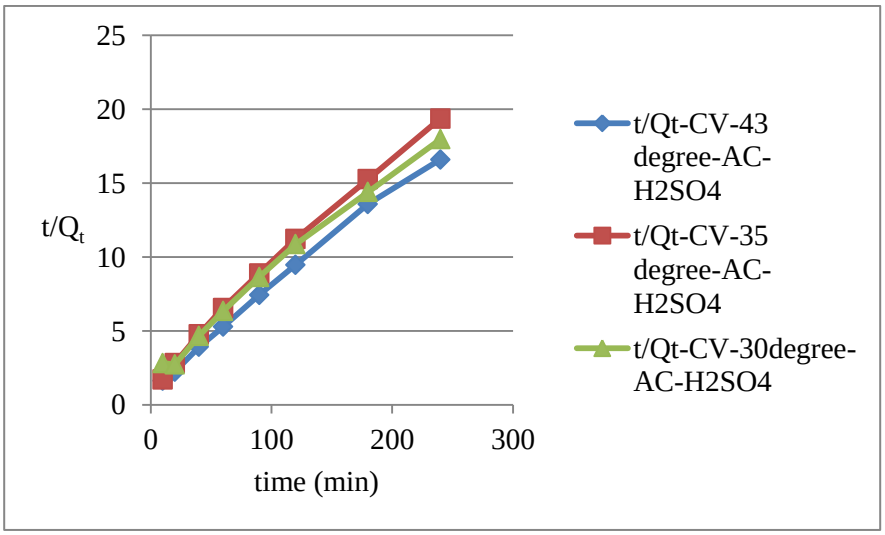

Figure 54: Presentation of the adsorption of CV on AC-H_2SO_4 at different temperatures as following second order kinetics

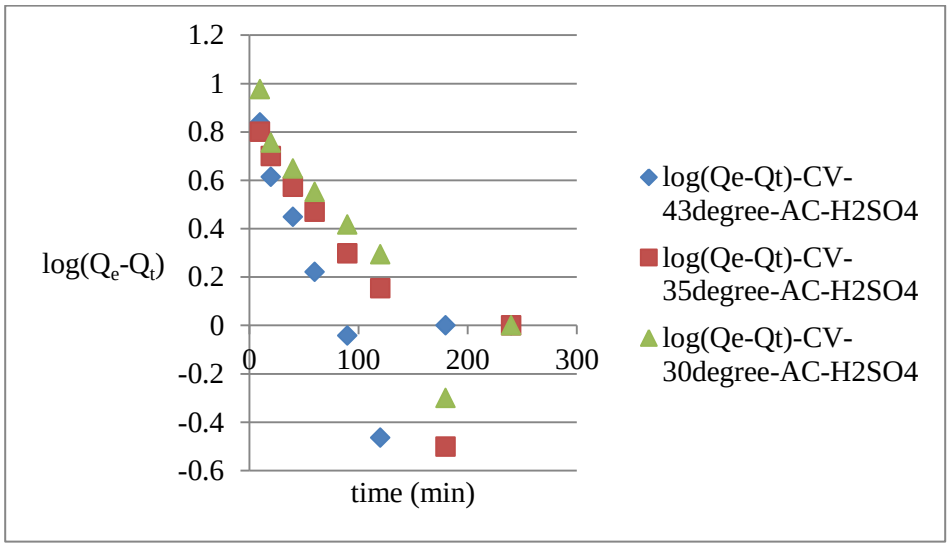

Figure 55: Presentation of the adsorption of CV on AC-H_2SO_4 at different temperatures as following first order kinetics

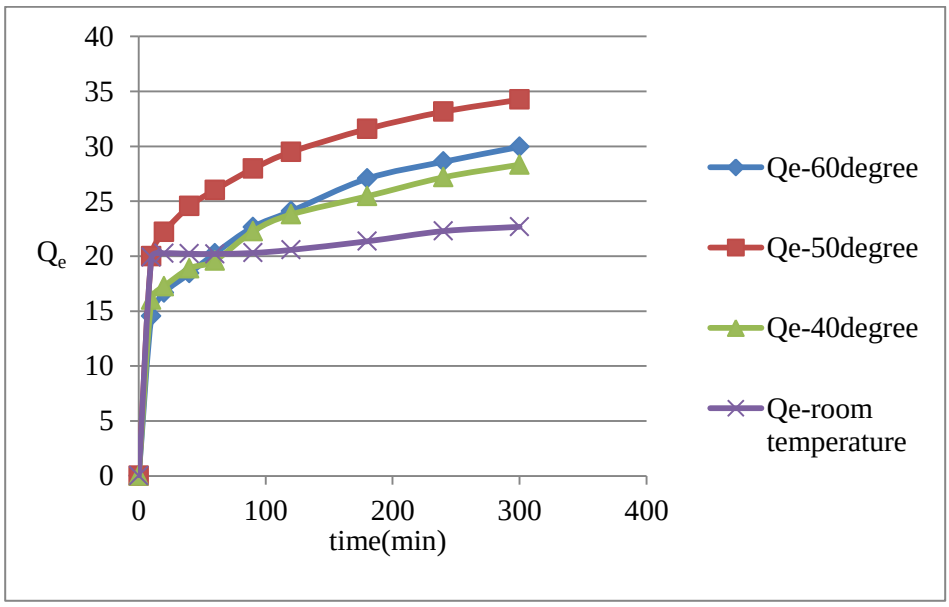

Figure 56: Effect of temperature on the adsorption of NB (40ppm) on AC-H_2SO_4

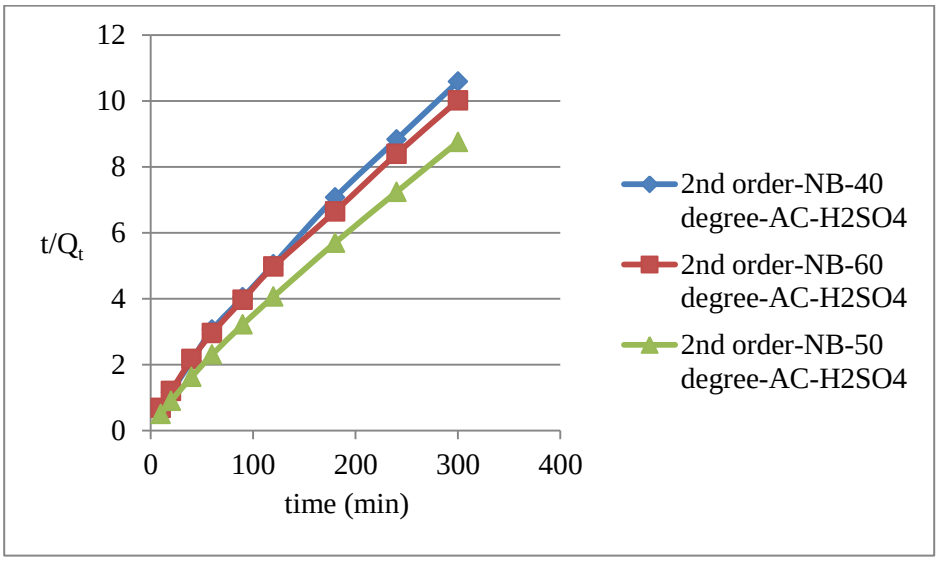

Figure 57: Presentation of the adsorption of NB on AC-H_2SO_4 at different temperatures as following second order kinetics

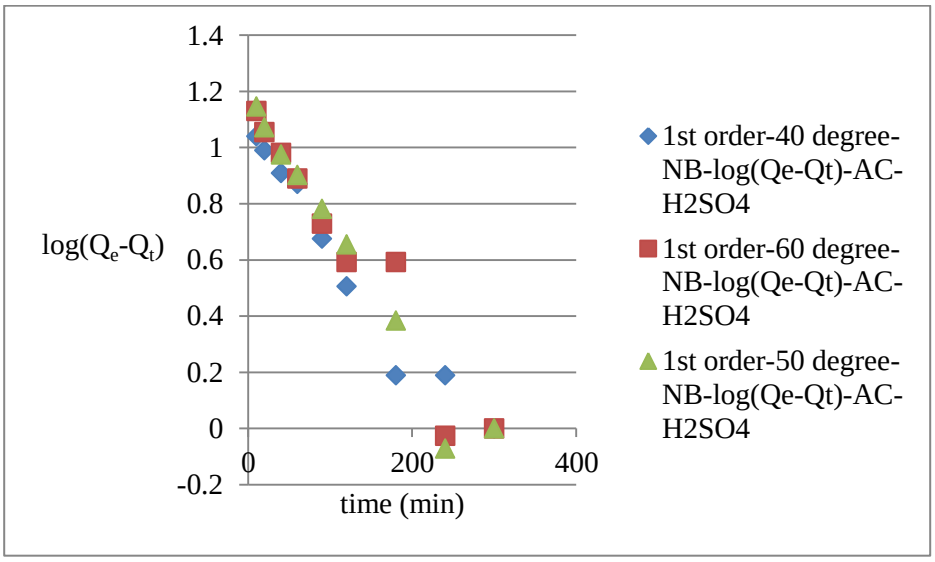

Figure 58: Presentation of the adsorption of NB on AC-H_2SO_4 at different temperatures as following first order kinetics

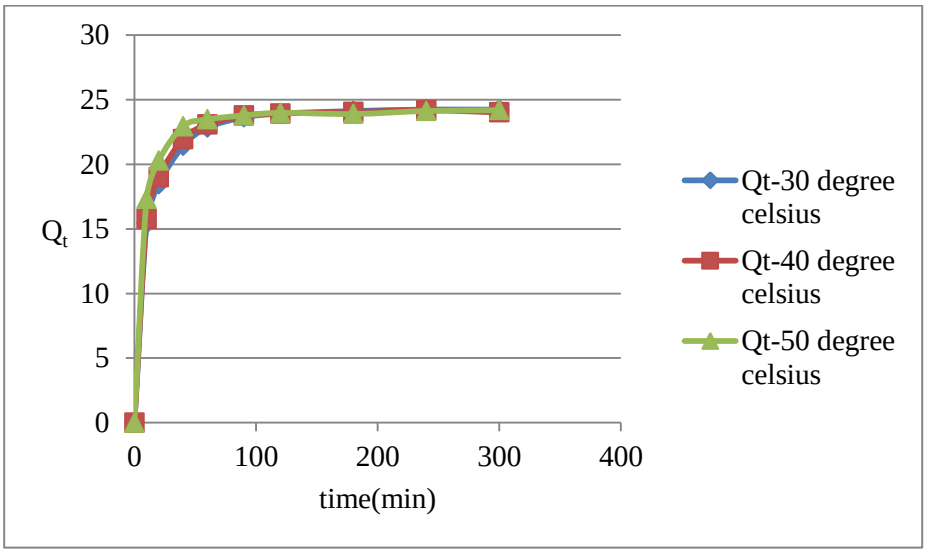

Figure 59: Adsorption of CV on AC-HNO_3 at different temperatures

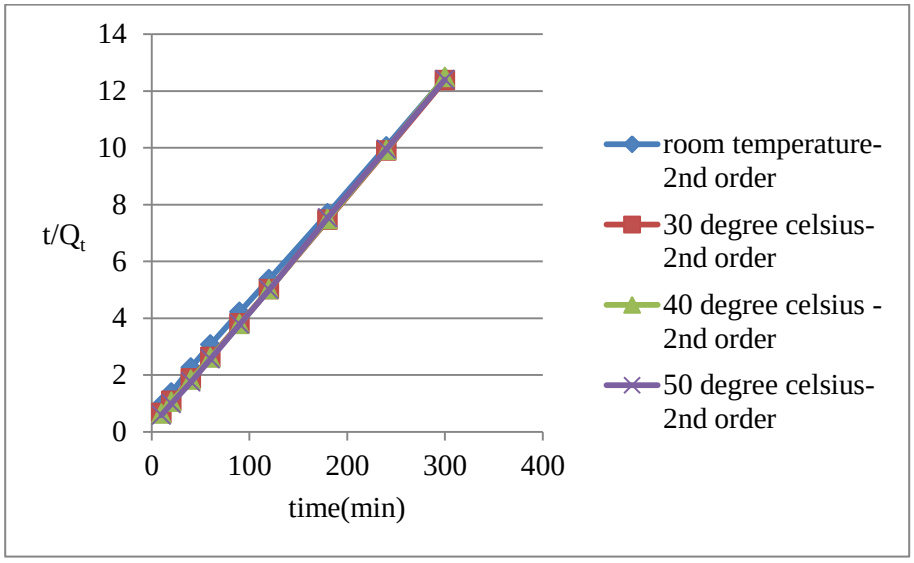

Figure 60: Presentation of the adsorption of CV on AC-HNO_3 at different temperatures as following second order kinetics

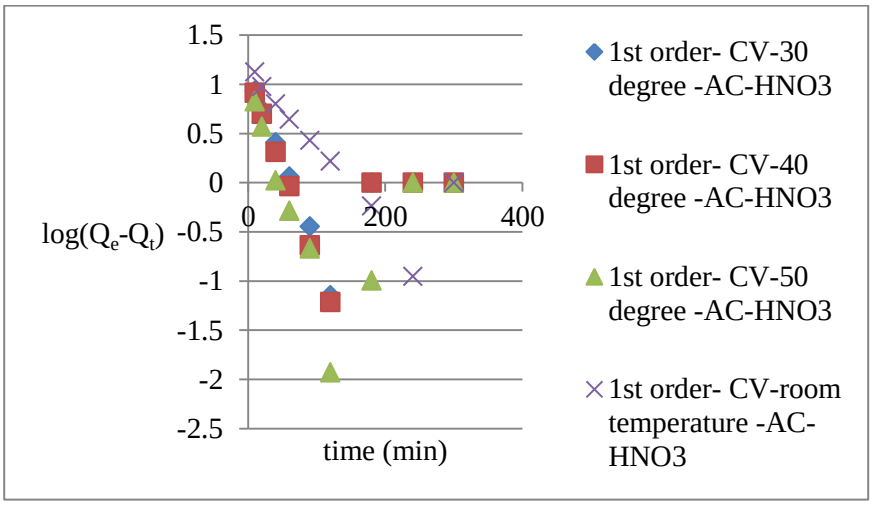

Figure 61: Presentation of the adsorption of CV on AC-HNO_3 at different temperatures as following first order kinetics

T^0C	Dye type	Activation method	(T+273)K	1/T	Qe	Ce	LnK_d
30^0C	CV	H_2SO_4	303	0.0033	13	11.033057	0.164053201
35^0C	CV	H_2SO_4	308	0.00324675	12.1	10.67849687	0.125
43^0C	CV	H_2SO_4	316	0.0031645	13	12.6569	0.027
40^0C	NB	H_2SO_4	313	0.003195	27	23.799	0.126
50^0C	NB	H_2SO_4	323	0.003096	34	29.48	0.143
60^0C	NB	H_2SO_4	333	0.003003	28	25.09	0.110
30^0C	CV	HNO_3	303	0.0033	24	23.928	0.003
40^0C	CV	HNO_3	313	0.003195	24	23.938	0.002
50^0C	CV	HNO_3	323	0.003096	24	23.988	0.0005

Table 15: Distribution of the values of co-efficient (K_d) for CV and NB onto AC at different temperatures

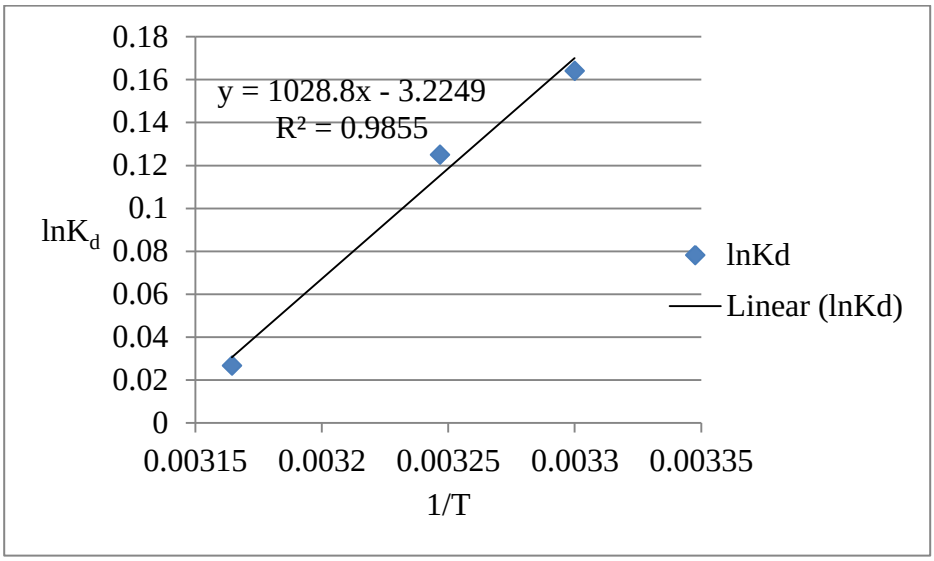

Figure 62: Determination of thermodynamic parameters (ΔG,ΔH,ΔS) for the adsorption of CV on AC-H_2SO_4

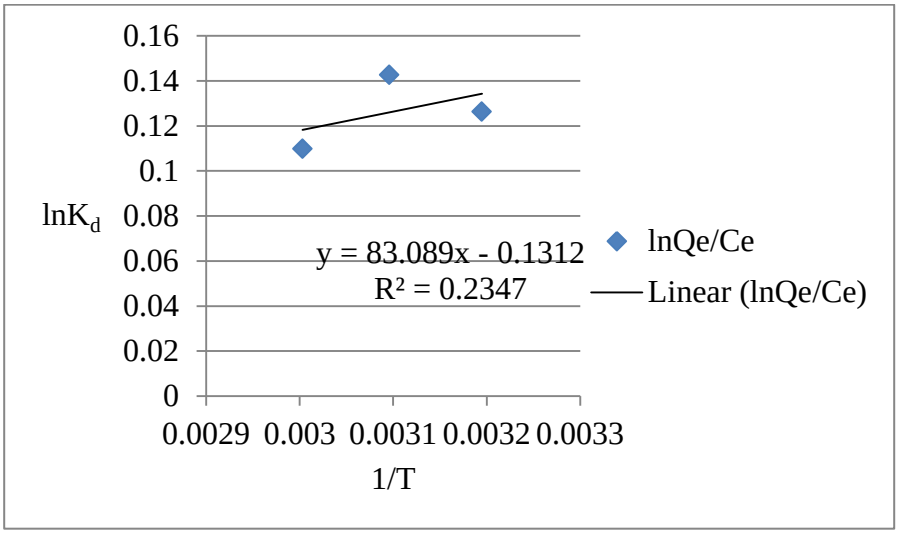

Figure 63: Determination of thermodynamic parameters (ΔG,ΔH,ΔS) for the adsorption of NB on AC-H_2SO_4

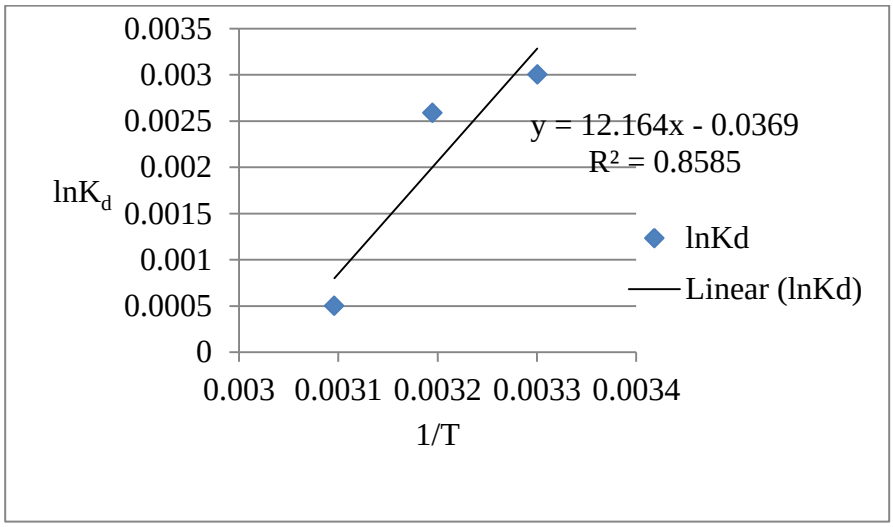

Figure 64: Determination of thermodynamic parameters (ΔG,ΔH,ΔS) for the adsorption of CV on AC-HNO_3

Temperature (K)	Dye	Activation method	ΔG^0 (kJmol^{-1} k^{-1})	ΔH^0 (kJmol^{-1} k^{-1})	ΔS^0 (kJmol^{-1} k^{-1})	R^2
303	CV	H_2SO_4	-0.413	-19.69	-0.0617	0.9855
308	CV	H_2SO_4	-0.32			
316	CV	H_2SO_4	-0.07			
313	NB	H_2SO_4	-0.328	-1.5909	-0.0025	0.2347
323	NB	H_2SO_4	-0.003			
333	NB	H_2SO_4	-0.002			
303	CV	HNO_3	-0.008	-0.2329	-0.000706	0.8585
313	CV	HNO_3	-0.007			
323	CV	HNO_3	-0.0013			

Table 16: Thermodynamic parameters calculated for the adsorption of CV and NB on AC-H_2SO_4 and of CV on AC-HNO_3

3.5.2 Determination of Activation Energy

The activation energy is calculated from the linear form of the Arrhenius equation (21)

$$lnk_2 = lnk_A - \frac{E_a}{RT} \quad (21)$$

With k_A being the pre-exponential factor and Ea the activation energy of the sorption process (kJ mol^{-1}). After plotting ln (k_2) as a function of 1/T (Fig. 65-67), the values of activation energy are determined from the slope of the regression line and k_0 from the intercept. The apparent activation energies are 42.88 KJ mol^{-1} for the sorption of CV on AC-HNO_3 and 9.14 kJ mol^{-1} and 31.57 kJ mol^{-1}, respectively, for the sorption of NB and CV on AC-H_2SO_4 (Table 18).

These findings were presented as evidence that most likely there is also chemical adsorption involved in the rate-controlling step for CV.

The sorption process of CV on AC-HNO_3 necessitates a higher activation energy than on AC-H_2SO_4, which could be explained by the potentially more microporous nature of AC-HNO_3 requiring more energy for the diffusion of the sorbate.

It is known that when the activation energy is low in the sorption process, the reaction rate can be controlled by an intra-particle diffusion mechanism, and hence it can be concluded that the adsorption of NB on AC-H_2SO_4-AC is governed by interactions of physical nature (ie., mainly physisorption is involved).

Moreover, Q_e values, calculated from the linear plots of t/q_t versus t for a pseudo-second-order kinetic equation, show a good agreement with experimental q_e values (Table 17). Consequently, it can be confirmed that the adsorption of CV and NB onto activated carbon obeys a pseudo-second-order reaction rate.

Temperature	Activation method	Dye		Pseudo-first order			Pseudo-2nd order		
			Experimental adsorption capacity(q_e) (mg/g)	Rate constant (K_1) (1/min)	Theoretical adsorption capacity(q_e) (mg/g)	R^2	Rate constant (k_2) (mg/g·min)	Theoretical adsorption capacity (q) mg/g	R^2
23°C	HNO_3	CV	24	0.012	9.58	0.072	$2.48X10^{-3}$	25.3	0.999
30^0C	HNO_3	CV	24	0.790	2.20	0.154	$7.21x10^{-3}$	24.81	0.999
40^0C	HNO_3	CV	24	$4.84x10^{-3}$	1.78	0.110	$9.32x10^{-3}$	24.50	0.999
50^0C	HNO_3	CV	24	$4.80x10^{-3}$	0.95	0.068	0.0127	24.4	0.999
23°C	H_2SO_4	NB	22	$2.99x10^{-3}$	1.98	0.647	$6.90x10^{-3}$	22.7	0.998
40^0C	H_2SO_4	NB	27	$8.52x10^{-3}$	10.9	0.956	$1.56x10^{-3}$	29.5	0.993
$50\ ^0$C	H_2SO_4	NB	34	$9.90x10-^{3}$	14.5	0.966	$1.63x10^{-3}$	35.5	0.996
60^0C	H_2SO_4	NB	28	$9.44x10^{-3}$	13.7	0.943	$1.19x10^{-3}$	31.6	0.992
30^0C	H_2SO_4	CV	13	0.0108	7.26	0.834	$2.22X10^{-3}$	14.7	0.993
35^0C	H_2SO_4	CV	12.1	0.0111	6.10	0.781	$4.15X10^{-3}$	13.0	0.994
43^0C	H_2SO_4	CV	13	$9.44X10^{-3}$	4.34	0.534	$3.93X10^{-3}$	14.9	0.996

Table 17: Parameters of the activation energy for the sorption processes of CV and NB as obtained from the effect of temperature the sorption processes of CV (on AC=15.6 M HNO_3) and of NB (on AC-H_2SO_4) - comparison of 1^{st}&2^{nd} order kinetics.

Temperature	Dye	Activation method	T+273	1/T	Rate constant($k2$)	LnK_2	E_a(KJ/mol)
23^0C	CV	HNO_3	296	$3.38X10^{-3}$	$2.48X10^{-3}$	-5.999	42.88
30^0C	CV	HNO_3	303	$3.30X10^{-3}$	$7.21x10^{-3}$	-4.932	
40^0C	CV	HNO_3	313	$3.19X10^{-3}$	$9.32x10^{-3}$	-4.676	
50^0C	CV	HNO_3	323	$3.09X10^{-3}$	0.0127	-4.36	
40^0C	NB	H_2SO_4	313	$3.20X10^{-3}$	$1.56x10^{-3}$	-6.463	9.14
50^0C	NB	H_2SO_4	323	$3.10X10^{-3}$	$1.63x10^{-3}$	-6.421	
60^0C	NB	H_2SO_4	333	$3.00X10^{-3}$	$1.19x10^{-3}$	-6.25	
30^0C	CV	H_2SO_4	303	$3.30X10^{-3}$	$2.22X10^{-3}$	-6.11	31.57
35^0C	CV	H_2SO_4	308	$3.25X10^{-3}$	$4.15X10^{-3}$	-5.4846	
43^0C	CV	H_2SO_4	316	$3.17X10^{-3}$	$3.93X10^{-3}$	-5.539	

Table 18: Calculation of the activation energy of sorption processes of NB and CV on AC-H_2SO_4 and of CV on AC-HNO_3-AC on NB and CV

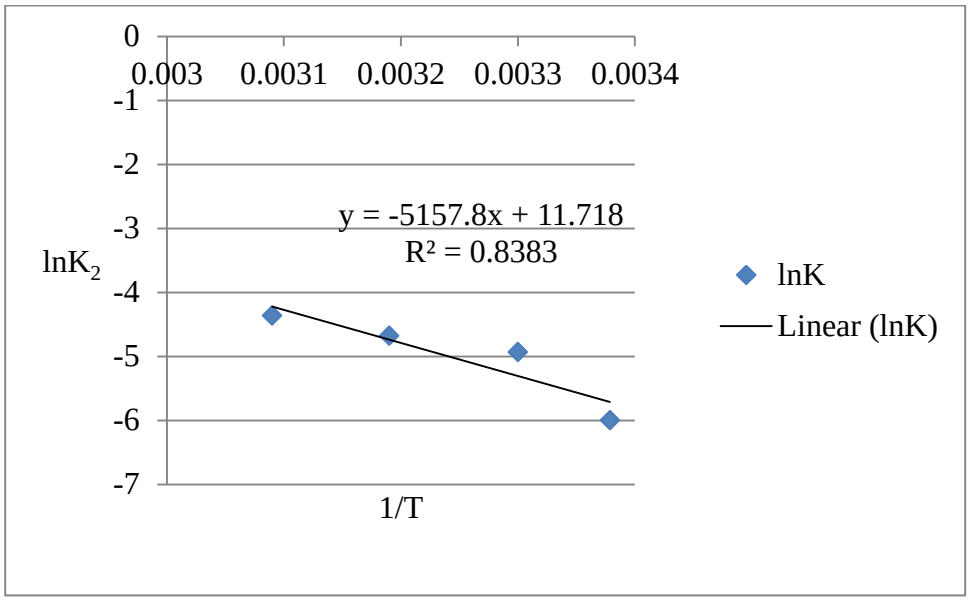

Figure 65: Determination of the activation energy for the sorption of CV on AC-HNO_3

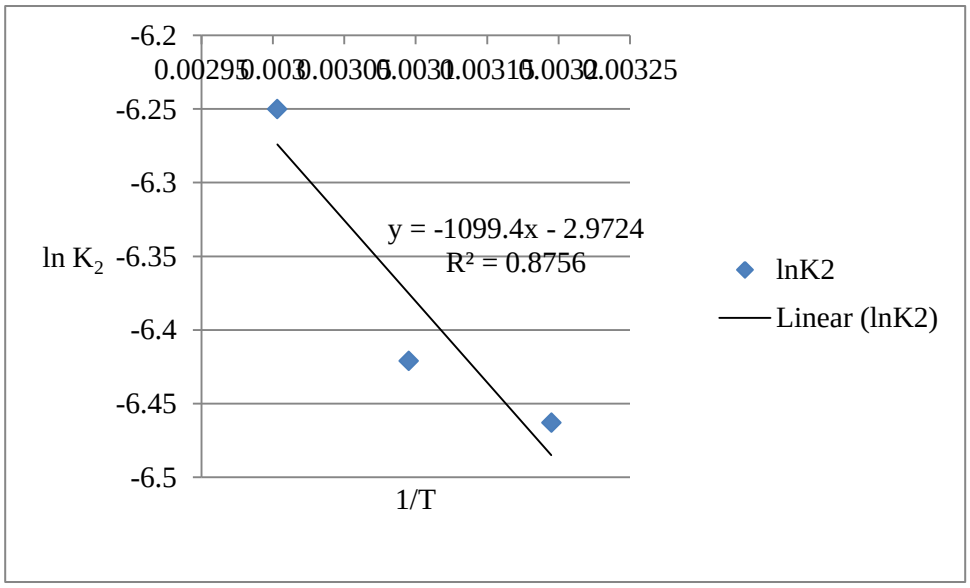

Figure 66: Determination of the activation energy for the sorption of NB on AC-H_2SO_4

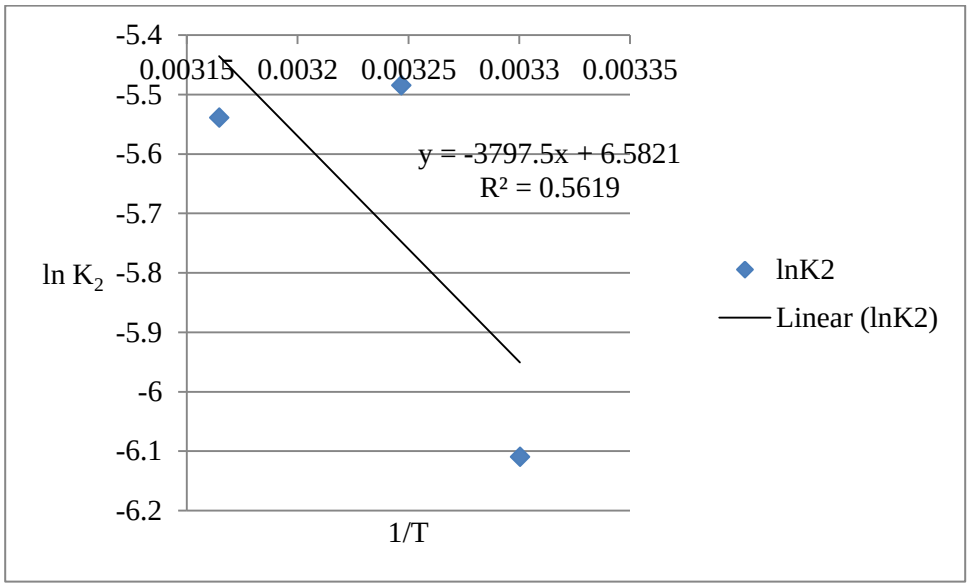

Figure 67: Determination of the activation energy for the sorption of CV on AC-H_2SO_4

The adsorption of CV and NB can be controlled by either the mass transfer through the boundary film of the liquid or by the intra-particular mass transfer.

In a batch reactor with rapid stirring, there is also a possibility that the transport of adsorbate ions from the solution into the pores of the adsorbent is the rate controlling step. This possibility was tested in terms of a graphical relationship between the amount of dye adsorbed and the square root of time at different initial dye concentrations (Fig. 68 and 69). For CV as adsorbate, all the plots have the same general aspect. They all have an initial curved portion, followed by an intermediate linear portion. The initial portion of these plots is related to mass transfer and the linear part is due to intraparticle diffusion. However, no linear relation is observed for NB and the regression coefficient is never higher than 0.93. This result clearly indicates that the uptake rate is not governed by mass transfer through a liquid film boundary, i.e., by a convective mass transfer. NB most probably is transported from the bulk of the solution into the solid

phase by intra-particle diffusion, which is often the rate limiting step in many adsorption processes.

Overall, it can be noted that adsorption process of NB is well correlated with an intra-particle diffusion model.

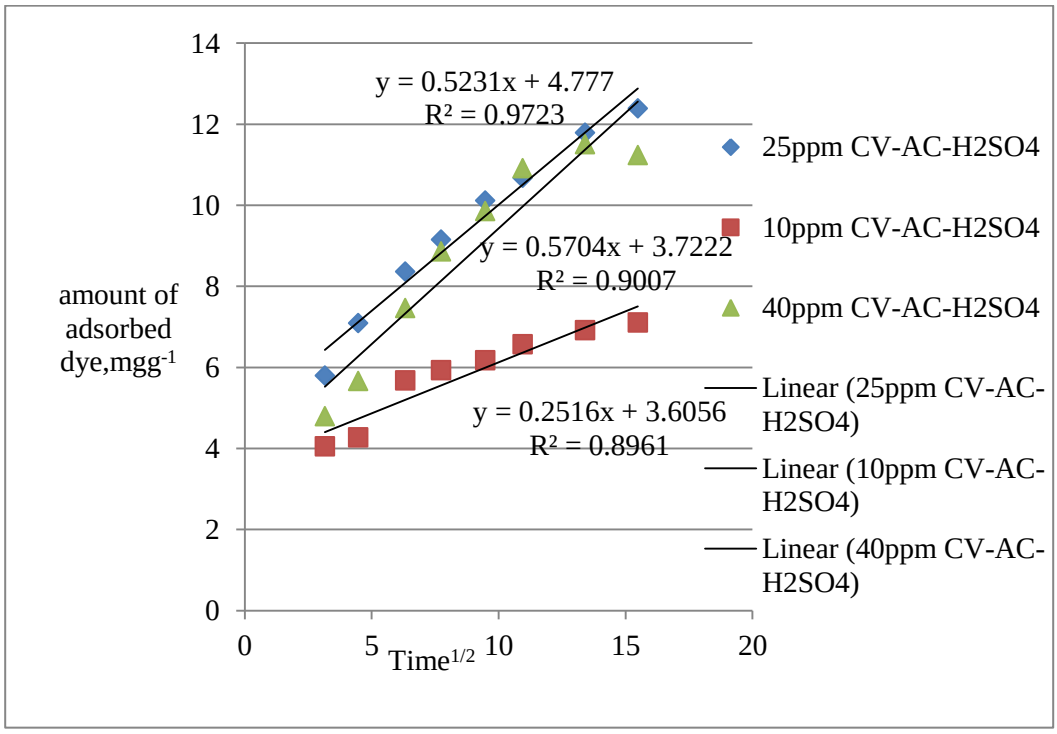

Figure 68: Intraparticle and pore diffusion for the adsorption of CV onto AC-H_2SO_4 at different concentrations

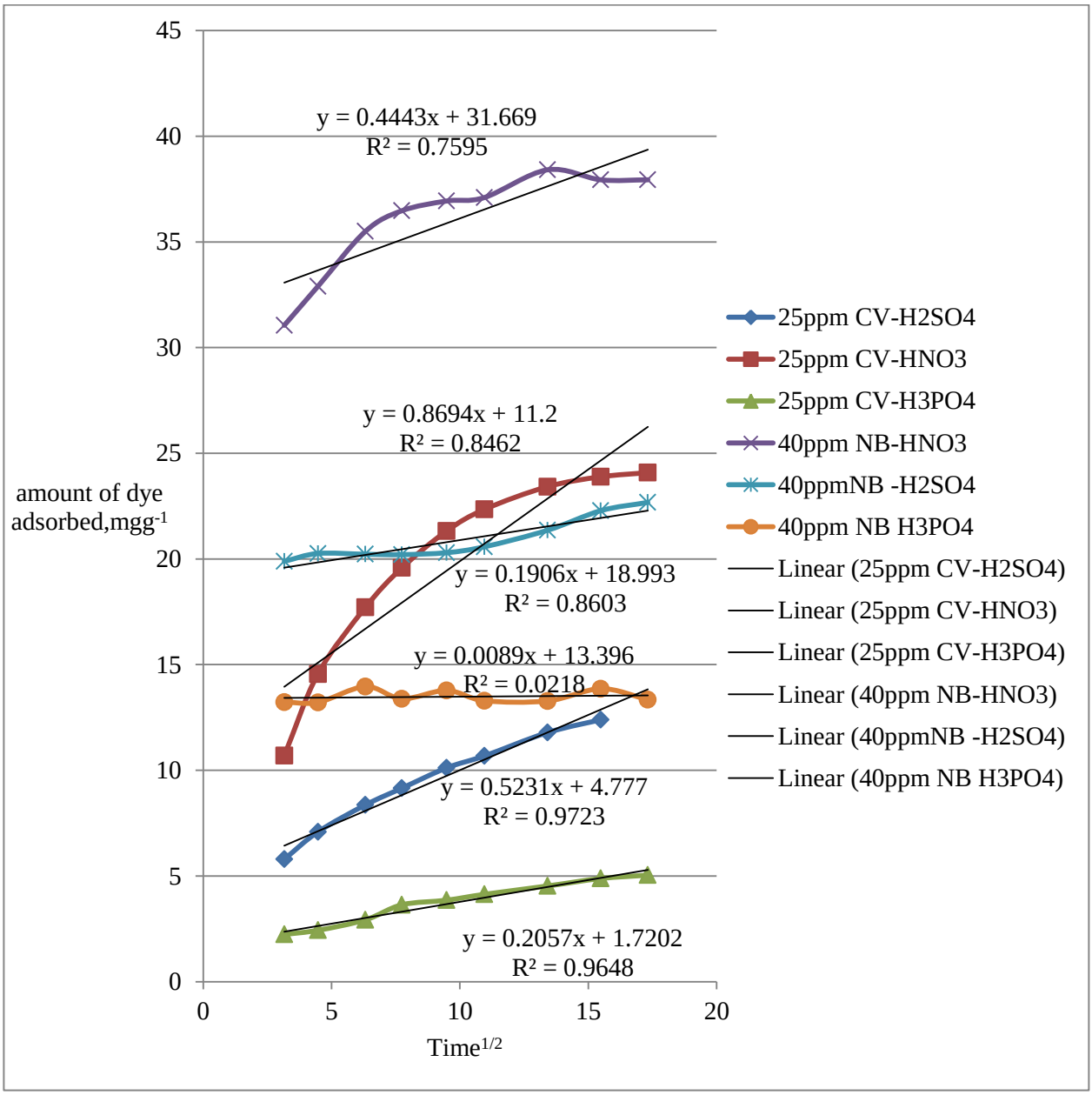

Figure 69: Intraparticle and pore diffusion for adsorption of CV and NB onto different types of AC at different concentrations of the sorbate

3.6 Dynamic Sorption Studies

3.6.1 Experimental Procedure

Dynamic experiments were carried out to explore the feasibility of using the activated carbon prepared above for the purification of dye-polluted water in larger quantities.

For constructing and modeling the dynamic sorption experiment, the breakthrough curve of the sorbate is used directly. A column (see methodology) was filled with 5.5 g of AC-H_3PO_4. The dye was injected in to column from the bottom, and samples were collected at different time intervals and analysed for dye in the effluent by UV-VIS spectrophotometer. The obtained data is presented in Fig. 70 and 71. After exhaustion, the column was regenerated using 1 M HNO_3. From Fig. 70 and 71, it can be seen that AC from date palm leaflet, activated with phosphoric acid, could be used for the purification of water polluted with CV (10 ppm) dye. The breakthrough time for the first adsorption experiment is 42.5 h, after 2.22 L completely cleaned water had been collected. However, after the first recycling of the column, a breakthrough time of 24.3 h was attained, with 1.45 L of completely cleaned water.

So, the regenerated column could be used again for another dynamic sorption experiment but the efficiency for the second adsorption cycle is less than the first one. The decrease of adsorption capacity of the column between the first cycle and the second one may be attributed to the incomplete removal of the adsorbed dye from the activated carbon surface. The only regenerated sites are the sites occupied by CV dye molecules via physical adsorption or ion exchange. Sites with chemically adsorbed CV

could not be regenerated; that is why the second cycle of adsorption is less than the first one.

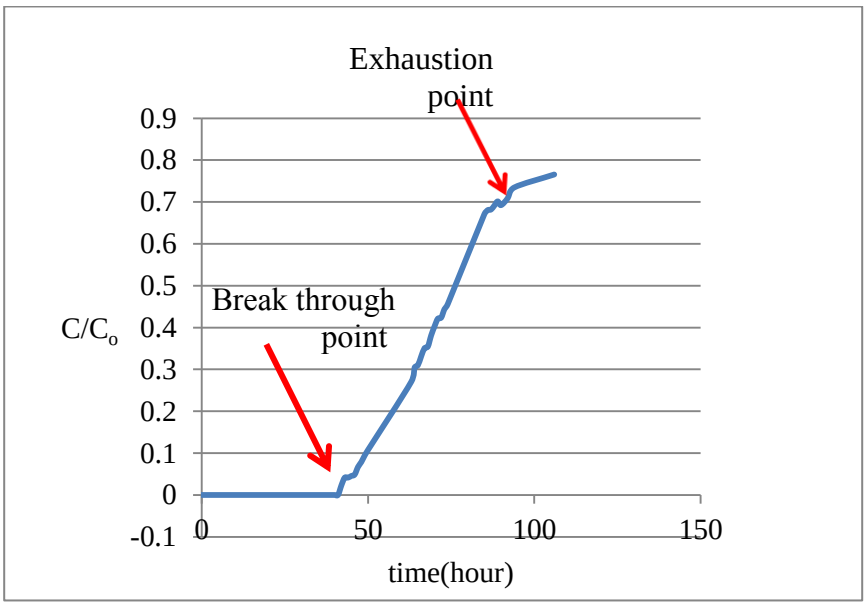

Figure 70: Dynamic adsorption curve for CV on freshly prepared AC-H_3PO_4

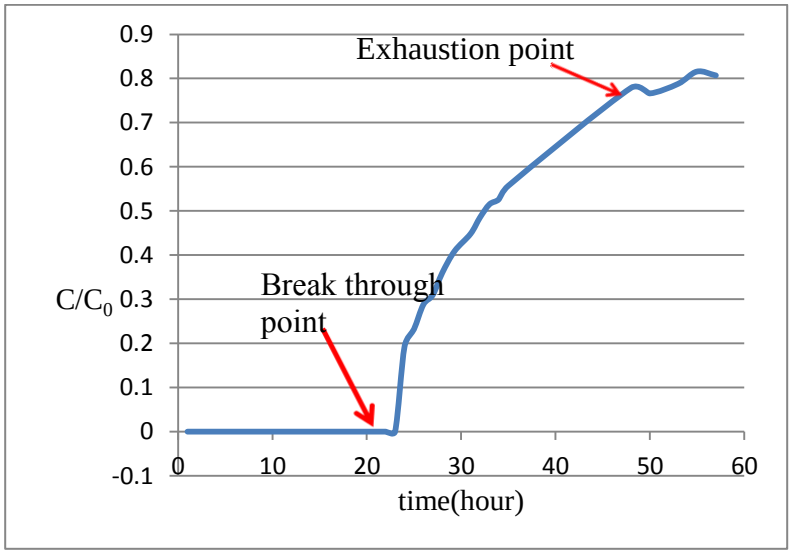

Figure 71: Dynamic adsorption curve for CV after 1st recycling of AC-H_3PO_4

3.6.2 Modelling of the Dynamic Adsorption Behaviour

Typically, the dynamic adsorption behaviour can be examined by applying Adam's–Bohart, Yoon–Nelson and Thomas models.

3.6.2.1 Adam's–Bohart Model

The basic mathematical correlation that relates C_t/C_0 and column operating time (t) for the purification of a flowing system was originally proposed by Bohart and Adam (Bohart & Adams, 1920) and can be presented as:

$$ln\frac{C_t}{C_0} = K_{AB}C_0t - K_{AB}N_0\frac{Z}{F} \qquad (22)$$

where C_0 and C_t (mg/L) are the inlet and effluent concentrations, K_{AB}(L/mg min) is the adsorption rate constant, F (cm/min) is the linear velocity determined by dividing the flow rate (mL/min) by the column sectional area (cm^2), N_0 (mg/L) is the saturation concentration,

t is the flow time (min), and Z (cm) is the adsorbent bed depth. This approach focuses on the estimation of characteristic parameters such as the saturation concentration N_0 (mg/L) and the adsorption rate constant, $k_{AB,}$ using a chemical kinetic rate expression. According to the model, the adsorption rate is proportional to both residual capacity of the adsorbent, and the concentration of the adsorbing species. The applicability of the Adam's–Bohart model was determined using a linear plot of ln C_t /C_0 against time (t) with a slope $k_{AB}C_0$ and an intercept, $k_{AB}N_0Z/F$. The validity of the adsorption equation was judged by determination of the coefficient R^2.

Although the Adam's–Bohart model provides a comprehensive approach for evaluating the adsorption-columns, its validity is limited to the range of conditions used. There is a good agreement between the experimental data and predicted values for the Adam's–Bohart model with R^2 of 0.8687 and 0.8194, respectively, for the adsorption of CV on pristine AC and recycled AC (Table 19).

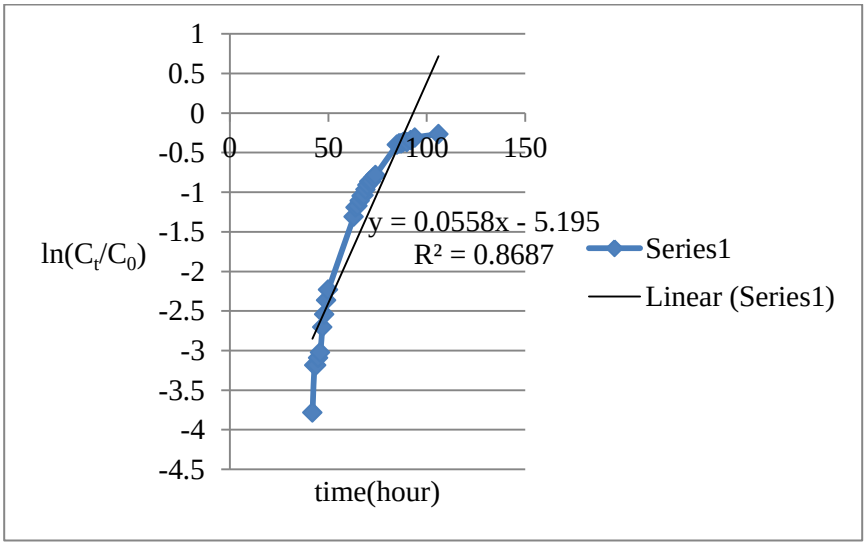

Figure 72: Presentation of the dynamic sorption data (CV on AC-H_3PO_4) in form of Adam's-Bohart model

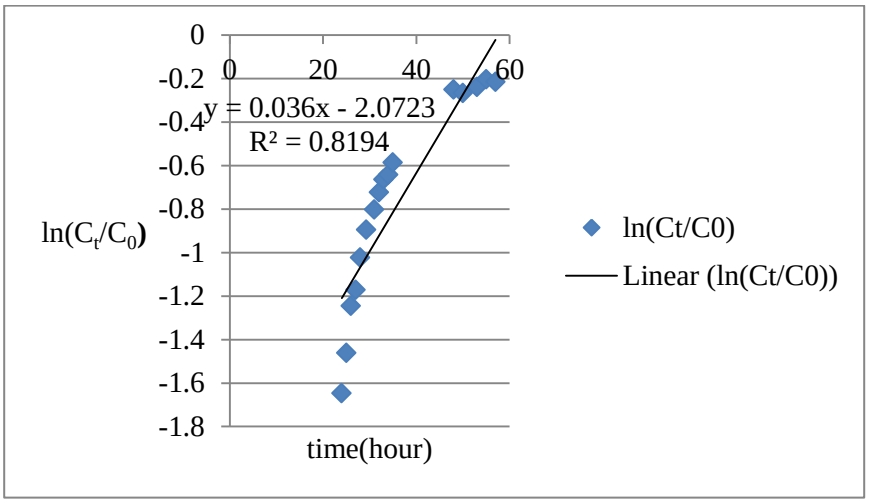

Figure 73: Presentation of the dynamic sorption data (CV on AC-H_3PO_4), using a recycled column, in form of Adam's-Bohart model

Bed height (cm)	Flow rate (ml/h)	Adam's –Bohart rate constant K_{AB}(L/mg.h)	Saturation concentration N_0(mg/L)	R^2
14	52.8	0.025	5079.6	0.8687
14	50.4	0.016	3022.1	0.8194

Table 19: Adam's-Bohart fitting parameters for the adsorption of CV (10 ppm) onto AC-H_3PO_4 in a dynamic experiment with a column of 0.45 cm in diameter.

3.6.2.2 Yoon–Nelson Model

A relatively simple theoretical model addressing the breakthrough behavior has been developed by Yoon and Nelson (Yoon &Nelson,1984). The model was derived based on the assumption that the rate of decrease in the probability of adsorption for each adsorbate molecule is proportional to the probability of adsorbate adsorption and the adsorbate breakthrough on the adsorbent. The mathematical equation of Yoon–Nelson model can be written as:

$$ln\frac{C_t}{C_0-C_t} = K_{YN}t - \tau K_{YN} \quad (23)$$

Where K_{YN} is the Yoon–Nelson velocity rate constant (1/min) and τ is the time (min) required for 50% of adsorbate breakthrough. A linear plot of ln (Ct/C_0-C_t) against the sampling time, *t*, was employed to determine the model parameters, K_{YN} and τ. Yoon-Nelson velocity rate constant, K_{YN}, increased with increasing the bed flow rate. Inspection of our data (R^2 = 0.9502) indicated that the model gave a good fit for the experimental data of the adsorption of CV on AC-H_3PO_4 with the used bed height and feed flow rate. The result suggests that the dynamic adsorption process was well described by the Yoon–Nelson model, with a negligible effect of axial dispersion.

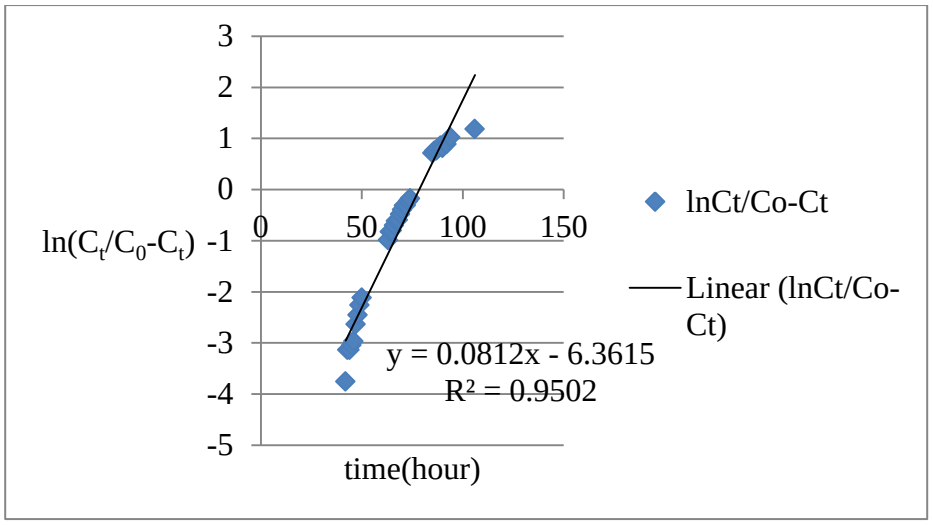

Figure 74: Presentation of the dynamic sorption data (CV on AC-H_3PO_4) in form of Yoon-Nelson model

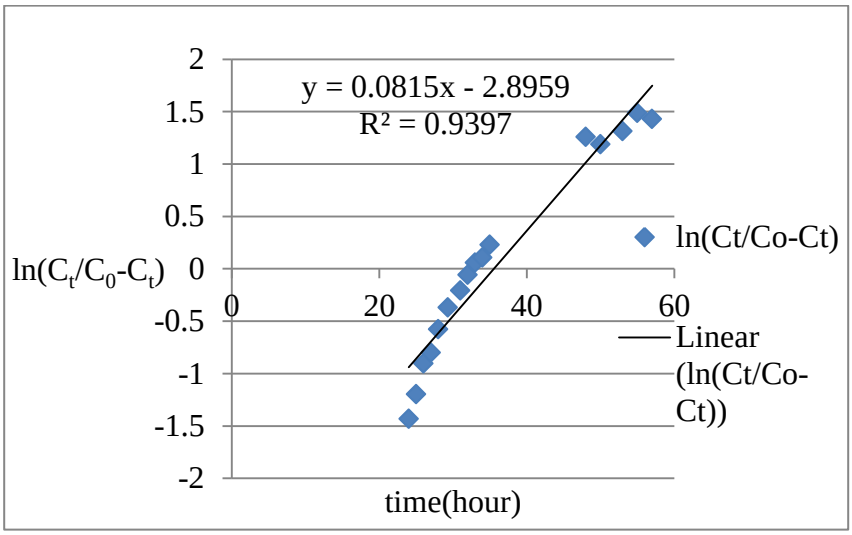

Figure 75: Presentation of the dynamic sorption data (CV on AC-H_3PO_4), using a recycled column, in form of Yoon-Nelson model

Flow rate (mL/min)	Yoon-Nelson velocity rate constant K_{YN}(L/mg.h)	τ,time(hour) for 50% of adsorbent break through	R^2
0.83	0.0812	78.34	0.9502
0.84	0.0815	35.53	0.9397

Table 20: Yoon–Nelson fitting parameters for the adsorption of CV (10 ppm) onto AC-H_3PO_4

Chapter 4: Conclusion

In this work, the use of the agricultural waste to address the problem of dye-loaded wastewater was addressed. For this purpose, three differently activated carbons were prepared from date palm leaflets and have been used successfully as an adsorbing agent for the removal of Crystal Violet (CV) and Nile Blue from aqueous solutions. The adsorption was influenced by various parameters such as temperature, initial dye concentration, different size of activated carbon (AC) and dose of adsorbent. The maximum adsorption of CV and NB dye on AC from the wastes of date palm leaves was obtained with AC prepared by the HNO_3 activation method. The removal efficiency increased with decreasing dye concentration and increasing dose of adsorbent. The Langmuir and Freundlich adsorption isotherm models were used for the description of the adsorption equilibrium of CV and NB dye onto activated carbon of date palm leaves. The data were in good agreement with the Langmuir isotherm rather than the Freundlich isotherm. It was shown that the adsorption of CV and NB onto AC best fit the pseudo second order model.

An intraparticle diffusion model developed by Weber and Morris was used to calculate the intraparticle diffusion coefficients. The adsorption is probably controlled by both external mass transfer and intraparticle diffusion.

Equilibrium data were validated with bench scale fixed bed column on a continuous basis. The result illustrated that the dynamic adsorption process was efficient for the adsorptive removal of CV with the dynamic adsorption capacities. Correlation coefficient determination (R^2) showed a good agreement with results predicted by the

Yoon–Nelson model rather than by the Adam's Bohart model, which implies versatility of the model for calculations for a potential scale up of the process.

Since date palm leaves, an agriculture solid waste locally available, were used in this study, the adsorption process is expected to be economically viable for wastewater treatment. Nevertheless, there are some problems that need to be addressed in the future. The carbon burn-off is too high, where the carbon burns off as carbon dioxide (another waste). The surface area achieved in the activations is still low. An activation of the date palm leaves in the absence of oxygen may be suitable to pursue. It was also realized that the reactive dyes Novacron Yellow S-3R and Novacron Deep Cherry S-D could not be adsorbed in sufficient quantity on the prepared activated carbons.

In the future, it is imagined that these reactive dyes will be removed by lignin based carbon, another agricultural waste, which would then have to be functionalized chemically.

Bibliography

Abo-Farha, S. A., Abdel-Aal, A. Y., Ashour, I. A., & Garamon, S. E. (2009). Removal of some heavy metal cations by synthetic resin purolite C100. Journal of hazardous materials, 169(1), 190-194.

Adams, C. D., & Gorg, S. (2002). Effect of pH and gas-phase ozone concentration on the decolorization of common textile dyes. *Journal of environmental engineering*, *128*(3), 293-298.

Ahmad, R. (2009). Studies on adsorption of crystal violet dye from aqueous solution onto coniferous pinus bark powder (CPBP). *Journal of hazardous materials*, *171*(1), 767-773.

Ahn, D. H., Chang, W. S., & Yoon, T. I. (1999). Dyestuff wastewater treatment using chemical oxidation, physical adsorption and fixed bed biofilm process. *Process Biochemistry*, *34*(5), 429-439.

Aksu, Z. (2001). Equilibrium and kinetic modelling of cadmium (II) biosorption by C. vulgaris in a batch system: effect of temperature. *Separation and Purification Technology*, *21*(3), 285-294.

Al-Kadhemy, M. F. H., & Abass, W. H. (2013). Optical properties of crystal violet doped PMMA films. *Research and Reviews on Polymer*, *4*(2), 45-51.

Anjaneyulu Y., Hima Bindu, V., (2001b). Application of mixed adsorbent (coconut shell activated carbon, OCSAC-fly ash China clay) for removal of basic dyes from industrial effluents. *J. Environ. Pollut. 8*: 117–121.

Anjaneyulu, Y., Chary, N. S., & Raj, D. S. S. (2005). Decolourization of industrial effluents–available methods and emerging technologies–a review. *Reviews in Environmental Science and Bio/Technology*, *4*(4), 245-273.

Baban, A., Yediler, A., & Ciliz, N. K. (2010). Integrated water management and CP implementation for wool and textile blend processes. *CLEAN–Soil, Air, Water*, *38*(1), 84-90.

Babić, B. M., Milonjić, S. K., Polovina, M. J., & Kaludierović, B. V. (1999). Point of zero charge and intrinsic equilibrium constants of activated carbon cloth. *Carbon*, *37*(3), 477-481.

Babu, B. R., Parande, A. K., Raghu, S., & Kumar, T. P. (2007). Cotton textile processing: waste generation and effluent treatment. *Journal of cotton science. 11*,141–153.

Bendahou, A., Dufresne, A., Kaddami, H., & Habibi, Y. (2007). Isolation and structural characterization of hemicelluloses from palm of Phoenix dactylifera L. *Carbohydrate Polymers*, *68*(3), 601-608.

Bhattacharyya, K. G., & Sarma, A. (2003). Adsorption characteristics of the dye, Brilliant Green, on Neem leaf powder. *Dyes and Pigments*, *57*(3), 211-222.

Bhattacharyya, K. G., & Sarma, N. (1997). Colour removal from pulp and paper mill effluent using waste products. *Indian journal of chemical technology*, *4*(5), 237-242.

Bohart, G. S., & Adams, E. Q. (1920). Behavior of charcoal towards chlorine. *J. Chem. Soc*, *42*(7).

Borrely, S. I., Cruz, A. C., Del Mastro, N. L., Sampa, M. H. O., & Somessari, E. S. (1998). Radiation processing of sewage and sludge. A review. *Progress in Nuclear Energy*, *33*(1), 3-21.

Bousher, A., Shen, X., & Edyvean, R. G. (1997). Removal of coloured organic matter by adsorption onto low-cost waste materials. Water Research, 31(8), 2084-2092.

Can, O. T., Kobya, M., Demirbas, E., & Bayramoglu, M. (2006). Treatment of the textile wastewater by combined electrocoagulation. *Chemosphere*, *62*(2), 181-187.

Canizares, P., Martínez, F., Rodrigo, M. A., Jiménez, C., Sáez, C., & Lobato, J. (2008). Modelling of wastewater electrocoagulation processes: Part I. General description and application to kaolin-polluted wastewaters. *Separation and Purification Technology*, *60*(2), 155-161.

Canizares, P., Martínez, F., Rodrigo, M. A., Jiménez, C., Sáez, C., & Lobato, J. (2008). Modelling of wastewater electrocoagulation processes: Part II: Application to dye-polluted wastewaters and oil-in-water emulsions. *Separation and Purification Technology*, *60*(2), 147-154.

Cardenas-Robles, A., Martinez, E., Rendon-Alcantar, I., Frontana, C., & Gonzalez-Gutierrez, L. (2013). Development of an activated carbon-packed microbial bioelectrochemical system for azo dye degradation. *Bioresource technology*, *127*, 37-43.

Carmen, Z., & Daniela, S. (2012). Textile organic dyes–characteristics, polluting effects and separation/elimination procedures from industrial effluents–a critical overview. In Organic Pollutants Ten Years After the Stockholm Convention-*Environmental and Analytical Update* (pp. 55-81). InTech: Croatia.

Cazetta, A. L., Vargas, A. M., Nogami, E. M., Kunita, M. H., Guilherme, M. R., Martins, A. C., ... & Almeida, V. C. (2011). NaOH-activated carbon of high surface area produced from coconut shell: Kinetics and equilibrium studies from the methylene blue adsorption. *Chemical Engineering Journal*, *174*(1), 117-125.

Chakraborty, S., Chowdhury, S., & Saha, P. D. (2011). Adsorption of Crystal Violet from aqueous solution onto NaOH-modified rice husk. *Carbohydrate Polymers*, *86*(4), 1533-1541.

Chakraborty, S., Purkait, M. K., DasGupta, S., De, S., & Basu, J. K. (2003). Nanofiltration of textile plant effluent for color removal and reduction in COD. *Separation and purification Technology*, *31*(2), 141-151.

CHAROENSRI, A., KOBAYASHI, F., KIMURA, A., & ISHII, J. (2006). Electrochemical Oxidation Process for Mineralization of Solvent. *Journal of Metals, Materials and Minerals*, *16*(2), 57-61.

Chen, G. (2004). Electrochemical technologies in wastewater treatment. *Separation and purification Technology*, *38*(1), 11-41.

Choy, K. K., McKay, G., & Porter, J. F. (1999). Sorption of acid dyes from effluents using activated carbon. Resources, *Conservation and Recycling*, *27*(1), 57-71.

Christie, R. (2014). *Colour chemistry*. Royal Society of Chemistry

Contaminant, A. O. (2014). Electrochemical Oxidation e A Versatile Technique for Aqueous Organic Contaminant Degradation. *Chemistry of Advanced Environmental Purification Processes of Water: Fundamentals and Applications*, 75.

Crini, G., & Badot, P. M. (2008). Application of chitosan, a natural aminopolysaccharide, for dye removal from aqueous solutions by adsorption processes using batch studies: A review of recent literature. *Progress in polymer science*, *33*(4), 399-447.

Das, K., Jain, B., & Patel, H. S. (2004). Nile Blue in Triton-X 100/benzene–hexane reverse micelles: a fluorescence spectroscopic study. *Spectrochimica Acta Part A: Molecular and Biomolecular Spectroscopy*, *60*(8), 2059-2064.

Dascalu, T., Acosta-Ortiz, S. E., Ortiz-Morales, M., & Compean, I. (2000). Removal of the indigo color by laser beam–denim interaction. *Optics and lasers in engineering*, *34*(3), 179-189.

Drogui, P., Elmaleh, S., Rumeau, M., Bernard, C., & Rambaud, A. (2001). Hydrogen peroxide production by water electrolysis: application to disinfection. *Journal of applied electrochemistry*, *31*(8), 877-882.

Duri, B. A., McKay, G., Geundi, M. E., & Wahab, M. A. (1990). Three-resistance transport model for dye adsorption onto bagasse pith. *Journal of Environmental Engineering*, *116*(3), 487-502.

El-Sayed, G. O. (2011). Removal of methylene blue and crystal violet from aqueous solutions by palm kernel fiber. *Desalination*, *272*(1), 225-232.

Foo, 5. 5. K., & Hameed, B. H. (2010). Insights into the modeling of adsorption isotherm systems. *Chemical Engineering Journal*, *156*(1), 2-10.

Foo, K. Y., & Hameed, B. H. (2010). Decontamination of textile wastewater via TiO 2/activated carbon composite materials. *Advances in colloid and interface science*, *159*(2), 130-143.

Fytianos, K., Voudrias, E., & Kokkalis, E. (2000). Sorption–desorption behaviour of 2, 4-dichlorophenol by marine sediments. *Chemosphere*, *40*(1), 3-6.

Georgiou, D., Aivazidis, A., Hatiras, J., & Gimouhopoulos, K. (2003). Treatment of cotton textile wastewater using lime and ferrous sulfate. *Water Research*, *37*(9), 2248-2250.

Ghaly, A. E., Ananthashankar, R., Alhattab, M., & Ramakrishnan, V. V. (2014). Production, characterization and treatment of textile effluents: a critical review. *J Chem Eng Process Technol*, *5*, 182.

Ghayeni, S. S., Beatson, P. J., Schneider, R. P., & Fane, A. G. (1998). Water reclamation from municipal wastewater using combined microfiltration-reverse osmosis (ME-RO): preliminary performance data and microbiological aspects of system operation. *Desalination, 116(1),* 65-80.

Glaze, W. H., Kang, J. W., & Chapin, D. H. (1987). The chemistry of water treatment processes involving ozone, hydrogen peroxide and ultraviolet radiation.

Güçlü, G. (2010). Removal of basic dyes from aqueous solutions by dimethyl terephthalate distillation residue. *Desalination*, *259*(1), 53-58.

Günay, A., Arslankaya, E., & Tosun, I. (2007). Lead removal from aqueous solution by natural and pretreated clinoptilolite: adsorption equilibrium and kinetics. *Journal of Hazardous Materials*, *146*(1), 362-371.

Guomin, C., Guoping, Y., Mei, S., & Yongjian, W. (2009). Chemical industrial wastewater treated by combined biological and chemical oxidation process.

Gupta, G. S., Singh, A. K., Tyagi, B. S., Prasad, G., & Singh, V. N. (1992). Treatment of carpet and metallic effluents by China clay. *Journal of chemical technology and biotechnology*, *55*(3), 277-284.

Hamada, K., Nishizawa, M., Yoshida, D., & Mitsuishi, M. (1998). Degradation of an azo dye by sodium hypochlorite in aqueous surfactant solutions. *Dyes and pigments*, *36*(4), 313-322.

Hanafi, F., Assobhei, O., & Mountadar, M. (2010). Detoxification and discoloration of Moroccan olive mill wastewater by electrocoagulation. *Journal of Hazardous Materials*, *174*(1), 807-812.

Herney-Ramírez, J., & Madeira, L. M. (2010). Use of pillared clay-based catalysts for wastewater treatment through Fenton-like processes. In *Pillared clays and related catalysts* (pp. 129-165). Springer New York.

Ho, Y. S., & McKay, G. (1998). A comparison of chemisorption kinetic models applied to pollutant removal on various sorbents. *Process Safety and Environmental Protection*, *76*(4), 332-340.

Hunger, K. (Ed.). (2007). *Industrial dyes: chemistry, properties, applications*. John Wiley & Sons.

Husain, Q. (2010). Peroxidase mediated decolorization and remediation of wastewater containing industrial dyes: a review. *Reviews in Environmental Science and Bio/Technology*, *9*(2), 117-140.

Ismadji, S., & Bhatia, S. K. (2001). Characterization of activated carbons using liquid phase adsorption. *Carbon*, *39*(8), 1237-1250.

İyim, T. B., & Güçlü, G. (2009). Removal of basic dyes from aqueous solutions using natural clay. *Desalination*, *249*(3), 1377-1379.

İyim, T. B., Acar, I., & Özgümüş, S. (2008). Removal of basic dyes from aqueous solutions with sulfonated phenol–formaldehyde resin. *Journal of applied polymer science*, *109*(5), 2774-2780.

Jiang, J. Q., & Graham, N. J. (1998). Pre-polymerised inorganic coagulants and phosphorus removal by coagulation- a review. *Water Sa*, *24*(3), 237-244.

Kasi, J. K., Kasi, A. K., Bokhari, M., & Afzulpurkar, N. (2013). Synthesis of Unique Structures of Carbon Nanotube at Anodic Aluminum Oxide Template. *Applied Mechanics and Materials*, *421*, 319-323.

Kattri, S. D., & Singh, M. K. (1999). Adsorption of basic dyes from aqueous solution by natural adsorbent. *Indian journal of chemical technology*, *6*, 112-116.

Kaur, R., Wani, S. P., Singh, A. K., & Lal, K. (2012, May). Wastewater production, treatment and use in India. In National Report presented at the 2 nd regional workshop on Safe Use of Wastewater in Agriculture.

Kent, F. C., Farahbakhsh, K., Mahendran, B., Jaklewicz, M., Liss, S. N., & Zhou, H. (2011). Water reclamation using reverse osmosis: Analysis of fouling propagation given tertiary membrane filtration and MBR pretreatments. *Journal of Membrane Science*, *382*(1), 328-338.

Kepa, U., Stanczyk-Mazanek, E., & Stepniak, L. (2008). The use of the advanced oxidation process in the ozone+ hydrogen peroxide system for the removal of cyanide from water. *Desalination*, *223*(1), 187-193.

Krihak, M., Murtagh, M. T., & Shahriari, M. R. (1997). A spectroscopic study of the effects of various solvents and sol-gel hosts on the chemical and photochemical properties of Thionin and Nile Blue A. *Journal of Sol-Gel Science and Technology*, *10*(2), 153-163.

Kundu, S., & Gupta, A. K. (2006). Arsenic adsorption onto iron oxide-coated cement (IOCC): regression analysis of equilibrium data with several isotherm models and their optimization. *Chemical Engineering Journal*, *122*(1), 93-106.

Kurniawan, A., Sutiono, H., Indraswati, N., & Ismadji, S. (2012). Removal of basic dyes in binary system by adsorption using rarasaponin–bentonite: Revisited of extended Langmuir model. *Chemical Engineering Journal*, *189*, 264-274.

Lai, K. C., Chen, J. W., Chen, W. T., Wan, T. J., Wen, J. C., & Shu, C. M. (2014). Applications of the Taguchi Method for Key Parameter Screening in Electrodialysis Reversal Used for High Salinity Wastewater. *CLEAN–Soil, Air, Water*, *42*(12), 1751-1758.

Lakowicz, J. R., Piszczek, G., & Kang, J. S. (2001). On the possibility of long-wavelength long-lifetime high-quantum-yield luminophores. *Analytical biochemistry*, *288*(1), 62-75.

Lee, I. H., Kuan, Y. C., & Chern, J. M. (2007). Equilibrium and kinetics of heavy metal ion exchange. *Journal of the Chinese Institute of Chemical Engineers*, *38*(1), 71-84.

Lee, S. H., Suh, J. K., & Li, M. (2003). Determination of bovine serum albumin by its enhancement effect of Nile Blue fluorescence. *BULLETIN-KOREAN CHEMICAL SOCIETY*, *24*(1), 45-48.

Legrini, O., Oliveros, E., & Braun, A. M. (1993). Photochemical processes for water treatment. *Chemical Reviews*, *93*(2), 671-698.

Limousin, G., Gaudet, J. P., Charlet, L., Szenknect, S., Barthes, V., & Krimissa, M. (2007). Sorption isotherms: a review on physical bases, modeling and measurement. *Applied Geochemistry*, *22*(2), 249-275.

Lin, C. D., & Chen, T. C. (1995). Relative antifungal efficacies of phosphoric acid and other compounds on fungi isolated from poultry feed. *Animal feed science and technology*, *54*(1), 217-226.

Lin, C. W., Shulok, J. R., Wong, Y. K., Schanbacher, C. F., Cincotta, L., & Foley, J. W. (1991). Photosensitization, uptake, and retention of phenoxazine Nile blue derivatives in human bladder carcinoma cells. *Cancer research*, *51*(4), 1109-1116.

Lin, Y., He, X., Han, G., Tian, Q., & Hu, W. (2011). Removal of Crystal Violet from aqueous solution using powdered mycelial biomass of Ceriporia lacerata P2. *Journal of Environmental Sciences*, *23*(12), 2055-2062.

Ma, W., Song, X., Pan, Y., Cheng, Z., Xin, G., Wang, B., & Wang, X. (2012). Adsorption behavior of crystal violet onto opal and reuse feasibility of opal-dye sludge for binding heavy metals from aqueous solutions. *Chemical Engineering Journal*, *193*, 381-390.

Maliwal, B. P., Kuśba, J., & Lakowicz, J. R. (1995). Fluorescence energy transfer in one dimension: Frequency-domain fluorescence study of DNA–fluorophore complexes. *Biopolymers*, *35*(2), 245-255.

Mall, I. D., Mishra, N., & Mishra, I. M. (1994). REMOVAL OF ORGANIC MATTERS FROM SUGAR MILL EFFLUENT USING BAGASSE FLY-ASH ACTIVATED CARBON. *Research and Industry*, *39*(2), 115-119.

Martínez-Huitle, C. A., & Brillas, E. (2009). Decontamination of wastewaters containing synthetic organic dyes by electrochemical methods: a general review. *Applied Catalysis B: Environmental*, *87*(3), 105-145.

McKay, G., El-Geundi, M., & Nassar, M. M. (1997). Equilibrium studies for the adsorption of dyes on bagasse pith. *Adsorption science & technology*, *15*(4), 251-270.

Mignani, M., Nosenzo, G., & Gualdi, A. (1999). Innovative ultrafiltration for wastewater reuse. *Desalination*, *124*(1), 287-292.

Mihara, Y., Inoue, T., & Yokota, K. (2005). [Relation between oxygen uptake rate and biosorption of activated sludge against chemical substance]. *Yakugaku zasshi: Journal of the Pharmaceutical Society of Japan*, *125*(2), 225-229.

Mittal, A., Mittal, J., Malviya, A., Kaur, D., & Gupta, V. K. (2010). Adsorption of hazardous dye crystal violet from wastewater by waste materials. *Journal of Colloid and Interface Science*, *343*(2), 463-473.

Mollah, M. Y., Morkovsky, P., Gomes, J. A., Kesmez, M., Parga, J., & Cocke, D. L. (2004). Fundamentals, present and future perspectives of electrocoagulation. *Journal of hazardous materials*, *114*(1), 199-210.

MOWR,(2000),*Annual Report on Wastewater Generation*, India.

Namasivayam, C., & Sumithra, S. (2005). Removal of direct red 12B and methylene blue from water by adsorption onto Fe (III)/Cr (III) hydroxide, an industrial solid waste. *Journal of environmental management*, *74*(3), 207-215.

Nassar, M. M., & El-Geundi, M. S. (1991). Comparative cost of colour removal from textile effluents using natural adsorbents. *Journal of Chemical Technology and Biotechnology*, *50*(2), 257-264.

Nassar, M. M., & El-Geundi, M. S. (1991). Comparative cost of colour removal from textile effluents using natural adsorbents. *Journal of Chemical Technology and Biotechnology*, *50*(2), 257-264.

Naveed, S., Bhatti, I., & Ali, K. (2006). Membrane technology and its suitability for treatment of textile waste water in Pakistan. *Journal of Research (Science)*, *17*(3), 155-164

Nigam, P., Armour, G., Banat, I. M., Singh, D., & Marchant, R. (2000). Physical removal of textile dyes from effluents and solid-state fermentation of dye-adsorbed agricultural residues. *Bioresource Technology, 72*(3), 219-226.

Nikas, D. C., Foley, J. W., & Black, P. M. (2001). Fluorescent imaging in a glioma model in vivo. *Lasers in surgery and medicine*, *29*(1), 11-17.

Nor, N. M., Lau, L. C., Lee, K. T., & Mohamed, A. R. (2013). Synthesis of activated carbon from lignocellulosic biomass and its applications in air pollution control—a review. *Journal of Environmental Chemical Engineering*, *1*(4), 658-666.

Ogugbue, C. J., & Sawidis, T. (2011). Bioremediation and detoxification of synthetic wastewater containing triarylmethane dyes by Aeromonas hydrophila isolated from industrial effluent. *Biotechnology research international*, *2011*.

Omura, T. (1994). Design of chlorine-fast reactive dyes: Part 4: degradation of amino-containing azo dyes by sodium hypochlorite. *Dyes and pigments*, *26*(1), 33-50.

Özcan, A. S., Erdem, B., & Özcan, A. (2004). Adsorption of Acid Blue 193 from aqueous solutions onto Na–bentonite and DTMA–bentonite. Journal of Colloid and Interface Science, 280(1), 44-54.

Philips, D. (1996). Environmentally friendly, productive and reliable: priorities for cotton dyes and dyeing processes. *Journal of the Society of Dyers and Colourists*, *112*(7-8), 183-186.

Pignon, H., Brasquet, C., & Le Cloirec, P. (2000). Coupling ultrafiltration and adsorption onto activated carbon cloth: application to the treatment of highly coloured wastewaters. *Water Science & Technology*, *42*(5-6), 355-362.

Poots, V. J. P., McKay, G., & Healy, J. J. (1976). The removal of acid dye from effluent using natural adsorbents—I peat. *Water Research, 10*(12), 1061-1066.

Raghavacharya, C. (1997). Colour removal from industrial effluents: a comparative review of available technologies. *Chemical engineering world*, *32*(7), 53-54.

Ramón, M. E., Gupta, A., Corbet, C., Ferrer, D. A., Movva, H. C., Carpenter, G., ... & Banerjee, S. K. (2011). CMOS-compatible synthesis of large-area, high-mobility graphene by chemical vapor deposition of acetylene on cobalt thin films. *Acs Nano*, *5*(9), 7198-7204.

Reemtsma, T., & Jekel, M. (Eds.). (2006). *Organic pollutants in the water cycle: properties, occurrence, analysis and environmental relevance of polar compounds*. John Wiley & Sons.

Robinson, T., McMullan, G., Marchant, R., & Nigam, P. (2001). Remediation of dyes in textile effluent: a critical review on current treatment technologies with a proposed alternative. *Bioresource technology, 77(3),* 247-255.

Saeed, A., Sharif, M., & Iqbal, M. (2010). Application potential of grapefruit peel as dye sorbent: kinetics, equilibrium and mechanism of crystal violet adsorption. *Journal of hazardous materials, 179*(1), 564-572.

Saleem, M., Afzal, M., Mahmood, F., & Hameed, A. (1994). Thermodynamics of adsorption of rhodamine B and nile blue sulphate on alumina from aqueous solutions. *JOURNAL-CHEMICAL SOCIETY OF PAKISTAN*, *16*, 83-83.

Saratale R. G., Saratale G. D., Parshetti G. K., Chang J. S. & Govindwar S. P. (2009). Outlook of bacterial decolorization and degradation of azo dyes: a review. *International Journal of Environmental Research and Public Health*, 11 – 59.

Saraydin, D., Karadağ, E., & Güven, O. (1996). Adsorption of some basic dyes by acrylamide-maleic acid hydrogels. *Separation science and technology*, *31*(3), 423-434.

Senthilkumaar, S., Kalaamani, P., & Subburaam, C. V. (2006). Liquid phase adsorption of crystal violet onto activated carbons derived from male flowers of coconut tree. *Journal of hazardous materials*, *136*(3), 800-808.

Singh A.K., & Tiwari, P.N., (2001). Adsorption of Malachite green from aqueous solution using low cost adsorbent. Proceedings of National Conference on Recent Advance in *Waste Management, Banaras Hindu University, Varanasi, India, 271*–274.

Slokar, Y. M., & Le Marechal, A. M. (1998). Methods of decoloration of textile wastewaters. *Dyes and pigments*, *37*(4), 335-356.

Soetaert, W., & Vandamme, E. J. (Eds.). (2010). *Industrial biotechnology: sustainable growth and economic success*. John Wiley & Sons.

Soliman, A. M., El-Naas, M. H., & Chaalal, O. (2013). Adsorption of Crystal Violet on Sludge produced from Refinery Wastewater Treatment: Characterization of Sludge Equilibrium and Kinetic Studies. *International Journal of Chemical & Environmental Engineering*, *4*(6).

Soloman, P. A., Basha, C. A., Velan, M., Ramamurthi, V., Koteeswaran, K., & Balasubramanian, N. (2009). Electrochemical degradation of Remazol Black B dye effluent. *CLEAN–Soil, Air, Water, 37*(11), 889-900.

UNSD (2013) *United Nations Statistics Division.*

Üstün, G. E., Solmaz, S. K. A., & Birgül, A. (2007). Regeneration of industrial district wastewater using a combination of Fenton process and ion exchange—A case study. Resources, *Conservation and Recycling, 52*(2), 425-440.

Üzüm, Ö. B., & Karadağ, E. (2006). Synthetic polymeric absorbent for dye based on chemically crosslinked acrylamide/mesaconic acid hydrogels. *Journal of applied polymer science, 101*(1), 405-413.

Venkatesh, S., Quaff, A. R., Pandey, N. D., & Venkatesh, K. (2014). Decolorization and mineralization of CI direct red 28 azo dye by ozonation. *Desalination and Water Treatment*, (ahead-of-print), 1-11.

Verma, A. K., Dash, R. R., & Bhunia, P. (2012). A review on chemical coagulation/flocculation technologies for removal of colour from textile wastewaters. *Journal of Environmental Management, 93*(1), 154-168.

Viraraghavan, T., & Mihial, D. J. (1995). Colour removal using peat. *Fresenius Environmental Bulletin, 4*(6), 346-351.

WHO, (2002). Water Pollutants. *World Health Organization: biological agents, dissolved chemicals, non-dissolved chemicals, Sediments, Heat*. WHO CEHA, Amman, Jordan.

Wiesmann, U., Choi, I. S., & Dombrowski, E. M. (2007). *Fundamentals of biological wastewater treatment. John Wiley & Sons.*

World Bank Group (Ed.). (2012). World Development Indicators 2012. *World Bank Publications.*

World Health Organization. (2000). *Air quality guidelines for Europe*.

Xu, X., & Zhu, X. (2004). Treatment of refectory oily wastewater by electro-coagulation process. *Chemosphere*, *56*(10), 889-894.

Yoon, Y. H., & NELSON, J. H. (1984). Application of gas adsorption kinetics I. A theoretical model for respirator cartridge service life. *The American Industrial Hygiene Association Journal*, *45*(8), 509-516.

Zaharia, C., & Suteu, D. (2013). Coal fly ash as adsorptive material for treatment of a real textile effluent: operating parameters and treatment efficiency. *Environmental Science and Pollution Research*, *20*(4), 2226-2235.

Zewail, T. M., & Yousef, N. S. (2015). Kinetic study of heavy metal ions removal by ion exchange in batch conical air spouted bed. Alexandria Engineering Journal.

Zhang, L., Zhang, H., Guo, W., & Tian, Y. (2014). Removal of malachite green and crystal violet cationic dyes from aqueous solution using activated sintering process red mud. *Applied Clay Science*, *93*, 85-93.

Zhang, Q., & Chuang, K. T. (2001). Adsorption of organic pollutants from effluents of a Kraft pulp mill on activated carbon and polymer resin. *Advances in Environmental Research*, *5*(3), 251-258.

Zhang, Z., Zhang, Z., Fernández, Y., Menéndez, J. A., Niu, H., Peng, J., ... & Guo, S. (2010). Adsorption isotherms and kinetics of methylene blue on a low-cost adsorbent recovered from a spent catalyst of vinyl acetate synthesis. *Applied Surface Science*, *256*(8), 2569-2576.

Zouboulis, A. I., Moussas, P. A., & Vasilakou, F. (2008). Polyferric sulphate: Preparation, characterisation and application in coagulation experiments. *Journal of Hazardous materials*, *155*(3), 459-468.

Appendix

Figure 76: Different concentration of Crystal Violet (CV)

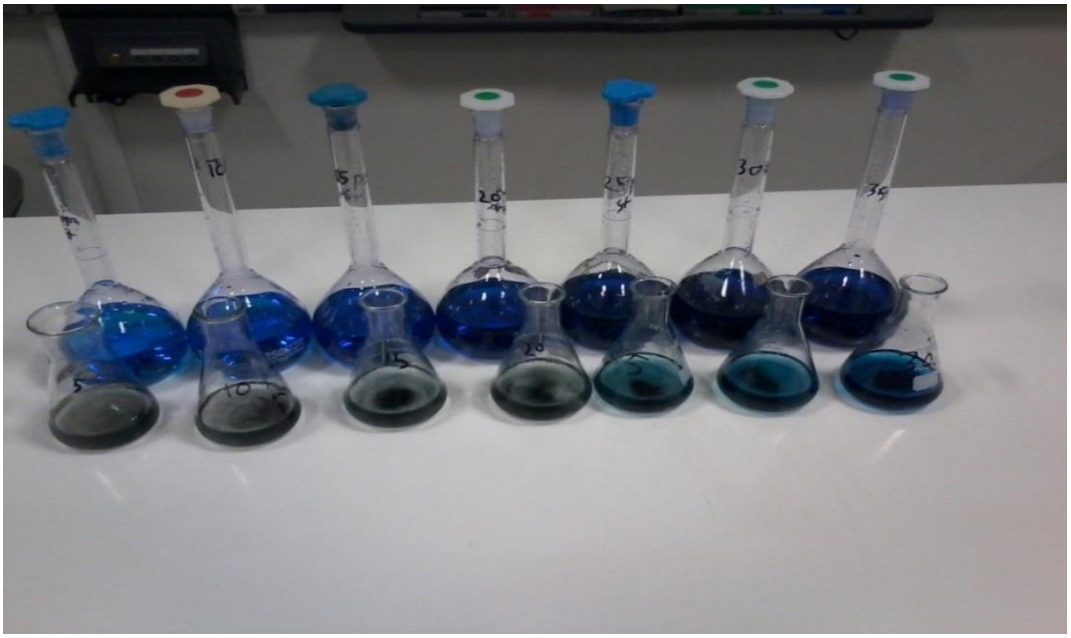

Figure 77: Different concentration of Nile Blue (NB)

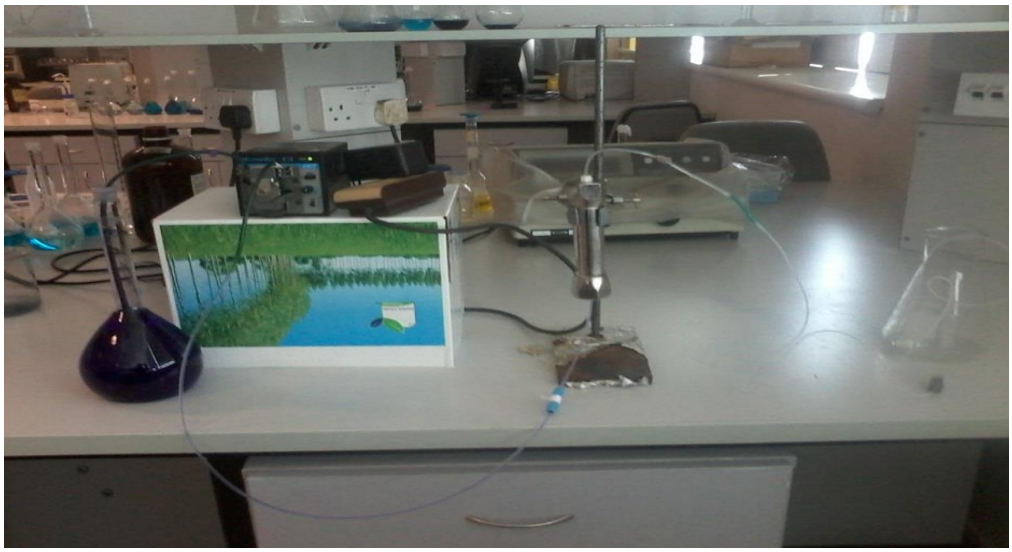

Figure 78: Dynamic adsorption study set-up for 10 ppm Crystal Violet (CV)

Figure 79: Treated date palm leaves

Figure 80: Activated Carbon